UNIVERSITY OF GHANA

APPLICATION OF DIRECT CURRENT ELECTRICAL RESISTIVITY AND HYDROGEOCHEMICAL METHODS IN INVESTIGATING GROUNDWATER CONTAMINATION: GA EAST MUNICIPAL ASSEMBLY AND ITS ENVIRONS, SOUTHERN GHANA.

PATRICK BANAHENE

(10442764)

THIS THESIS IS SUBMITTED TO THE UNIVERSITY OF GHANA, LEGON IN PARTIAL FULFILMENT OF THE REQUIREMENT FOR THE AWARD OF MASTER OF PHILOSOPHY GEOLOGY DEGREE.

JULY, 2015

DECLARATION

This is to certify that this is the result of research carried out by Patrick Banahene towards the award of Master of Philosophy in Geology in the Department of Earth Science, University of Ghana.

…….. Date……

PATRICK BANAHENE

(Student)

……Date……....

DR. THOMAS E. K. ARMAH

(Principal Supervisor)

……Date……....

DR. PATRICK ASAMOAH SAKYI

(Co-Supervisor)

ABSTRACT

A combined electrical resistivity and hydrogeochemical methods have been used in investigating groundwater contamination in the Ga-East municipality. Thirty five vertical electrical sounding (VES) using the Schlumberger array configuration (with a maximum of AB/2 = 500 m) and one azimuthal array resistivity sounding were conducted and analysed using the single channel Scintrex Automated Resistivity Imaging System (SARIS) and IPI2WIN software. The resistivity survey revealed mainly four geoelectric layers correlating very well with the borehole logs used in constraining the interpretation in the area. The interpreted pseudo and resistivity sections showed that the water quality at the Pantang dumpsite is contaminated and it is on a downward trend with a tendency of affecting deeper depth with time. The low resistivity signatures of the VES has positive correlation with areas of high electrical conductivity (EC) of groundwater in the study area. The analysis of trace metals revealed that only few areas were affected by the disposal of solid waste. The study also characterised the hydrochemistry of the area and assessed the suitability of groundwater for domestic and agricultural purposes. The study area was found to be characterized by the Na-Cl and Na-HCO_3^-water types from the piper diagram. Na^+ and Ca^{2+} were the dominant cations whiles Cl^- and HCO_3^- were the dominant anions detected. Sodium adsorption ratio (SAR) and hydrochemical index revealed that the groundwater around the dump site is generally unsuitable for drinking and irrigation whiles the groundwater samples from around the Legon, Pantang hospital and Ghana Atomic Energy Commission (GAEC) areas are generally good for irrigation but only about 50% are good for drinking.

DEDICATION

This work is dedicated to the Almighty God for the gift of life, and being my source of strength, knowledge and inspiration. To my parents, Mr. Osei Badu Banahene and Madam Agnes Boadu, and my siblings Yaw Badu Banahene Snr. & Jnr., and Portia Abena Banie Banahene.

ACKNOWLEDGEMENT

I am grateful to the Almighty God for his love, protection and mercies. I shall forever remain indebted to my parents Mr. Osei Badu Banahene and Madam Agnes Boadu, my siblings Yaw Badu Banahene Snr. and Jnr. and Portia Abena Banie Banahene, for their love, spiritual, moral and material support throughout this journey.

My sincere thanks and appreciation goes to my supervisors, Dr. Thomas E. K. Armah and Dr. Patrick Asamoah Sakyi for their kind supervision, constructive criticism, guidance, and motivation. I must admit your invaluable advice and support in reviewing this thesis has brought me this far. I would like to thank all the lecturers of the Department of Earth Science who have contributed immensely to my knowledge. I also appreciate the effort of Prof. Shiloh Osae, Prof. Samuel Dampare, Dr. P. Amponsah, Dr. S. Ganyoglo, Mr. Afful, Nash O. Bentil, David Saka and Adwoba Edjah, all of the Ghana Atomic Energy Commission.

To all my fellow Earth Scientists especially Sampson Renner, Kofi Duku and Emmanuel Haruna who served as research and field assistants, Patience Bosompemaa, Elizabeth Darko and Jeremiah Anno-Onumah my study mates, I salute you all. I cannot forget the assistance of the department driver for all your services, God bless you Mr. Michael Obeng.

My heartfelt and profound gratitude also goes to Akua Yeboah Oduro Owusu, Mr. Abubakar. Shehu Yaradua of Tubman University Liberia, Francis Torgbor and his family and my dear friend Shirley-Anne Lutterodt, you deserve a lot of thanks and you have been exceptionally unique in my life and I am indeed proud of you.

TABLE OF CONTENTS

LIST OF FIGURES

LIST OF TABLES

CHAPTER ONE

INTRODUCTION

1.1 BACKGROUND

Groundwater is an important natural resource that exists on earth, and it plays a major role in the daily activities of man. Groundwater resource has been identified as the solution to the water delivery system because of the susceptibility of surface water to pollution (Quist et al., 1988). The patronage of groundwater is becoming common than surface water as it occurs naturally and known to be less prone to the negative effects of anthropogenic activities and adverse climatic conditions. Because of these advantages and uses, a significant quantity of groundwater is being used for domestic, agricultural and industrial activities. The capital cost of exploiting groundwater is known to be modest as compared to treating contaminated surface waters before use (Yidana, 2010).

It is however important to note that the quality of groundwater is sometimes negatively affected by dissolved minerals resulting from weathering and interaction with the geologic formation which may affect human health (Freeze and Cherry, 1979; Domenico and Schwartz, 1990; Kortatsi, 2007; Aghazadeh and Mogaddam, 2010). Groundwater flow is relatively slow and it is very difficult and expensive to treat when contaminated. Contamination of groundwater may also occur due to the potential of leachate from waste, increasing rate of urbanization and saline water intrusion (Makey, 1982).

In Accra, groundwater has become an alternate source of potable water for many people. This includes several people residing in the Ga East municipality who have turned their

attention to groundwater for domestic, agricultural and industrial purposes without much attention to the quality of the groundwater, with the general belief that groundwater is pure and clean. The Ga East municipal assembly and its immediate environs, all in the Greater Accra Region of Ghana, host some of the prominent institutions such as the Pantang Hospital, Pantang Nursing Training College, Ghana Atomic Energy Commission (GAEC), the University of Ghana, Presbyterian Boys Senior High School, and the West African Senior High School. In spite of the immense contributions that these institutions offer to the socio-economic development of the country, they have not been spared of the perennial water shortage syndrome in the area; therefore, all these institutions have resorted to the exploitation of groundwater resources in order to meet the needs and demands of their work.

The Pantang dump site, which serves as one of the major dump sites in Accra for the disposal of solid waste is also located within the municipality, posing serious threats to the groundwater resources, especially for those living very close to the dump site who use the groundwater for their daily activities. Individuals who live close to, and afar from the dumpsite within the municipality have also complained about high iron content and the salinity of the groundwater amongst other contaminants.

To investigate and assess the quality of groundwater in the area, a combination of direct current electrical resistivity and geochemical methods have been employed. In the absence of large number of observation wells, surface geophysical survey is known to provide an effective way to image the subsurface and the groundwater zone. The electrical resistivity

method has been widely used to investigate shallow subsurface geology, to determine the groundwater sources and their quality (Kearey and Brooks, 2002).

Groundwater flow is mostly restricted to joints and fractures within crystalline rock formations. In such formations, the primary permeability is very much reduced. Groundwater flow varies in space and time, and it is dependent on the hydraulic properties of the rocks and the boundary conditions imposed on the groundwater system (Stallman, 1971). Water quality analysis is an important aspect in groundwater studies. Variation of groundwater quality in an area is found to be a function of the physical and chemical parameters and they are greatly influenced by geological formations and anthropogenic activities (Kumaresan and Riyazuddin, 2006; Majolagbe et al., 2011).

1.2 PROBLEM STATEMENT

Increasing population density and urbanization has led to perennial water shortage in the area. There is therefore high demand for water resources by residents and institutions located in the study area. This has resulted in the exploitation of groundwater resources without necessarily paying attention to potential sources of pollution in order to avoid tapping groundwater that are contaminated.

A number of the wells are located very close to the Pantang dump site where varieties of solid waste collected within and around the municipality are disposed of. The waste dumped contains a lot of metals that are washed and infiltrated into the groundwater (Achampong et al., 2013). The contaminants may also include interaction of weathered rocks in the aquifers.

Literature reviewed and reconnaissance survey prior to the research revealed that quite a number of the boreholes and hand dug wells found in the area are contaminated in different forms. The predominant contaminants are high salinity and iron content (Kortatsi and Jorgensen, 2001), and therefore this raises concerns about the quality of the water being used in the area.

1.3 OBJECTIVES

The research work is aimed at investigating groundwater contamination by the application of direct current electrical resistivity (geophysical method) and physico-chemical analyses (hydrogeochemical method) of water samples. The specific objectives are;

- To assess the impact of dump site on groundwater quality.
- To investigate the effect of geological formation on groundwater quality.
- To generate interpreted resistivity and pseudo cross-sections of the Schlumberger sounding curve(s) for the area.
- To determine the groundwater types in the area.

1.4 JUSTIFICATION

The most popular form of assessing groundwater quality is by analysing the physico-chemical and the bacteriological parameters. Aside this, there are also the geophysical techniques often employed in the study of groundwater resources, including investigating groundwater quality and delineating contaminated zones (El-Hussaini et al., 2003; Banoeng-Yakubo et al., 2005; Abdalla, 2008).

The application of direct current electrical resistivity survey combined with geochemical methods, as an integrated approach in investigating groundwater contamination for hydrogeological studies is not common in Ghana. Detecting groundwater contaminants and advising on groundwater resource management by applying geophysical techniques helps in reducing cost, as the approach is non-intrusive, faster, and less expensive. It will also aid in pollution prevention and control. The findings of the research will contribute to the existing knowledge on groundwater quality studies using different methods. This will serve as a useful reference for other researchers to explore the assessment of groundwater quality studies using different approach at different locations.

CHAPTER TWO

LITERATURE REVIEW

2.1 GROUNDWATER RESOURCE OCCURRENCE AND DEVELOPMENT

Water is an essential commodity in everyday life of human activities, and it plays a major role in the economies of many countries, by providing means of transport, generation of hydropower, tourism activities and also used by many manufacturing industries. The occurrence and availability of water throughout the Earth is driven by the hydrologic cycle. Quantifying groundwater, hydrogeochemical evolution and solute transport in aquifers is important for their evaluation as sites for long term hazardous waste containment, protective natural covers and geochemical influence to underlying regional fresh water aquifers (Ortega-Guerrero, 2003).

Groundwater use is becoming common in Ghana's water supply system as it is relatively cleaner and less susceptible to pollution as compared to surface water. It is also partly because of the non-reliability of the water supply from the Ghana Urban Water Limited (GUWL) thereby compelling individuals and organisations to resort to drilling their own boreholes.

A lot of surface water bodies have also dried out due to bad cultural practices and adverse weather conditions. It is in view of this that Yidana et al., (2007) indicated that the proper management of groundwater resources in rural communities requires a good understanding of the dynamics of the resource.

The occurrence of groundwater in a coastal setting is often accompanied by high salinity, and as a result when groundwater types are being classified in coastal areas the major determining factor is considered to be the salinity (Stuyfzand, 1986). Over withdrawal of groundwater also leads to head loss, which causes saline water to be drawn into a freshwater body thereby increasing the salinity of the groundwater (Obikoya and Bennell, 2012).

2.2 GROUNDWATER USE

Groundwater is globally important for human consumption, and changes in quality with subsequent contamination can undoubtedly affect human health (Tay and Kortatsi, 2008). The role of groundwater in the water supply system in Ghana cannot be overlooked, especially in the rural areas where they mostly rely on groundwater for their activities. According to the Ghana National Water Policy (GNWP, 2007), the projected irrigation water demand by the year 2020 will be about 400,000 m^3over a projected area of 100,000 hectares. Groundwater is used across the country for drinking and other domestic purposes as well as industrial and agricultural needs. In spite of the increasing reliance on groundwater, the resource is reported as not only inadequate but is also saline at most places within the Accra Plains (Kortatsi and Jørgensen, 2001).

In recent times, exploitation of groundwater for industrial use by way of sachet and bottling water production is on the increase and irrigation of agricultural farms as well as livestock watering. A number of boreholes have been drilled purposely for the large scale commercial bottled water industries in southern Ghana (Gyau-Boakye et al., 2008).

The Ghana National Water Policy (GNWP, 2007) reported that the main consumptive usages of water are water supply, irrigation and livestock watering. The Reformed Ghana Rural Water Supply Sector Policy outlined procedures for an integrated use of pipe-borne water and groundwater to meet the increasing demands of rural settlements and the peri-urban areas (Kleemeier, 2002). However, the usage of groundwater is dependent on its availability, quality, quantity and the purpose for which it will be used for. In an area where the location of the borehole is farther than a nearby surface water and depending on its intended purpose it may not be resorted to that much (Kleemeier, 2002).

For various reasons including low yield of boreholes and the relatively good quality of groundwater compared to surface sources, groundwater abstracted from boreholes in 9 out of the 10 administrative regions of Ghana with the exception of Greater Accra region is exclusively used for domestic water supply (Gyau-Boakye et al., 2008). It is estimated that over 95% of groundwater use in the country is for domestic purposes (Gyau-Boakye et al., 2008).

In terms of irrigation, groundwater usage is generally on the low and not much is seen especially in the Ga East municipality. However, few people are seen using hand dug wells or channels that intercept shallow aquifers for irrigating vegetable farms and gardens. In Ghana, the use of groundwater for irrigation is often seen in the three northern regions where rainfall is limited as compared to the other parts of the country. Groundwater for irrigation is also prevalent in Volta Region and the Accra Plains in the Greater Accra Region (Kortatsi and Jorgensen, 2001). About 70% of Ghana's 1.34 Million Heads (MH) cattle (2003

estimated figure) and 40% of other livestock and poultry (sheep-3.02 MH; goats-3.56 MH; pigs-3.03 MH; and poultry-2.64 MH) are produced in the 3 northern regions are watered mainly through groundwater (MOFA, 2004). The usage of groundwater in livestock watering is also seen in the Accra plains.

2.3 SITING AND DRILLING OF BOREHOLES

Siting of boreholes is very important in the study of groundwater contamination. When boreholes are not sited properly it may be faced with dangers of getting polluted by potential contaminants ranging from rock water interaction, leachate from dump sites, pollution of surface water bodies that serve as recharge and interacts with groundwater and chemicals resulting from fertilizer application.

According to the report of the British Geological Survey (2011), it is a good practice to site a borehole as far away as possible, and preferably upslope, from any potential sources of pollution. These includes septic or fuel tanks, soakaways, slurry pits and areas of intensive grazing. A minimum distance of 50 m between a water borehole and any potentially polluting activity is recommended (Adetunji and Odetokun, 2011; British Geological Survey, 2011).

2.4 THE EFFECTS OF GEOLOGY ON THE HYDROCHEMISTRY OF GROUNDWATER

Aquifers are the rocks and sediments that not only contain significant quantities of groundwater but are also able to store and transmit water when it has sufficient porosity and

permeability to allow the passage of groundwater to flow at a speed based on the hydraulic parameters of the formation (Freeze and Cherry, 1979).

Anthropogenic activities ranging from agricultural practices to industrial discharges are some of the sources of groundwater quality problems faced in most parts of the world through infiltrations and percolations into the ground water. This may not be the only contributing factor to the contaminants seen in groundwater hydrochemistry. Another major factor is the influence of the local geology the area under study. Groundwater and surface water co-exist in the hydrologic cycle and sometimes interact. The origin of high groundwater salinity can be attributed to several probable causes which includes leaching of salt during or after infiltration; seawater intrusion; mixing with brines and surface evaporation before recharge (Slater et al., 2000; Morrow et al., 2010).

Groundwater flows through almost all rocks and sediments below the water table. Because some are less porous and permeable than others, water flows through different rocks and sediments at different speeds. The quality of groundwater may be compromised when the water flowing through the pore spaces interacts and dissolves some rocks and parts of the rocks especially the weathered rocks. The elements of the dissolved rocks ends up contaminating or polluting the groundwater and when a well is drilled to tap, it eventually renders the groundwater unsafe for drinking and sometimes unsuitable for other purposes.

2.5 POLLUTION AND CONTAMINATION OF GROUNDWATER

Groundwater and surface water are interconnected and therefore, pollution of surface water is most likely to affect groundwater. Aquifers are highly vulnerable to chemical and microbial contamination due to rapid recharge of water from the land surface (Ford and Williams, 2007). Any activity which involves the pollution of the environment for example chemical spillage and application of fertilizers has the potential of polluting the groundwater. Although groundwater is generally good for drinking and other domestic and industrial activities, it may be dangerous to human health when contaminated by spillage from the surface (Appelo and Postma, 2005).

Groundwater resources have been under rapidly increasing stress in large parts of the world due to pollution (Ogungbe et al., 2012). Several people have conducted research into groundwater pollution and contamination (e.g., Aristodemou and Thomas-Betts, 2000; Mota et al., 2004; Nartey et al., 2012). Mostly groundwater pollution is as a result of several factors which includes anthropogenic and geogenic activities (Yidana et al., 2011). The anthropogenic contaminants sometimes results from nitrates from agricultural activities, animal waste, manures, sewages, industrial discharge and leachate. Decaying organic matter found in the soil, and the occurrence of irons and manganese from rocks as well as seawater intrusion also contributes to groundwater contamination (Rao et al., 2005; Kortatsi, 2007; Jianshua et al., 2008; Yidana et al., 2012). The contamination also results in an increase in hardness and conductivity of the water (Schneider, 1978). The liquid drains from dump site, mainly organic carbon which occurs in the form of fulvic acids migrate downward and contaminate the groundwater (Taylor and Allen, 2001). This makes the water quality a major

health problem, particularly causing diseases such as cholera, heart related diseases and kidney failures.

Fluorine occurs in the environment as fluoride and its characteristics in groundwater is dependent on the pH since it has a low solubility between the pH of 6.0 to 6.5 (Apelo and Postma, 2005). Occurrence of excessive fluoride in groundwater when taken into human body can cause diseases such as dental and skeletal fluorosis (Apambire et al., 1997).

2.6 EFFECTS OF DUMPSITE ON GROUNDWATER QUALITY

The urban wastes that are generated in the Ga East municipality coupled with the industrial and domestic waste produced in some parts of Accra are disposed of at the Abokobi-Pantang dump site. Groundwater contamination from dump sites often results from leaking leachate that has percolated through waste and accumulated as various ions in solution (Rushbrook and Pugh, 1999; Carpenter et al., 2012; Aweto and Mamah, 2014). A study conducted using electrical resistivity soundings in a municipal dump site in Jordan indicated that the leachate plume migration from industries affects the quality of groundwater along its flow direction (Al-Tarazi et al., 2006).

In Ghana, the use of dump site is still the preferred option for waste disposal in all the metropolitan areas, municipalities and districts (Keelson, 2014). Siting of dump sites often do not follow any planning considerations and lead to pollution of nearby surface water bodies which may tend to recharge the groundwater and subsequently pollute the aquifers (Nartey et al., 2012; Keelson, 2014). Contamination from dump sites typically forms a

"plume" that moves outward and downward into surrounding and underlying aquifers (Carpenter et al., 2012). The environmental hazards posed by open dumpsites may not stop even after waste disposal activities have ceased at the locations.

In Accra, research studies on abandoned waste disposal sites by (Essumang et al., 2009; Osei et al., 2011; Denutsui et al., 2012) shows that leachate could have high concentration of nutrients and polycyclic aromatic hydrocarbons and significant concentrations of heavy metals such as iron, zinc and aluminium. The contamination subsequently becomes part of the groundwater flow system immediately they reach the water table. The extent of pollution and the negative effects on human health is greater in high rainfall areas than less humid and arid areas (Al-Yaquot and Hamoda, 2003).

The contamination of groundwater and soil is the major environmental risk related to unsanitary dump site of solid waste (Raman and Narayanan, 2008). Siting of boreholes at the dump sites to draw groundwater threatens to contaminate the water (Kumar and Alappat, 2003). The adverse effect of pollution has brought about the widespread of the various waterborne diseases such as typhoid fever, guinea worm infestation, bilharzias and many more (Adomako et al., 2010).

A study conducted at the Pantang dump site by Achampong et al., (2013) revealed that;

- The leachate from the dump site has contaminated the groundwater making it unsafe to drink.
- High levels of heavy metals such as lead, iron, magnesium, zinc, cobalt and manganese in some of the neighbouring wells.

- The geology of the study area is not an ideal site for a dump site due to high water table levels, and the presence of numerous secondary porosities such as faults, joints and highly weathered rocks.

2.7 APPLICATION OF GEOPHYSICS IN GROUNDWATER STUDIES

Geophysical techniques have been employed in the field of geology in many parts of the world and it can be used in prospecting for groundwater as well as detecting groundwater contamination (Wilson et al., 2006; Duque et al., 2008; Song et al., 2012; Akankpo and Igboekwe, 2011; Werner et al., 2013). Electrical resistivity and electromagnetic techniques have been applied in groundwater studies based on the geologic formation and its properties like porosity and permeability by correlating it with electrical conductivity signatures (Obikoya and Bennell, 2012). This helped in the investigation of freshwater intrusion by saline water and subsequently delineated the fresh-saline water interface at the inter-tidal area in North Wales.

Among the various geophysical techniques, the electrical resistivity method is widely used in groundwater studies because of its ability to detect a change in pore water conductivity (Abdul Nassir et al., 2000; Adepelumi et al., 2008). Several researchers (e.g, Barker, 1990; Telford et al., 1990) established the significance of using the Schlumberger resistivity sounding in Yorkshire in UK and Novo in Brazil respectively in detecting contaminated substrate of sandstone.

Onions et al. (1996) applied surface geophysical surveys to investigate a contaminated old collieries site by identifying hazards on contaminated sites. The resistivity technique enabled the reclamation and redevelopment of the land and equipped the site engineers with more complete surveys. However, guidelines of good practice did not exist at the time and hence could not establish geophysics as a more widely used technique for site investigations (Onions et al., 1996).

Zaidman et al. (1999) in a different study employed the electrical resistivity imaging techniques to investigate solute transport of the unsaturated zone in the chalk at Yorkshire and reported about the several advantages it has over pore solution sampling. This is because the spatial distribution of the solute obtained is much better as sampling is limited to few points. Subsequently, the solutes were detected through localized pathways such as fractures.

Geophysical methods however presents more challenges at the stage of interpretation as geological and hydrogeological changes have to be inferred from the characteristics of a geophysical survey (Zaidman et al., 1999; Edet and Okereke, 2002; Attwa et al., 2011; Li et al., 2012). That notwithstanding, application of electrical resistivity in the characterisation of a hydrogeological setting has proved to be very successful (Daily et al., 1992; Slater et al., 1996). Direct current resistivity was applied to demarcate possible areas for groundwater development away from a possible contaminated zone in the Lekki area of Lagos state (Adepelumiet al., 2008). The results revealed a dominant trend of decreasing resistivity with depth, indicating an increase in salinity with depth.

A geochemical study has also been used to determine the possibility of seawater intrusion (Lee and Song, 2007). Results from a combination of geophysical and geochemical analysis have proved useful and very effective in groundwater quality studies (Akankpo and Igboekwe, 2011; Obikoya and Bennell 2012; Hwang et al., 2004).

A study conducted in Ahoada, south-south Nigeria after an oil spillage arising from ruptured pipeline in the area by (Nwankwo and Emujakporue, 2012) suggested that using geophysical methods can be helpful in mapping areas of contaminated soil and groundwater. A study of this nature was to examine the subsoil conditions and groundwater quality of the area. The method employed in the investigation involved the vertical electrical sounding technique using the Schlumberger configuration and the horizontal profiling. The two methods correlated well and the profiles generated helped to map the contaminant plume, which was delineated as an area of high interpreted resistivities (Hwang et al., 2004; Nwankwo and Emujakporue, 2012).

Benson (1991) observed in a geophysical studies that hydrocarbon plumes may be delineated as resistivity highs since hydrocarbons typically have high resistivities relative to water, or as resistivity lows if inorganic compounds are added to contaminated water to stimulate bioremediation, therefore increasing the total dissolved solids (TDS) in the water. Previous studies by (Apambire et al., 1997; Srinivasamoorthy et al., 2010) focused mainly on groundwater quality assessment by using hydrogeochemical data. Many different methods have been developed for assessing this vulnerability but combined hydrogeochemical and geophysical techniques have been the goal of recent studies to evaluate the potential for

groundwater vulnerability to contamination (Srinivasamoorthy, 2011). This is because the combine methods take into consideration both qualitative and quantitative assessment.

Combined resistivity and hydrogeochemical investigations in parts of south Giza, Egypt identified seepage of irrigation water, sanitary water and other domestic activities as the main causes for groundwater pollution (Abdalla, 2008). Another study also examined the geoelectric and hydrochemical data and identified the presence of a very high conductive zone (contaminated zone) with low resistivity value extending from the ground surface down to a depth of about 47 m (El-Hussaini et al., 2003).

Electrical resistivity technique has been used to delineate formations bearing fresh and saline water, distinguished between sandy and clay layers and established depth to the freshwater-saline water interface (Banoeng-Yakubo et al., 2005). The results obtained from the VES indicated that the northern portions of the area were basically underlain by four-layered lithological structure with varying resistivity range. This helped to establish the freshwater-saline water interface.

In Ghana, both electromagnetic profiling and vertical electrical sounding have been employed to determine the aquifer freshwater lens along the sea (Kortatsi, 2005). Resistivity value in sedimentary rocks are also known to be controlled by parameters such as water contents, salinity, texture, matrix conductivity and the presence of clay materials (Telford et al., 1990). The resistivity ranges of some common geological formations are as shown in Table 2.1. The resistivity values are employed in interpretation of sounding results.

Table 2.1: Resistivity values of some common geological formation recorded by (Telford et al., 1990)

Material	**Nominal resistivity (Ω-m)**
Quartz	3×10^2 - 10^6
Granite	3×10^2 - 10^6
Granite (weathered)	30 – 500
Consolidated shale	20 - 2×10^3
Sandstones	200 – 5000
Sandstone (weathered)	50 – 200
Clays	1 - 10^2
Boulder clay	15 – 35
Clay (very dry)	50 – 150
Gravel (dry)	1400
Gravel (saturated)	100
Lateritic soil	120 – 750
Dry sandy soil	80 – 1050
Sand clay/clayed sand	30 – 215
Sand and gravel (saturated)	30 – 225
Mudstone	20 – 120
Silstone	20 – 150

2.8 SCHLUMBERGER AZIMUTHAL ARRAY

Azimuthal resistivity surveys were done to cover 360 degrees rotation and taking measurements along a sufficient number of azimuths to define any variation of apparent resistivity with orientation (Taylor and Fleming, 1988). The apparent resistivities for each electrode spacing are plotted against azimuth in a polar diagram. Areas with no measurable fracture sets show a circular plotted figure. The circular plot also show that the volume of rock investigated was insufficient because the structure and material sampled were, to the limit of measurement, isotropic.

A resultant elliptical plot indicates the presence of anisotropic conditions in the subsurface resulting from heterogeneity within the subsurface. Habberjam (1975) first studied the case of homogeneity and its effect on the anisotropy of the subsurface and showed that the

anisotropy if a subsurface can be characterized by four parameters (ρ1, ρ2, ρm and λ) which are the measureable apparent resistivities. The strike and the dip also play a significant role in the anisotropy of the subsurface. A surface point P, at a distance "r" from the surface source where OP makes an angle ϑ with the strike direction has an electric potential of

$$V(r,\vartheta) = \frac{I\rho_m}{2\pi r\sqrt{1+(\lambda^2-1)sin^2\alpha sin^2\vartheta)}} \qquad \text{(Habberjam, 1975)} \qquad (2.1)$$

Because the apparent parameters are the only measureable parameters, the square root of the ratio of the maximum apparent resistivity to the minimum apparent resistivity, and the paradox of anisotropy applies such that the maximum apparent resistivity is obtained with current flowing parallel to the strike. Graphical interpretation of the plots also infer that the directions of maximum apparent resistivity are the directions of the trend of the fracture set (Taylor and Flemming, 1988).

The azimuth of the principal fracture set can be defined for elliptical plots. The major axis of the ellipse is coincident with the strike of the fractures for co-linear array, but for non-linear arrays, such as the Square array (Habberjam and Watkins, 1967), the minor axis of the ellipse is parallel to the fracture strike.

2.9 RESISTIVITY CURVE TYPES

For three layers resistivities in two interface case, four possible curve types exist, which are:

1. Q – Type ρ1> ρ2> ρ3
2. H – Type ρ1> ρ2< ρ3
3. K – Type ρ1< ρ2> ρ3
4. A – Type ρ1< ρ2< ρ3

There are also eight possible relations in four-layer geoelectric sections. However, in situations where more than three layers exist the resulting type curve is obtained by combining these curve types to represent the layers below (Telford et al., 1990). The different types of curves characterized by the four geoelectric layers are listed.

1. HA- Type $\rho1 > \rho2 < \rho3 < \rho4$
2. HK -Type $\rho1 > \rho2 < \rho3 > \rho4$
3. AA -Type $\rho1 < \rho2 < \rho3 < \rho4$
4. AK -Type $\rho1 < \rho2 < \rho3 > \rho4$
5. KH -Type $\rho1 < \rho2 > \rho3 < \rho4$
6. KQ -Type $\rho1 < \rho2 > \rho3 > \rho4$
7. QH -Type $\rho1 > \rho2 > \rho3 < \rho4$
8. QQ -Type $\rho1 > \rho2 > \rho3 > \rho4$

CHAPTER THREE

METHODOLOGY

3.1 STUDY AREA

3.1.1 Location and Accessibility

Ga East municipal assembly is located in the northern part of Greater Accra Region of Ghana and bordered by longitude 0.16518°W to 0.24689°W and latitude 5.62978°N to 5.74725°N (Fig 3.1). The total land area of the municipality is approximately 166 km^2 (Yeboah and Ameyaw, 2012). The municipality has a population of about 244,226 with a population density of 1214 persons per km^2 according to the provisional results of the population and housing census released by the Ghana Statistical Service (2010). The municipality shares boundaries with four municipal/district assemblies. To the south east by the La-Nkwantanang Madina municipal assembly (LaNMMA) and it is bordered to the west by the Ga West municipal assembly (GWMA), to the east by the Adenta municipal assembly (AdMA), to the south by Accra metropolitan assembly (AMA) and to the north by the Akwapim south district assembly.

The area is fairly accessible and the municipality can be accessed using the Tetteh Quarshie-Aburi road. The other road networks are well connected to the major road with the minor roads well connected to each other. Some of the popular towns within the municipality are Abokobi, Pantang, Teiman, Oyarifa, Agbogba, Kwabenaya and Ashongman.

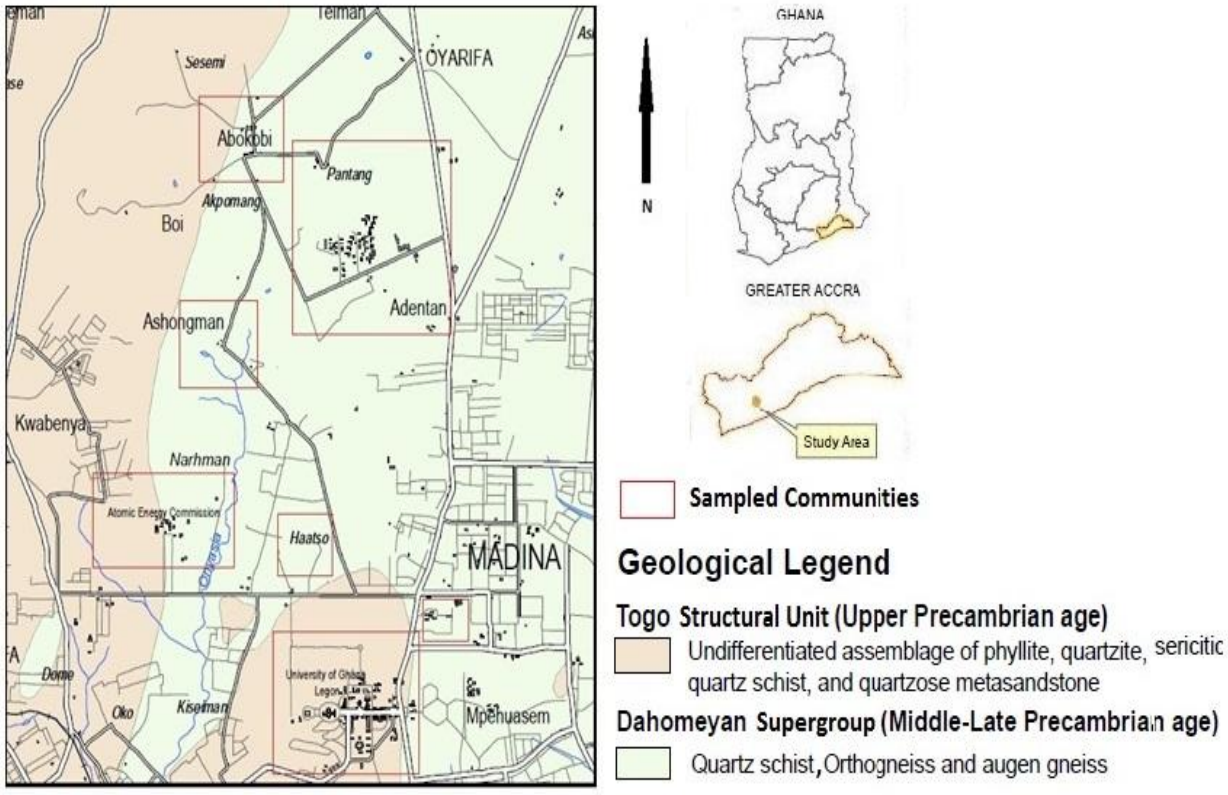

Figure 3.1: Sketched map of the study area indicating areas of sampling (after Anokwa et al., 2005). Not drawn to scale.

3.1.2 Vegetation

The vegetation of the area is the savannah zone type and it is occupied by grassland and clusters of shrub (Dickson and Benneh, 1998). Wetlands, dune vegetations, dense grass, palms and coconut are also found in the area with large trees like baobab trees sometimes found in the eastern lowlands with dense shrub land or thicket covers most of the Akwapim Range (Muff and Efa, 2006). The area is peri-urban and as such some people practice agriculture which is mostly backyard. Irrigated vegetable production is the most important type except areas like Abokobi, Teiman and Oyarifa where some farmers engage in cassava, maize and plantain farming (Ga East Municipal Report, 2006; Muff and Efa, 2006). Urban

agriculture plays a very important role in supplying food to support the economy and the ever growing population.

3.1.3 Climate

Much of the working area lies in the coastal savannah zone, which is the driest climatic zone in Ghana (Dickson and Benneh, 1998). Two rainy seasons are recognized: April to June, and mid-August to October, the first being the heaviest. Average annual rainfall is about 730 mm (Kortatsi and Jorgensen, 2001). The rainfall is usually intensive and short, this gives rise to local flooding where drainage channels are obstructed, or imperviousness of the urban soil and thus causes sheet floods which cannot be handled by the natural river system. The variation in temperature throughout the year is minimal. Mean monthly temperatures range from 24.7°C in August to 28°C in March, with an annual average of about 26.8°C (Kortatsi and Jorgensen, 2001).

3.1.4 Geology

The geology of the study area comprises largely of the Dahomeyan Structural Unit (Middle-Late Precambrian age) and the Togo Structural Unit (Upper Precambrian age) covering small portions around Legon and Kwabenya areas (Mani, 1978; Wright, 1985; Muff and Efa, 2006). In Ghana, the southeastern corner is occupied by the Dahomeyide with predominantly NE trending Structural Units (Kesse, 1985). It is more or less in fault contacts with the Voltain Supergroup and the Birimian Supergroup (Griffis et al., 2002). The local strike of rocks in the study area was found to be NE/SW from structural attitudes taken from the outcrops encountered during field survey.

The Togo Structural Unit refers to the structurally complex units of rocks along the border of Ghana and Togo and it can be traced further into northern Benin (Griffis et al., 2002). In Ghana, it is largely defined by the narrow, elongate Buem Structural Unit on the western margin and the Dahomeyan Structural Unit on the eastern margin which contains some high-grade metamorphic units, usually referred to as Dahomeyan metamorphics. The Togo Structural Unit marks the western limits of a very large area affected by the Pan-African thermotectonic event that peaked at about 600-550 Ma and whose effects extend right across Nigeria (Griffis et al., 2002). Studies by Koert (1910) and Crook (1970) have suggested that the Togo Structural Unit is younger than the Dahomeyan Structural Unit based on the occurrence of Dahomeyan gneisses within the Togo sediments. Mani (1978) and Blay (1991) suggested that the Dahomeyan Structural Unit is older than the Togo Structural Unit since the Togo occurs as outliers in the Dahomeyan.

The shape of the Togo Structural Unit is irregular, and it is a fault-bounded belt of metamorphic units that comprise the series of hills and ridges that start from west and north of Accra and extend along the Ghana-Togo border and into northern Benin where it is referred to as the Atakora Range (Kesse, 1985). The rock types found within the Togo Structural Unit are phyllite, quartzite, schist, and marble but are mainly described as being metamorphosed sediments (Robertson, 1925; Junner and Hirst, 1946; Grant, 1969).

The rocks of the Togo Structural Unit are highly deformed and metamorphosed, but the degree of metamorphism and deformation increases towards the southeast (Wright et al.,

1985). The current consensus is that the Togo Structural Unit correlates with the lower Bombouaka Group of the Voltaian Supergroup (Wright et al., 1985). Significant amount of groundwater is gained from boreholes if fracture openings in the Togo Structural Unit are wide and are not filled with impervious material. Borehole yields in the Togo Structural Unit ranges from 0.7–24 m^3/hr with an average of about 9.5m^3/hr (Agyekum, 2002). The overall, borehole success rate in the Togo Structural Unit is between 85 – 90% (WRI, 2001).

The Dahomeyan Structural Unit is located to the east of the Togo Structural Unit and it is generally a low-lying area normally referred to as the Accra plains (Attoh et al., 1997; Nyarku et al., 2011). The level of metamorphism is largely of amphibolite facies although there are areas of high-grade granulite facies with garnet, pyroxene, and scapolite. However, during the field work, observed rock outcrops were quartzo-feldspathic gneisses, which have been reported in literature as quartz-schist (Anokwa et al., 2005). The geological map of Ghana (Loh and Hirdes, 1996) distinguishes two broad belts of more mafic composition with an intervening zone of more felsic units. The typical rock lithologies include migmatites, gneisses, mica schists, amphibolites, syenites and granitoids (Agyei et al., 1987).

The age and nature of the Dahomeyan Structural Unit have always been a mystery (Griffis et al., 2002). The high degree of metamorphism of the Dahomeyan made early researchers (Koert, 1910) suggest that it is an old Archean basement. However, isotope and age dating gave a better understanding of the plate-tectonics, and revealed that the Dahomeyides were largely as a result of the Pan-African orogeny (Griffis et al., 2002). Some isotopic data suggests an inheritance from Kibaran (approximately 1000 Ma) and possibly Birimian

(approximately 2200 Ma) basement and contributions from older Archean (Liberian) crust cannot be excluded (Wright et al., 1985).

3.1.5 Water Supply in the Area

The water supply system in the municipality is mostly by Ghana Urban Water Limited (GUWL). Several individuals and institutions within the area have also drilled boreholes and hand dug wells as a result of lack of constant supply from the GUWL. The municipality has three small town water supply schemes which serve semi-rural areas, including Abokobi-Oyarifa-Teiman, Pantang area and Kweiman-Danfa water schemes.

The Abokobi-Oyarifa-Teiman water scheme serves about 10,750 people, Pantang area water scheme serves about 12,401 people and Kweiman-Danfa water scheme serves 5,400 people (Amfo-Otu et al., 2012). The three schemes cover about twenty-three communities within the municipality and all the three boreholes serving as the sources of supply are located in the valley of the Akwapim Ridge which falls within the Togo Structural Unit (Amfo-Otu et al., 2012).

3.2 ELECTRICAL RESISTIVITY SURVEY

Direct current survey was carried out at 35 different locations in the study area to determine the subsurface resistivity distribution. Different factors affect the resistivity in the subsurface, which include the presence of pore space and how they are interconnected, the degree of saturation, the presence of chemical salts in solution and temperature of the electrolyte (Telford et al., 1990).

The instrument used in measuring the earth's resistance was the single channel Scintrex Automated Resistivity Imaging System (SARIS) from Canada. Steel electrodes of 70 cm long and 20 cm wide with tapering were used. 3 mm-wide copper wires wound round reels were employed in the survey. Bearings were taken with the Konustar compass. Hammers, tape measures, clips and connectors were the other accessories utilized. The coordinates of the stations were picked and registered using a hand-held Garmin Etrex Geographical Position System (GPS), and metal pegs were planted at the stations for easy identification.

VES using the Schlumberger configuration was adopted to measure the earth's resistance to the flow of current injected because it is very fast and can be carried out with less number of personnel. The method employed involves two outside electrodes, and the resultant electrical potential is measured between two central electrodes (Fig 3.1). In the Schlumberger electrode arrangement, the central electrodes (MN) are kept relatively close together as compared to the separation of the outside current electrodes (AB). The distance between A and M is equal to the distance between N and B. The resistance readings at every VES point were automatically displayed on the digital readout screen and then written down on the field data sheet. In ensuring consistency and accuracy of the data, electrodes were hammered deep into the ground and two to three measurements at a particular station were made before moving to the next location. The data was plotted on the field sheet to monitor the trend of the curve to cross check readings with higher deviations in order to repeat such readings and make the appropriate corrections.

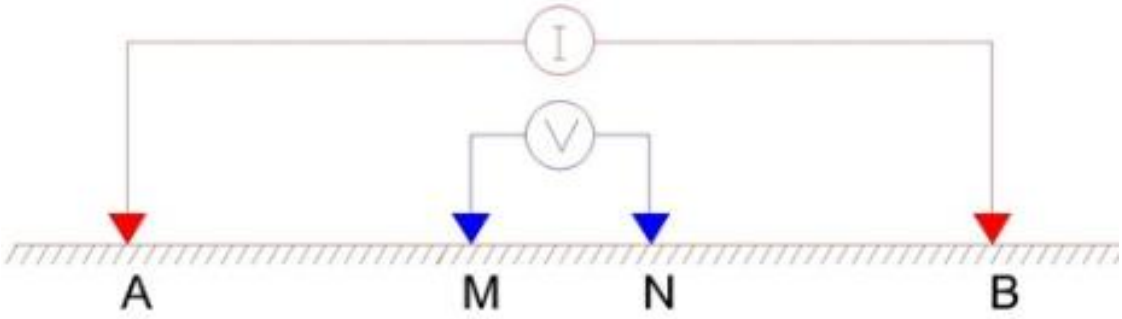

Figure 3.2: Electrode arrangement for the Schlumberger array electrode configuration.

The apparent resistivity ρα, of the bulk earth can be determined by the appropriate equations. The potential electrodes were kept fixed at 0.5 m away from the centre while the current electrode positions were varied at predetermined intervals. As the distance increased, the potential electrodes were expanded to 5 m and 25 m to cater for the expansion of the current electrodes. The distance as it increases laterally also increases the depth of current penetration into the subsurface (Fig 3.3).

As a quality control measure, series of measurements of resistivity were made by increasing the current electrode spacing in successive steps. The data of the 35 Schlumberger VES with a maximum of AB/2 = 500 m was obtained. The method of vertical exploration is known as the expanding electrode method or vertical electrical sounding (VES).

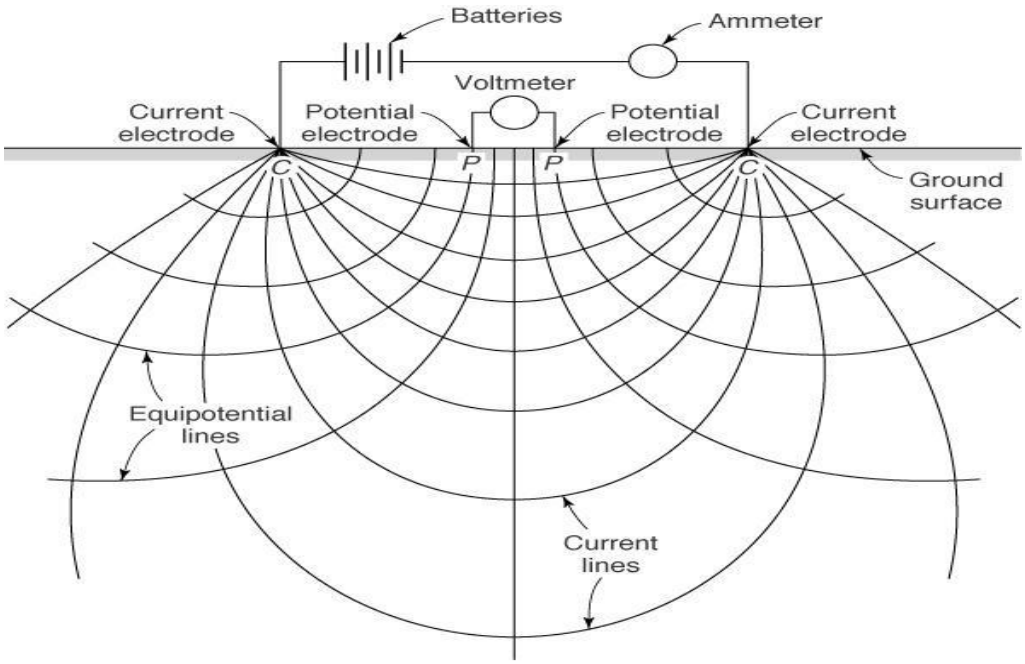

Figure 3.3: Schematic diagram illustrating basic concept of electrical resistivity measurement (Walton, 2010)

The apparent resistivity values obtained with increasing values of electrode separations were used to estimate the thickness and the true resistivities of the subsurface formations using IPI2WIN software. In the software, a bi–log plot was made with apparent resistivity on the ordinate axis and the current electrode spacing (AB/2) along the abscissa. The Schlumberger configuration was selected and an automatic iteration was adopted for data inversion. This then gave a model of how the subsurface resistivities vary with depth by matching the observed curve with a standard one. A correlation was then made with the resistivity and the lithology which aided interpretation of the VES results.

The models were constrained using the lithologies of the boreholes to give a real meaning to the curves in order to obtain the actual depths of investigations so as to match the layers.

The 35 VES carried out in the study area were situated at stations BAN 1 to BAN 35 (Fig 3.4). Sounding is best done along strike direction but settlements in the area permitted only about half of the VES in the strike direction. The station intervals were without specific intervals as the VES depended on borehole availability and space since it is more or less an urban geophysics with a lot of impediments.

3.2.1 Schlumberger Azimuthal Sounding

For the study area, one Schlumberger azimuthal sounding was done at the Pantang hospital which is more central in the study area. This was done to measure anisotropy caused by near-vertical dipping structure resulting from fracture or bedding plane. Following the regular Schlumberger array configuration, a minimum current electrode spacing of approximately 1.6 m and a maximum of 100 m was used. The rotation was done at 10 degrees intervals to cover the entire 360 degree rotation. Using a similar Schlumberger array configuration as indicated earlier, the current electrodes were expanded up to a length of $^{AB}/_{2} =$ 100 meters.

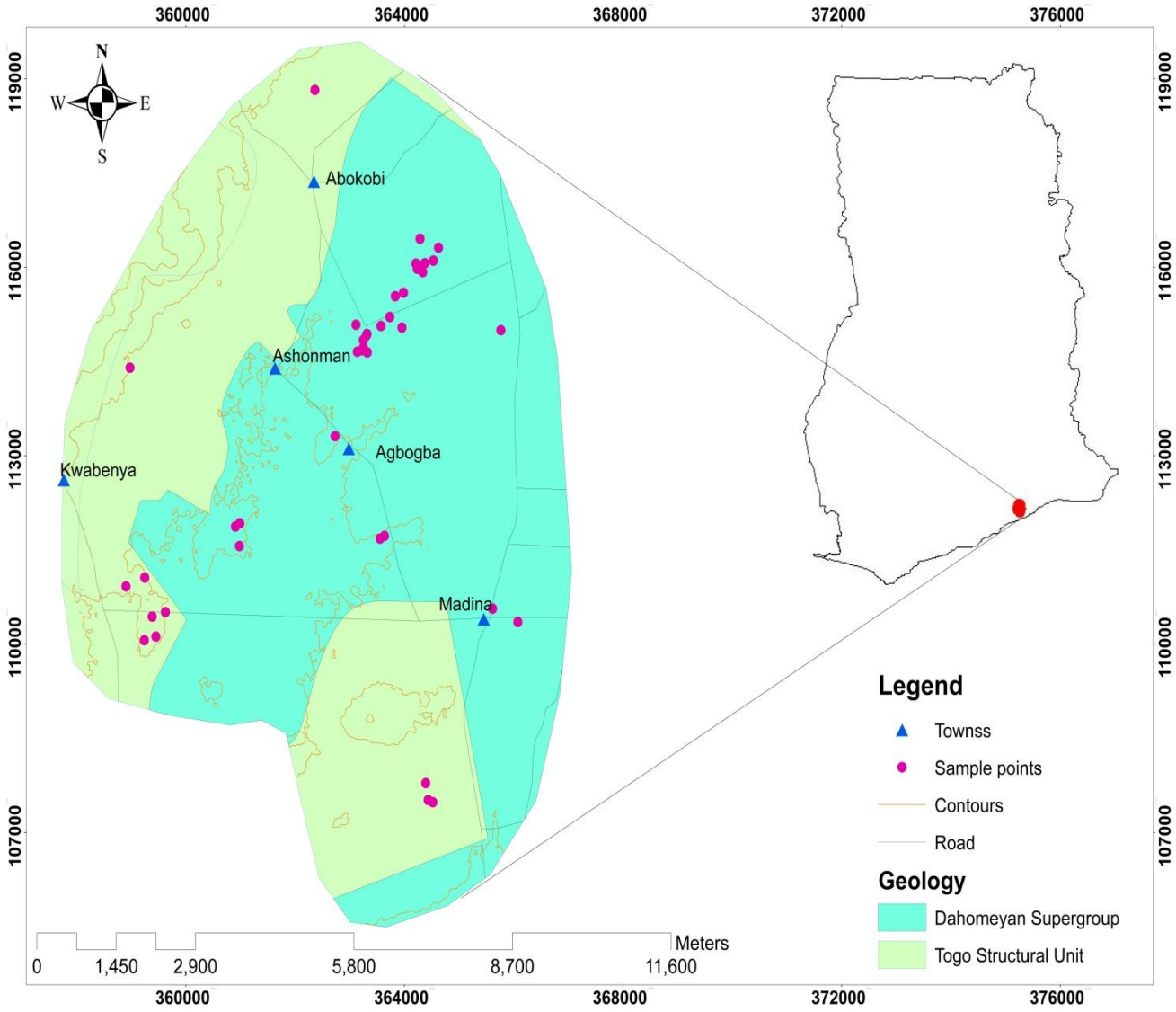

Figure 3.4: VES stations and sampling points in the study area

3.3 WATER SAMPLE COLLECTION AND ANALYSIS

Collection of water samples was done in January and February, 2015. Water samples were taken from different source which includes drilled boreholes and hand dug wells within the study area. The total number of samples taken was 80, but the sampling point was 40 which implies that two samples were taken from each sampling point; one for physico-chemical analysis and the other one for the trace metals analysis. For the purpose of this research,

samples were taken from sites where vertical electrical soundings were carried out except for five locations where VES were not possible. The space required for the geophysical survey limited the water sampling to boreholes and hand dug wells where the VES were carried out and therefore the spatial distribution of the sampling points may not be evenly distributed.

The water samples collected were analysed for temperature, pH, conductivity, total dissolved solids (TDS), calcium (Ca^{2+}), magnesium (Mg^{2+}), sodium (Na^{+}), potassium (K^{+}), bicarbonate (HCO_3^{-}), chloride (Cl^{-}), Fluoride (F^{-}), sulphate (SO_4^{2-}), Alkalinity (OH^{-}), Phosphate (PO_4^{2-}), and nitrate (NO^{3-}). The trace metals analysed include, Lead (Pb), Manganese (Mn), Zinc (Zn), Iron (Fe), Cobalt (Co), Nickel (Ni) and Cromium (Cr).

The samples were taken following standard protocols described by USGS (2006) and Duncan et al. (2007). At each sampling point, purging was done for a minimum of 10 minutes to flush out the stagnant water retained in the pipes. The purpose of the purging was to ensure that stale and stagnant water was not sampled.

A potable EC meter (HachSension 5) was used to measure some field parameters like total dissolved solids, electrical conductivity and potable pH meter (Hach Sension 1) was also used to measure the pH. 500 m/L pre-sterilized polyethylene bottles were used in collecting the samples at each location point. Few drops of nitric acid (10% by volume) were added immediately to the samples labeled cations for digestion in the laboratory. Samples were kept under safe conditions, the filled bottles labeled anion and cation were all stored in an ice chest with ice of temperatures below 4°C.

The samples were prepared and made ready for the National Nuclear Research Institute (NNRI) of the Ghana Atomic Energy Commission's chemistry laboratory and stored at temperature below 4^{o}C until they were all analyzed.

At the laboratory, the water samples were filtered with a white 0.45 µm membrane placed in a filter holder. HCO_3^- determination was carried out in the laboratory using double-indicator titration of 25 ml sample against 0.01M HCl, with phenolphthalein and methyl orange as the indicator as described by Eaton et al., (2005).

The Sodium and potassium were analyzed using Flame Emission Photometer (Sherwood Model 420). The amount of potassium in the water samples was determined in a direct-reading type of flame photometer at a wavelength of 766.5 nm whilst the concentrations of sodium were determined at a wavelength of 589 nm. Fluoride (F^-) concentrations were obtained with the use of Hach Colorimeter (DR/890) (Franson et al., 1995).

The following anions, NO_3^-, PO_4^{3-} and SO_4^{2-} were analysed using Brucine reagent, Ascorbic Acid, Turbidimetric methods and Ultra Violet Spectrometer (UV- 1201) respectively. Mg^{2+} and Ca^{2+} were analyzed using digestion, followed by atomic spectrometry using the AA240S Fast Sequential Atomic Absorption Spectrometer (Franson et al., 1995; Sood et al., 2004; Eaton et al., 2005).

For magnesium, 1mol of the sample was pipette into a test tube and 9 ml of lanthanum solution added as a suppressant to dissolve the magnesium ions in solution. The magnesium ions were then analyzed using the AAS. To digest the water sample to determine the concentration of calcium, 5 ml of raw water sample was pipette into a Teflon bomb or beaker in three replicate. 6 ml of 65% of concentrated HNO_3^- was added to dissolve the metal in solution, 3 ml of 35% HCl and 0.25% or five drops of H_2O_2 which served as a catalyst was added to each vessel containing the sample. The beakers were swirled gently to mix well and fitted vertically into the microwave digester and digested for 20 minutes. After digestion, the solution containing the sample was allowed to cool in water bath for 20 minutes to reduce high temperature and pressure build-up within the vessels. The mixture was then transferred into volumetric flask and diluted to 20 ml using deionised water. After the digestion process, the solutions were transferred into test tubes and ready for the analysis.

To ensure quality control and quality assurance, the charge balance error (CBE), is usually calculated to check on the accuracy of the analysis using the relation;

$$CBE = \frac{\sum zxm_c - \sum zxm_a}{\sum zxm_c + \sum zxm_a} x100\% \qquad (3.1)$$

where z and m are respectively the valence and molality of the ion. For a fairly accurate or balanced analysis, the CBE should not exceed 5%. The concentrations of the major anions and the major cations obtained from the hydrochemical analysis were inputted in excel and converted from milligram per litres to milliequivalent. Following the CBE, the electrical balance which fell beyond 5% were not include in the results and discussion.

CHAPTER FOUR

RESULTS AND DISCUSSION

4.1 ELECTRICAL RESISTIVITY RESULTS AND CORRELATION WITH HYDROCHEMICAL ANALYSIS

The application of the direct current electrical resistivity in the study was to assist in the investigation of groundwater contamination in the area. Vertical electrical sounding curves were analysed and interpreted quantitatively to indicate the various layers and the depth of the layers with their respective thicknesses and resistivities.

The borehole logs acquired for some of the boreholes (40% of the boreholes) provided the number of layers, thicknesses and depth of the subsurface which were used to constrain the resistivity models in order to enhance the interpretation. The root mean square (RMS) error obtained from the VES models were generally lower than 10%. Only 2 of the models had RMS greater than 10% with the highest among them being 13.9%. This may have occurred as a result of high lateral variations existing within the surface, an example may be the variation between the material on top of the dump site and the nearby ones (Porsani et al., 2004).

From this study, 8 different resistivity sounding curve types were determine from the VES result as presented in (Fig. 4.1), with their percentage and spatial distribution shown. For the three layers, only the Q-type curve was missing in the study area whiles three out of the eight of the four-layer geoelectric sections (QQ, AK, KQ) were not obtained in the study area. In

total, 11 VES models had three layers whiles 24 VES models were represented by four layers.

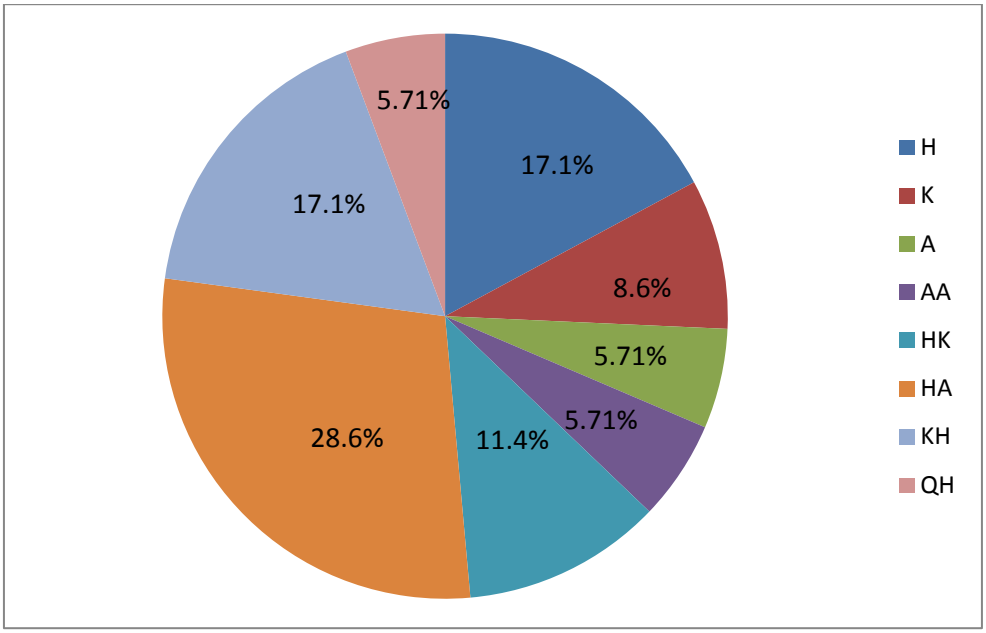

Figure 4.1: Distribution of curve types in the study area

4.1.2 Results of the Schlumberger Azimuthal Sounding

The polar plots for the current electrodes 1.58, 1.99, 2.51, 3.16, 10, 12.5, 15.8, 19.9 and 25.1 meters showed prominent northeast-southwest trends (Fig. 4.2) while the 6.31 m current electrode expansion showed a slight northwest-southeast direction (Fig. 4.3). The 50.1 and the 79.4 m current electrode spacing gave plots that shows an east-west trend.

The occurrence of lobes and ellipses in the polar plots show that that the subsurface at the area of investigation is anisotropic and this is resultant from heterogeneities within the subsurface. The heterogeneity may be attributed to different lithologies or discontinuities in the rocks at the subsurface.

From the polar plots in the Figures, it can be inferred that that the major fracture direction is the northeast-southwest trending one whereas the minor ones are in the east-west and the northwest – southeast directions. The effect of the presence of more than one fracture set can be linked to the ground water system as they tend to be more source flow directions.

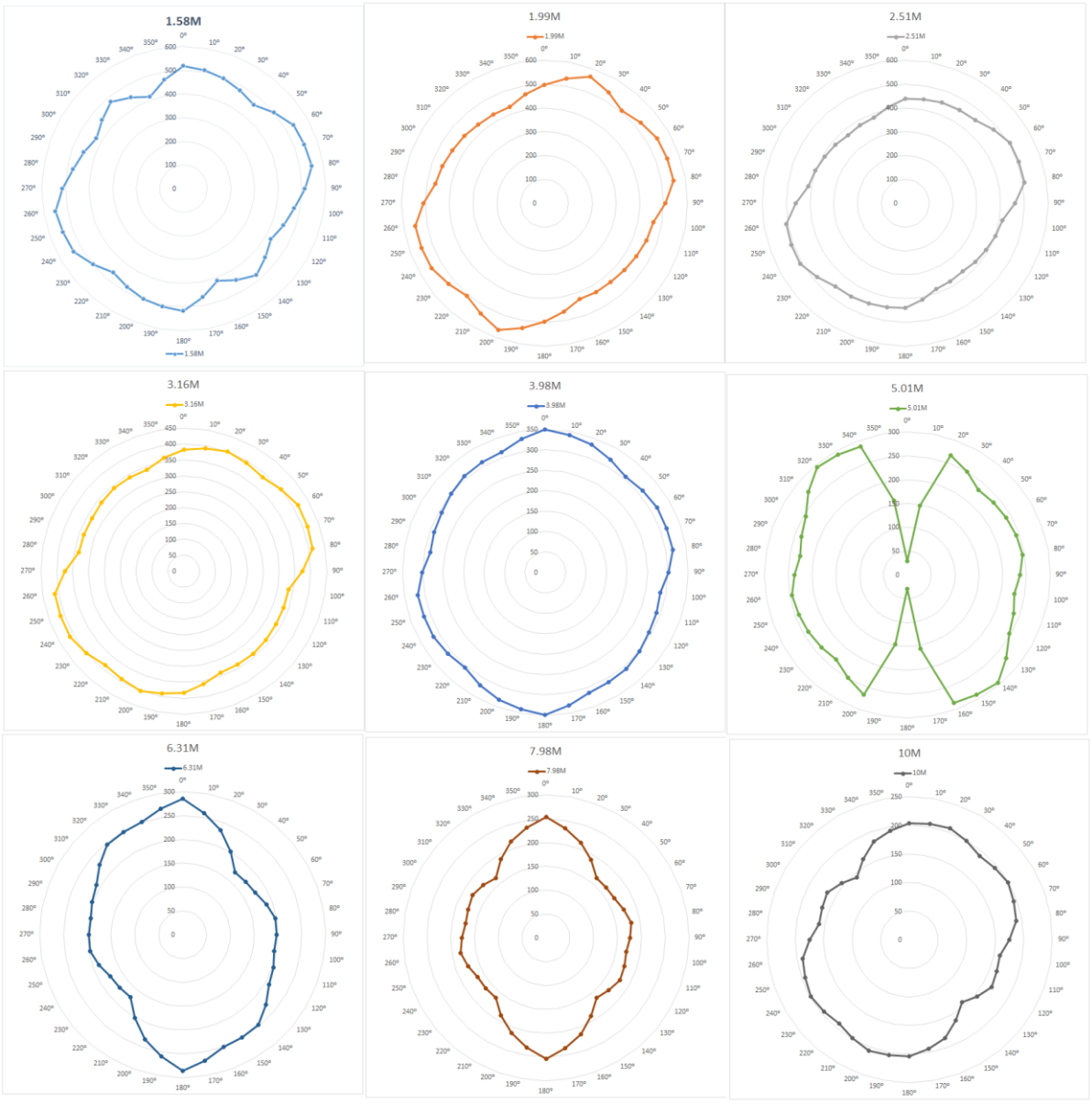

Figure 4.2: Schlumberger azimuthal array results 1

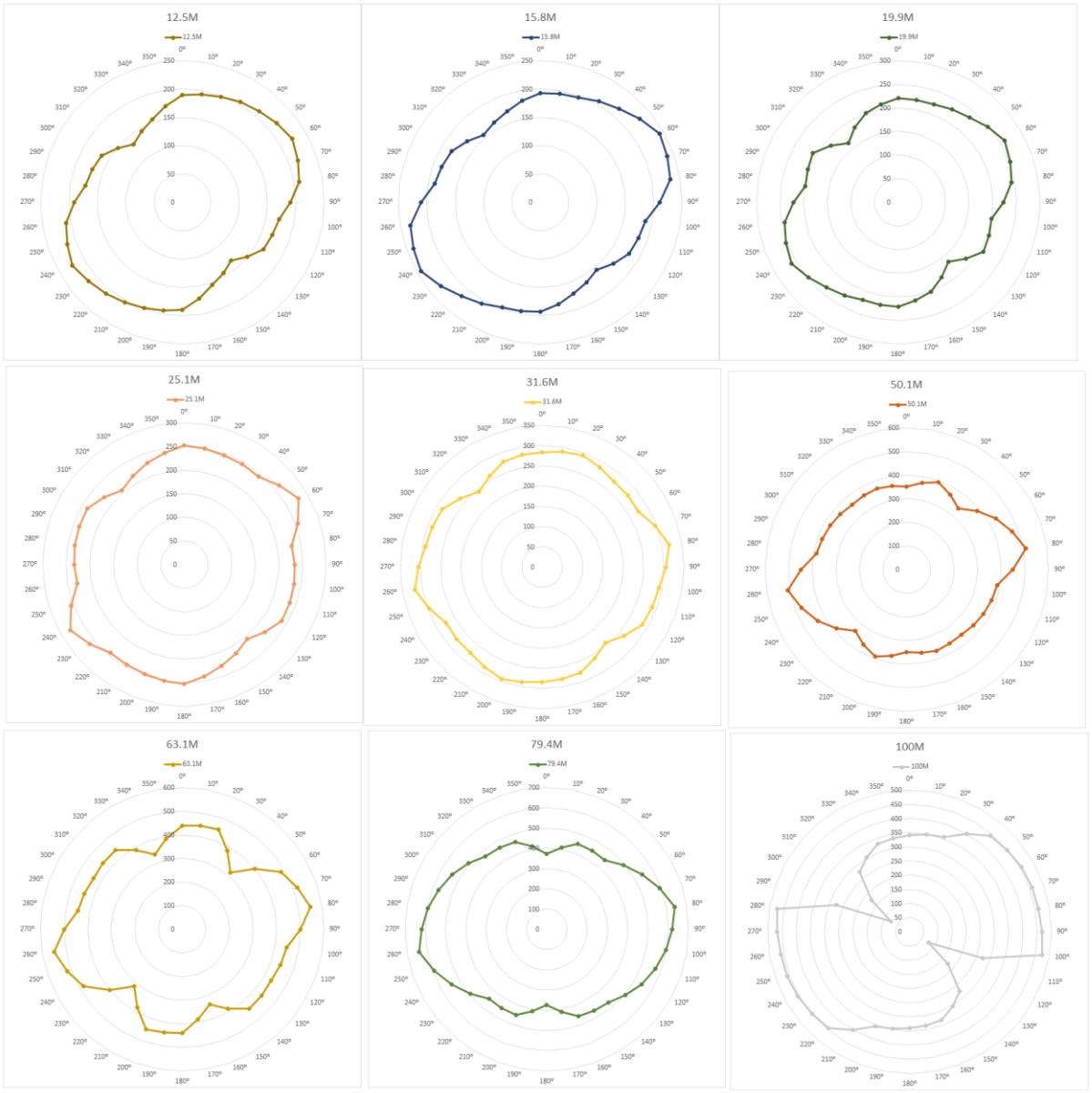

Figure 4.3: Schlumberger azimuthal array results 2

Table 4.1: Summary of some borehole logs within the study area obtained from GAEC and HEISA Engineering Ltd. depicting the general trend.

Depth Range(m)	Geological Formation
0 to 9	Laterite
9 to 38	moderate to highly weathered quartzite/phyllite
38 to 60	moderately weathered quartzite/phyllite
60 to 85	low weathered to fresh quartzite/ phyllite

For a better assessment, the study area was sub-divided into four 4 sections,

- The Pantang dump site area
- The Pantang hospital area
- Ghana Atomic Energy Commission (GAEC) area
- University of Ghana, Legon area

4.2 VES RESULTS AND THE HYDROGEOCHEMICAL ANALYSIS AT THE PANTANG DUMP SITE AREA

At the Pantang dump site, 7 of the VES points were sited very close to the dump site and 4 of the points located farther away from the dump site to observe possible migration of the contaminant and also draw a comparison between the results of the hand dug wells closer and those further away from the dump site. The results of the VES models and the physico-chemical parameters at the dump site are discussed under this section. The hand dug wells closer to the dump site are represented by BAN 1 to BAN 5 and BAN 8 and BAN 9 whiles the four distant from the dump site are represented by BAN 6 and 7 and BAN 10 and BAN 11.

The resistivity signatures for the top geoelectric layers were very low compared to that of the second layer at the stations closer to the dumpsite. In an open dump, different kinds of waste are discarded haphazardly such that it is not in any particular order. These wastes ranges from chemical, biological, organic and inorganic wastes. With time, the components of these waste substances found at the dump site deteriorate and undergoes several changes and reactions. At dump sites, carbon based acids may be produced under certain conditions when water comes into contact with carbon dioxide.

Heavy metals that are also discarded such as metal scraps usually found at dump sites subsequently come into contact with the acid produced and increases the electrical conductivity of the medium which eventually contaminates the groundwater (Schneider, 1978). From the field and laboratory analysis, the conductivity of the water samples at the dump site were found to be higher as compared to the VES stations farther away from the dump site.

Lower resistivity of (<20 Ωm) when noted indicates groundwater contamination in the absence of clay minerals and shallow water table with saturated regolith (Barker et al., 2001). Figures 4.4 and 4.5 are typical resistivity models obtained from the stations BAN 5 and BAN 8, both closer to the dump site whiles the Figures 4.6 and 4.7 (BAN 6 and BAN 7) are VES models obtained from two of the four wells further away from the Pantang dump site. The models reveals four geoelectric layers with relatively lower resistivities at the first and second layers.

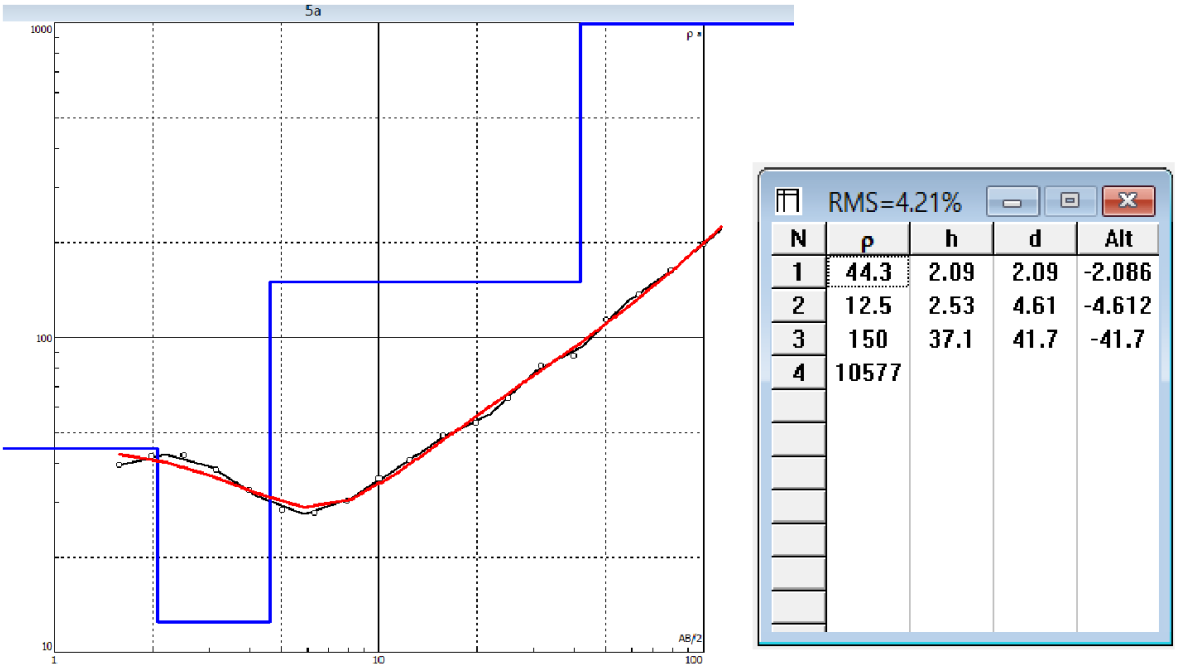

Figure 4.4: Sounding curve at BAN 5

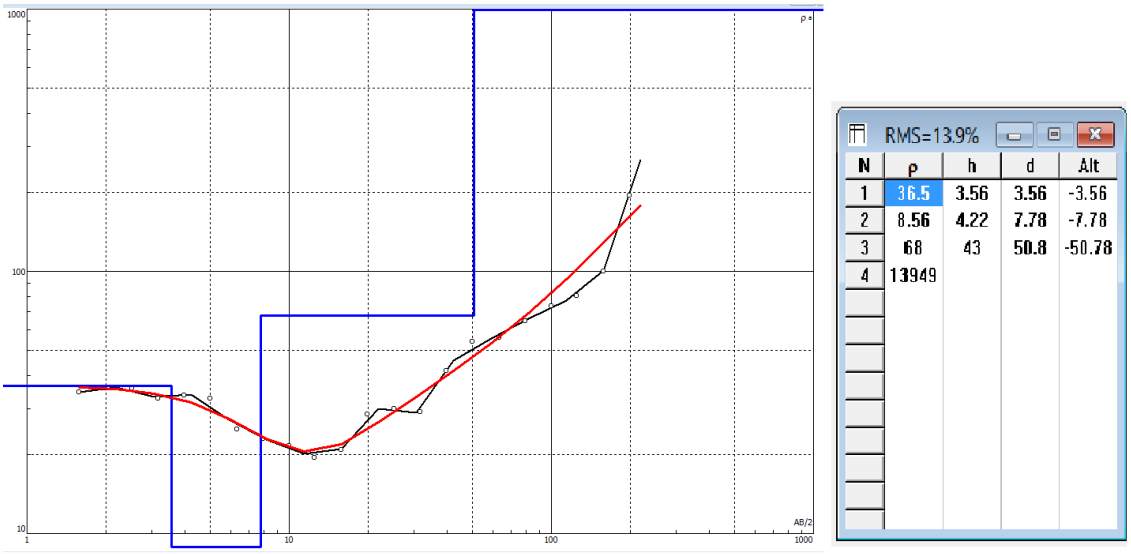

Figure 4.5: Sounding curve at BAN 8

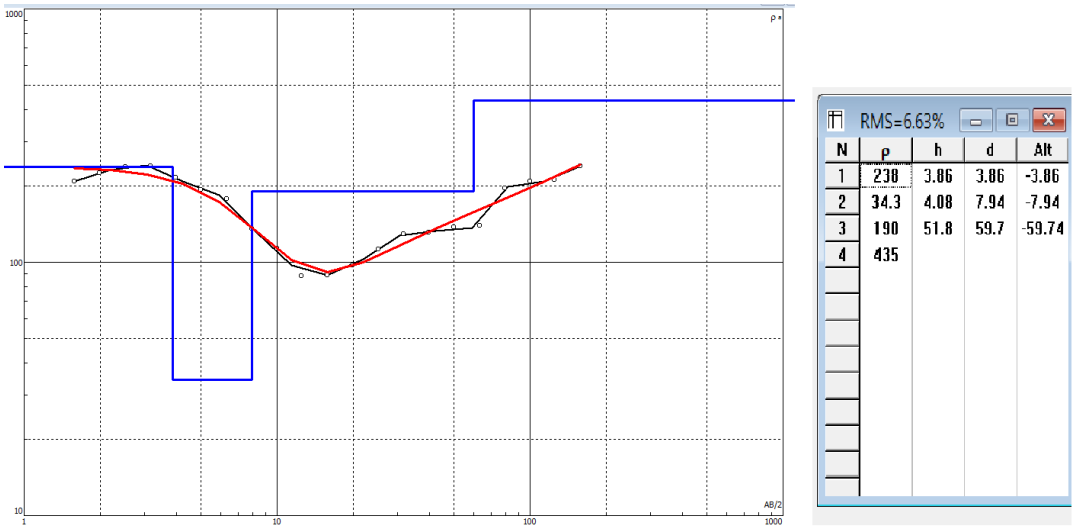

Figure 4.6: Sounding curve at BAN 6

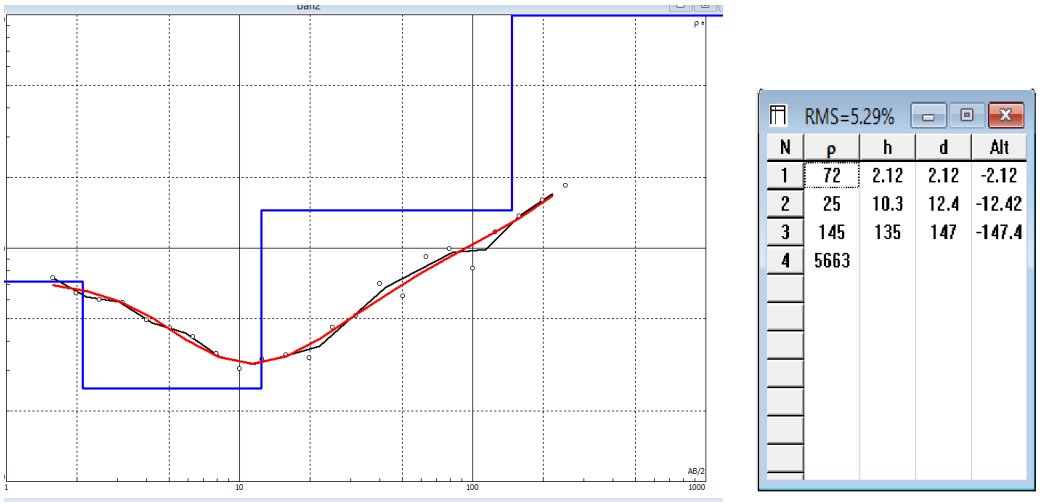

Figure 4.7: Sounding curve at BAN 7

The pH of the water samples around the dump site are generally low, and falls within the acid range that may contribute to release of the carbon based acids from the reactions with

carbon dioxide as $CO_2 + H_2O \rightarrow H_2CO_3$. The concentration of chloride ranges from 212 to 520 mg/L at the dump site and it also has higher concentrations at the four wells further away from the dump site. In this study, chloride concentration was found to be one of the major inorganic anions in the water and as such the low resistive subsurface might be as a result of contribution from elevated concentrations of chloride as it is very conductive (Yadav et al., 2015). Although chloride is not noted to have any serious human health implications, the WHO has a limit of 250 mg/L acceptable in portable water.

From Table 4.2, 4 of the wells (BAN 1 - BAN 4) out of the eleven in the Pantang dump site area recorded high iron content and could be from the disposal of heavy metals. Lead (Pb) concentrations detected at the hand dug wells from the dump site were all higher than the (WHO, 2004) standards except BAN 7 and BAN 9 to BAN 11. These could be coming from car batteries disposed at the dump site (Achampong et al., 2013). The leachate plume at the dump site can also be credited with the presence of manganese and this was evident in the water sampled from the wells at the dump site. Four of the wells closer to the dump site (BAN 2 to BAN 5) recorded Mn concentrations higher than the WHO permissible limit of 0.5 mg/L whiles all of the four farther away from the dump site recorded less Mn concentrations.

Table 4.2: Physico-chemical results of hand dug wells at the Pantang dump site area

Station	Cl(mg/L)	PH	EC(µS/cm)	TDS(mg/L)	Fe(mg/L)	Mn(mg/L)	Pb(mg/L)
BAN1	212	5.70	3998	1996	0.2580	0.0254	0.190
BAN2	256	4.48	1546	775	0.4217	0.5421	0.214
BAN3	412	6.13	1815	898	0.8624	0.6125	0.020
BAN4	257	5.31	2217	1109	0.3713	0.5841	0.018
BAN5	263	6.05	1451	729	0.1389	0.8762	0.081
BAN6	240	4.44	897	449	0.1333	nd	0.015
BAN7	257	5.28	1144	593	0.1020	nd	0.008
BAN8	425	4.80	3999	2000	0.1388	0.013	0.018
BAN9	312	6.12	1790	895	0.0548	0.015	0.005
BAN10	520	3.93	3999	2000	0.0750	0.089	0.005
BAN11	170	5.76	393	193	0.0870	0.019	0.006
WHO	**250**	**6.5-8.5**	**1500**	**500**	**0.3**	**0.5**	**0.01**

The VES models obtained from the IPI2WIN software at the Pantang dump site area are characterized by the following curve types, two AA-type, two of the K-type and one each of the A-type, HK and HA types. Four of the curves that represented the VES farther away from the dump site exhibited HA-type of curves throughout. From Table 4.3, the descriptive statistics of the resistivity, thickness and depth of the model shows that the maximum depth penetrated by the current was 147 m and occurred at the station BAN 2.

Table 4.3: Descriptive statistics of the VES results at the Pantang dump site area

Parameters	Number	Range	Minimum	Maximum	Mean	Std. Deviation
ρ1 (Ωm)	12	229	9	238	72	77
ρ2 (Ωm)	12	1238	6	1244	201	373
ρ3 (Ωm)	12	1697	68	1765	373	477
ρ4 (Ωm)	9	13939	10	13949	5604	5599
h1 (m)	12	5	1	6	2.50	1.68
h2 (m)	12	36	2	38	10.83	11.13
h 3 (m)	9	134	1	135	57.78	45.60
Depth (m)	9	132	15	147	67.22	45.60

4.2.1 Results from Resistivity Pseudo-Section at the Pantang Dump Site Area

Pseudo cross-sections and resistivity sections were generated from the VES models obtained from the dump site to provide a clear image of the spatial distribution of the leachate plume (Fig. 4.8). From the pseudo cross-section, it shows a very low resistivity zone (13.3 Ωm to 23.7 Ωm) from AB/2 spacing of 3.7 m extending vertically at VES BAN 3 and extends laterally towards VES BAN 2. It is characterised by the colour black and depicted by a dip in contour. This zone is resulting from the contaminants from the leachate deposited on top of the soil at the dump site.

The point indicated by VES BAN 3 with the colour black shows that the location is polluted and perhaps a lot of the waste are disposed of at that location, or the waste accumulates and leaches down the station. It can be observed from the pseudo-section that AB/2 spacing range of 5.18 m - 19.3 m indicated by blue, green and the yellow colour scale is the water bearing zone. The water table at the dump site is on the average of 2.3 m (Achampong et al., 2013 and references therein).

The resistivity cross-section shows that all the resistivity values of the second layer are also lower and gives an indication of groundwater contamination resulting from the dump site. The selection of sounding stations for cross sections were based on closeness to each other along the survey line and the availability of enough space to carry out the survey.

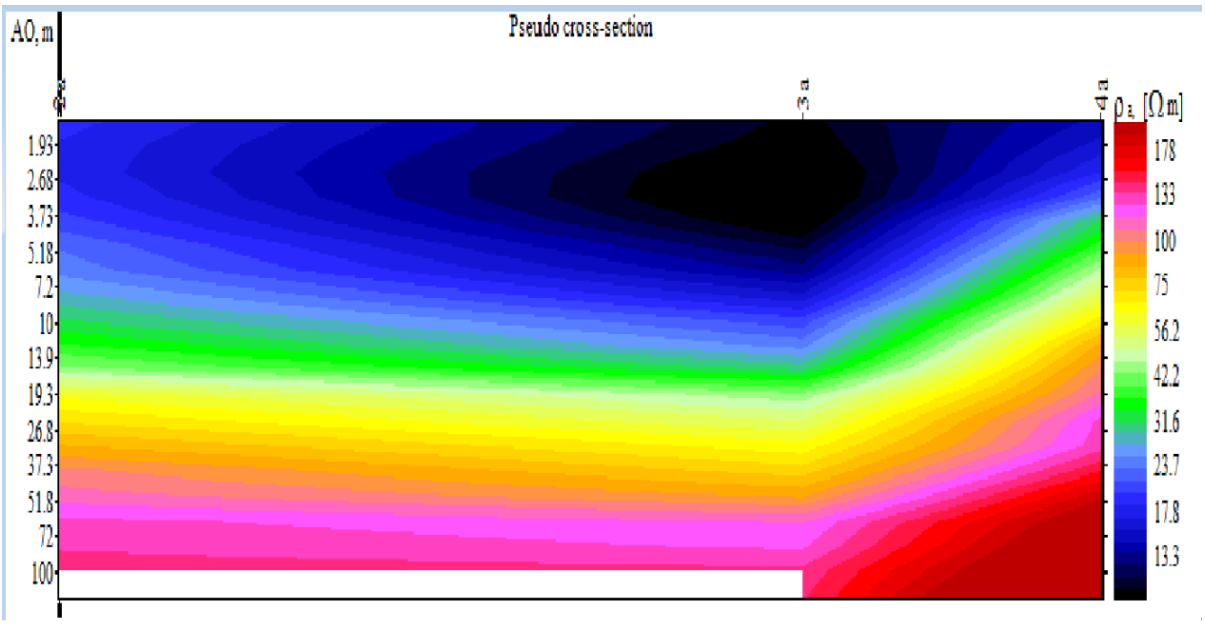

Figure 4.8: Pseudo cross-section of VES BAN 2 - BAN 4

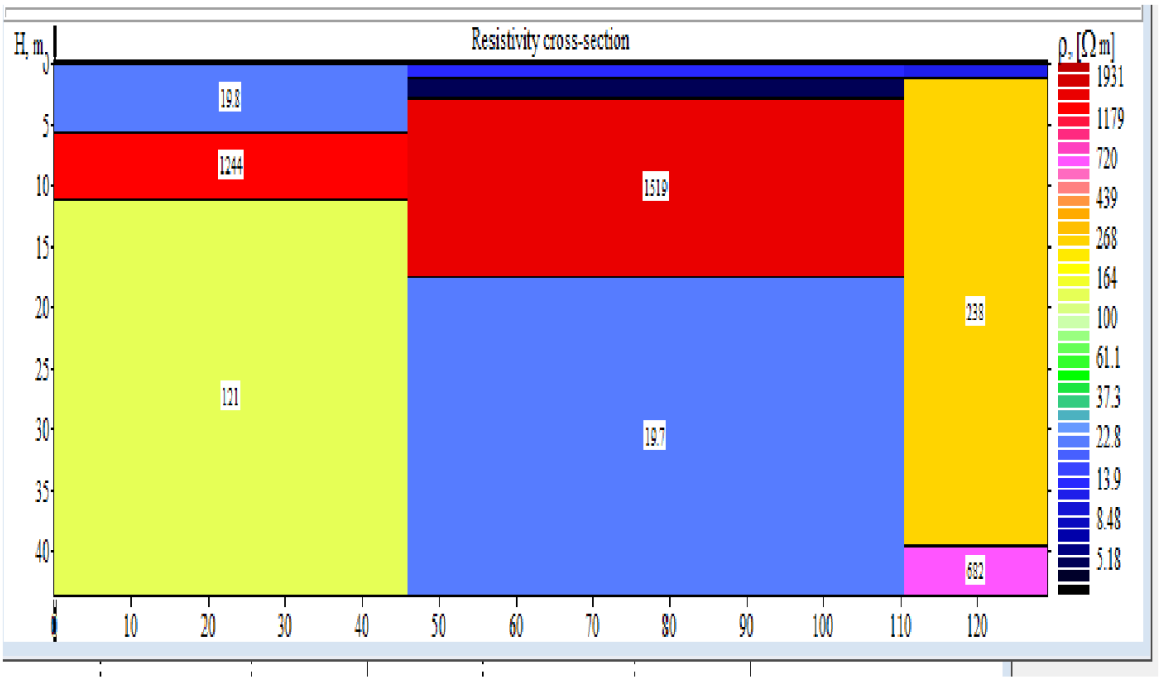

Figure 4.9: Resistivity cross section of VES BAN 2 - BAN 4

4.3 VES RESULTS AND THE HYDROGEOCHEMICAL ANALYSIS AT THE PANTANG HOSPITAL AREA

At the Pantang hospital area, eight of the VES were carried out at eight borehole locations. Generally, the resistivity models in the Pantang hospital area gave relatively low resistivity values and suggestive of the fact that the terrain have more weathered rocks and fractured zones with enough pore spaces. The study area is underlain by the Dahomeyan Structural Unit with the rocks being inherently impermeable with groundwater occurrence controlled basically by the development of secondary porosities such as fractures, faults, joints and the associated weathered zone. The acid gneisses weather to slightly permeable calcareous clay whiles the quartzites and phyllites weather to sandy clay (Kortatsi and Jorgensen, 2001).

The entire Pantang hospital area revealed four geoelectric layers by the models (e.g., Fig 4.10 and 4.11). The low resistivities shown in this region suggests that the fairly weathered bedrock could be a potential zone for groundwater accumulation with high conductivity since the borehole log (Table 4.1) in the area showed the water bearing zone to be within 33 m to 65 m. The very low resistivity of 4.81 Ωm at the third layer of BAN 28 with total depth of investigation revealed as 4.91 m which suggest that depth of investigation is contaminated as the particular station is an old dump site and a gutter upstream that runs down may have leached into the subsurface to contaminate the zone without necessarily getting to the groundwater (Ga East Municipal Report, 2006).

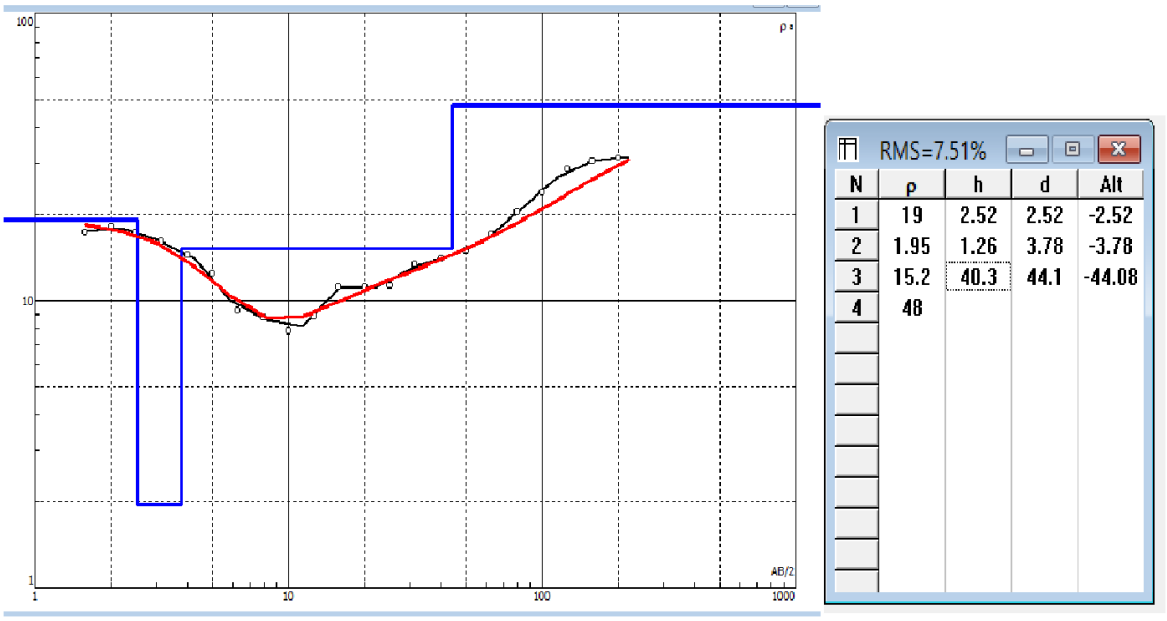

Figure 4.10: Sounding curve at BAN22

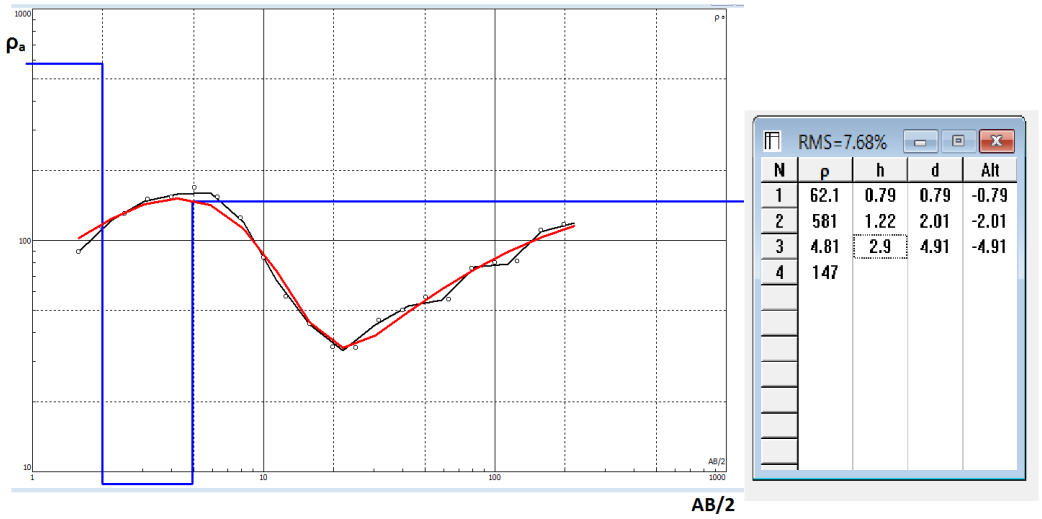

Figure 4.11: Sounding curve at BAN 28

The low value of resistivity is also likely to be a contribution from the TDS. The electrical conductivity measured when water samples were taken from six of the boreholes at the

hospital area recorded conductivities higher than the WHO permissible limit of 1500 µS/cm, except for BAN 31 and BAN 32.

The Fe concentrations were higher than the WHO permissible limits in two of the boreholes at (BAN 22 and 28). The high iron content in the area can be a contributory factor to the low resistivity signatures that were picked by the VES, since dissolved irons in water increases its conductivity. The presence of iron in the aquifers might be as a result of some weathered rocks in the subsurface. Pb and Mn concentrations were only elevated at BAN 22 and 26 respectively. Again, the pH of BAN 31 and BAN 32 and also BAN 23 were very low as indicated in Table 4.4.

Table 4.4: Physico-chemical analysis of hand dug wells at the Pantang hospital area

Station	Cl(mg/L)	PH	EC(µS/cm)	TDS(mg/L)	Fe(mg/L)	Mn(mg/L)	Pb(mg/L)
BAN22	231	7.05	1687	846	0.454	0.356	0.076
BAN23	251	3.02	2806	1406	0.111	0.489	0.008
BAN24	218	6.58	1890	943	0.058	0.043	0.005
BAN26	246	7.40	1640	820	0.138	0.504	0.009
BAN27	220	7.10	1581	801	0.119	0.389	0.008
BAN28	275	7.40	1592	795	0.521	0.368	0.006
BAN31	200	5.45	343	171	0.014	0.030	0.005
BAN32	130	4.91	762	380	0.060	0.002	0.008
WHO	**250**	**6.5-8.5**	**1500**	**500**	**0.3**	**0.5**	**0.01**

The results of the VES interpretation suggest that four layers exist at this sub-section and the maximum depth obtained from the VES result was 91 m occurring at station BAN 26 and a minimum depth of 5 m occurring at station BAN 32. The least resistivity value was recorded at the second layer of BAN 22 whiles the highest resistivity encountered was 5269 Ωm of the

third layer at BAN 24. The Pantang hospital area is dominated by the HA type of curve representing 50% of the curve types whiles KH and HK represented 25% each.

Table 4.5: Descriptive statistics of the VES results at the Pantang hospital area

Parameters	Number	Range	Minimum	Maximum	Mean	Std. Deviation
ρ1 (Ωm)	8	412	12	424	116	139
ρ2 (Ωm)	8	579	2	581	114	191
ρ3 (Ωm)	8	1676	5	1681	364	619
ρ4 (Ωm)	8	5258	11	5269	1074	1809
h1 (m)	8	7	1	8	2.88	2.36
h2 (m)	8	23	1	24	6.88	8.71
h 3 (m)	8	87	3	90	43.75	29.92
Depth (m)	8	86	5	91	53.38	30.55

4.4 VES RESULTS AND THE HYDROGEOCHEMICAL ANALYSIS AT THE GAEC AREA

A total of 10 vertical electrical soundings were performed at the GAEC area. Two of the boreholes (BAN 15 and BAN 30) had faulty pumps and therefore the water could not be sampled. The analysis indicates that six of the models revealed three geoelectric layers whiles four shows four layers. Three (BAN 20, 21 and 25) out of the eight boreholes recorded high EC concentrations beyond the WHO standards (Table 4.6).

Fe and Pb concentrations were beyond the acceptable limits at stations BAN 16 and from BAN 18 - 20. whiles Mn concentrations were generally okay except for BAN 25 which is beyond the limit. The GAEC area is characterized by four of the H-type curves, and one each of the A, K, HA, HK, KH and QH-type. The minimum and the maximum depth of investigation was found to be 16 m and 110 m respectively with an average depth of 52.5 m as shown in Table 4.7.

Table 4.6: Physico-chemical analysis of boreholes at the GAEC area

Station	Cl(mg/L)	PH	EC(µS/cm)	TDS(mg/L)	Fe(mg/L)	Pb(mg/L)	Mn(mg/L)
BAN 16	268	6.26	1484	739	0.701	0.028	0.108
BAN 17	125	6.11	1370	683	0.067	0.008	0.318
BAN 18	120	6.09	405	197	2.671	0.158	0.024
BAN 19	213	5.87	303	150	0.667	0.026	0.192
BAN 20	325	6.76	3999	2000	1.949	0.152	0.425
BAN 21	456	7.22	2215	1107	0.060	0.005	0.002
BAN 25	230	7.36	1556	777	0.068	0.008	0.512
BAN 29	281	7.08	1207	602	0.049	0.002	0.003
WHO	**250**	**6.5-8.5**	**1500**	**500**	**0.3**	**0.01**	**0.5**

Table 4.7: Descriptive statistics of the VES results at the GAEC area

Parameters	Number	Range	Minimum	Maximum	Mean	Std. Deviation
ρ1 (Ωm)	10	830	40	870	288	278
ρ2 (Ωm)	10	6046	12	6058	760	1890
ρ3 (Ωm)	10	5022	23	5045	1189	1794
ρ4 (Ωm)	4	797	130	927	357	382
h1 (m)	10	3	1	4	2.40	0.96
h2 (m)	10	38	2	40	15.30	11.57
h 3 (m)	4	92	7	99	43.75	39
Depth (m)	4	94	16	110	52.50	41

4.4.1 VES at Station BAN 20

The geological section at BAN 20 shown by Figure 4.12 indicates three layers with resistivity range of 17.2 Ωm to 5045 Ωm making a very sharp contrast. The resistivity of the second layer is the lowest recorded as 17.2 Ωm at a thickness of 25.5m. The high salinity of the water at this level measured might account for the low resistivity value at this point and subsequently making the subsurface very conductive. The electrical conductivity measured at this station was as high as 3999 µS/cm therefore correlating with the VES model and suggestive of groundwater contamination. This very borehole has been left undeveloped after

drilling as the physico-chemical parameters (Table 4.6) measured were so high that the water was found to be unsuitable for use.

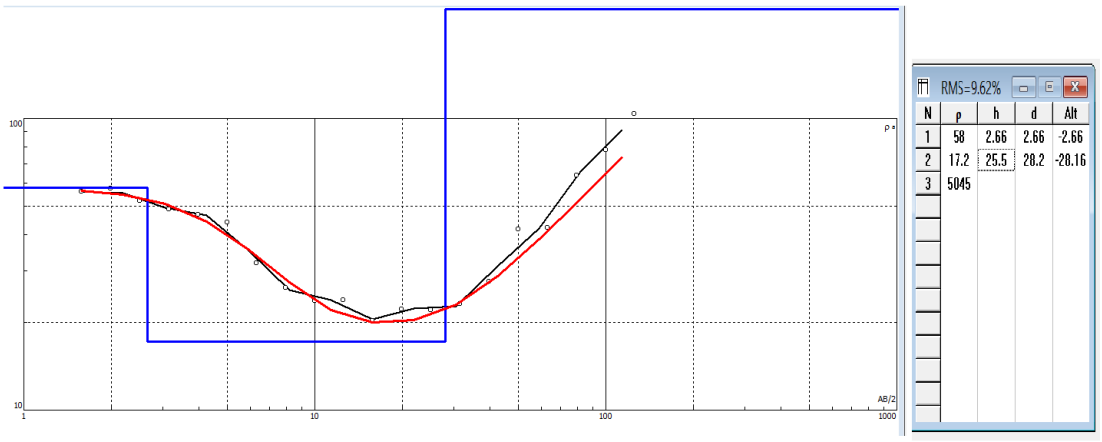

Figure 4.12: Sounding curve at BAN 20

4.4.2 VES Station at BAN 21

The curve analysis at station BAN 21 revealed a three geoelectric layered structure shown in Figure 4.13. The resistivity values ranged between 26.6 Ωm and 533 Ωm. The second layer recorded the lowest resistivity of 26.6 Ωm within a thickness of 23.2m. The low resistivity value at this depth correlates well with the depth within which the groundwater was encountered and the high EC value of 2215 µS/cm coupled with a very high chloride concentration of 455.86 mg/L (Table 4.6). The water from this borehole was found to be very hard and does not lather easily with soap. The groundwater might be contaminated as the EC, Ca^{2+}, Mg^{2+} and the resistivity signatures suggests.

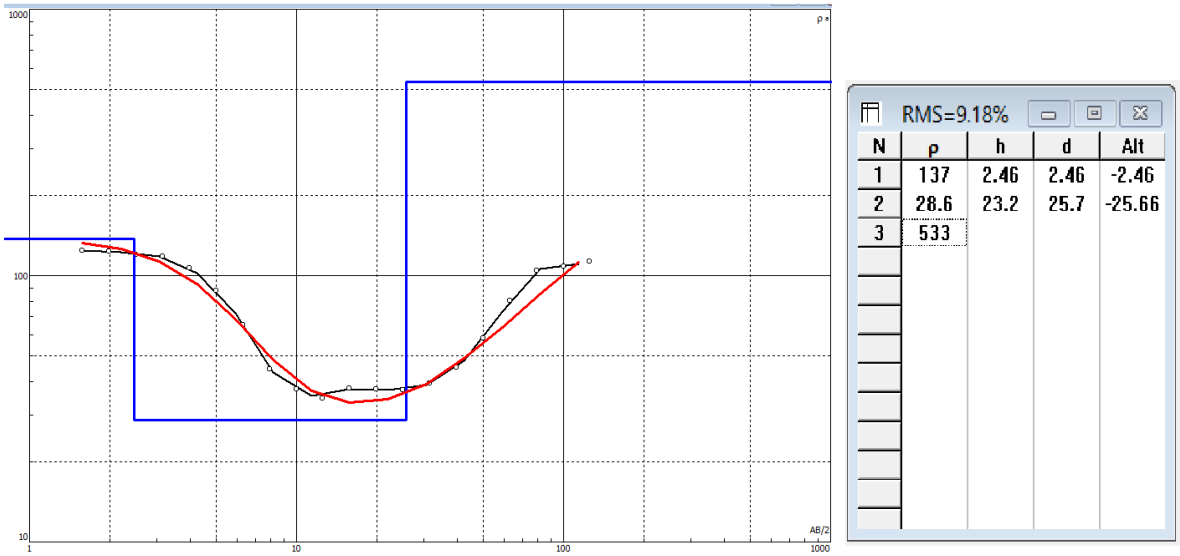

Figure 4.13: Sounding curve at BAN 21

4.4.3 VES at Station BAN 29

The third layer of this model with a very low resistivity value of 23.4 Ωm recorded at the thickness of 31.3 m and a depth of 35.6 m might be the zone of groundwater storage whiles the resistivity of the first layer, 40.5 Ωm is also low and can therefore be attributed to the fact that the borehole is fitted with a hand pump used by the residents, hence the water infiltration into the near surface through continuous pumping and washing of items around the borehole might be the cause of the conductive nature of water. Figure 4.14 represents the VES curve at BAN 29.

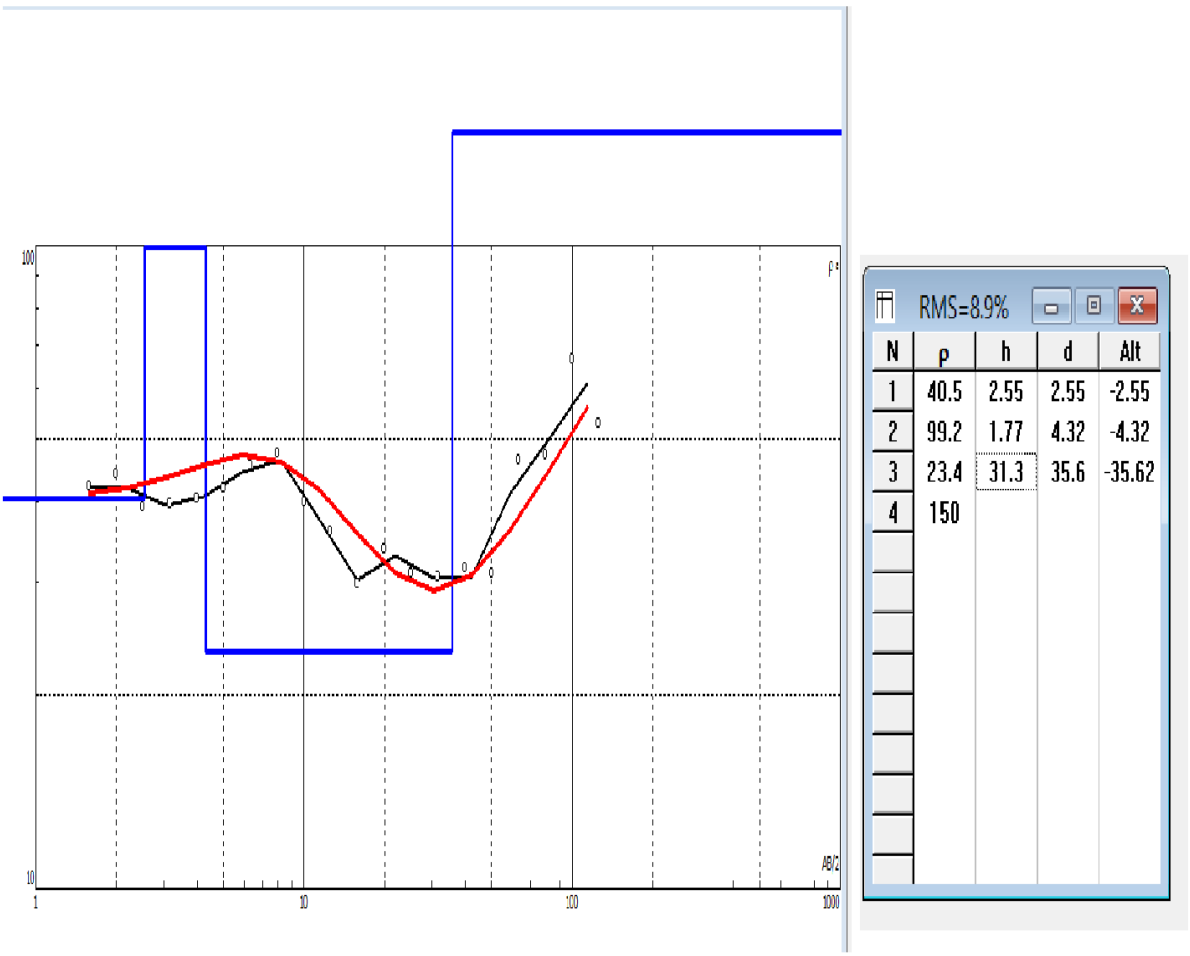

Figure 4.14: Sounding curve at BAN 29

4.4.5 VES AT STATION BAN 30

The nature of the curve generated by inversion at this station revealed a three layer structure and the resistivity increased after the first layer and evens out with increasing depth which implies that the bedrock is closer to the surface and hence the survey could not pick out much needed information about the subsurface. Figure 4.15 shows resistivity range between 522 Ωm and 1290 Ωm with a maximum depth of investigation being 10.2 m. This obviously cannot give any information about the quality of the water.

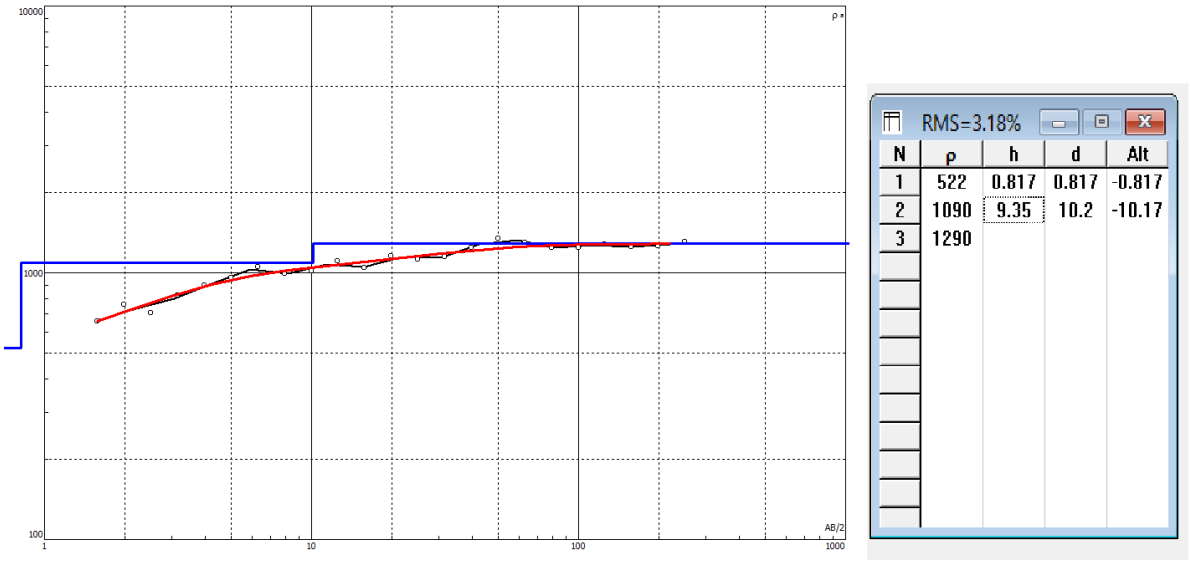

Figure 4.15: Sounding curve at BAN 30

4.5 VES RESULTS AND THE HYDROGEOCHEMICAL ANALYSIS AT THE UNIVERSITY OF GHANA, LEGON AREA.

Within this area, there were 5 VES carried out. All the five recorded chloride concentrations higher than the (WHO, 2004) standards (Table 4.8) therefore contributing to the conductivity of the subsurface. With the exception of BAN 35, all the boreholes gave EC values beyond the permissible limit. Pb concentrations were elevated in 3 samples (BAN 12, 34 and 35) whiles Mn and Fe concentrations were either not detected or within the acceptable range as shown in Table 4.8. From Table 4.9, the maximum depth of penetration reached was 74 m which occurred at BAN 33. This area also picked some very low resistivity signatures of 7, 5 and 23 Ωm at the first and second layers of BAN 13 and the third layer of BAN 34 respectively.

Table 4.8: Physico-chemical analysis of boreholes at the University of Ghana area

Station	Cl(mg/L)	PH	EC(µS/cm)	TDS(mg/L)	Fe(mg/L)	Mn(mg/L)	Pb(mg/L)
BAN 12	350	6.91	2402	1205	0.07	0.006	0.0246
BAN 13	310	6.87	2970	1486	0.05	0.021	0.0045
BAN 33	323	5.28	1675	922	0.06	Nd	0.0089
BAN 34	323	5.33	1223	673	0.05	Nd	0.0121
BAN 35	315	7.14	353	176	0.05	Nd	0.0173
WHO	**250**	**6.5-8.5**	**1500**	**500**	**0.3**	**0.5**	**0.01**

Table 4.9: Descriptive statistics of the VES results at the University of Ghana area

Parameters	Number	Range	Minimum	Maximum	Mean	Std. Deviation
ρ1 (Ωm)	5	251	7	258	124	93
ρ2 (Ωm)	5	1592	5	1597	393	675
ρ3 (Ωm)	5	12705	23	12728	3198	5448
ρ4 (Ωm)	3	45080	406	45486	15800	25714
h1 (m)	5	2	1	3	1.40	0.894
h2 (m)	5	68	4	72	22.40	28.09
h 3 (m)	3	50	19	69	47.33	25.66
Depth (m)	3	45	29	74	56.67	24.21

4.6 PHYSICO-CHEMICAL RESULTS

The hydrochemical analysis included all the major cations and anions, the physical parameters, bicarbonate, nitrate, sulphate, ammonia and the trace metals. Table 4.10 represents the basic statistics of the physico-chemical parameters of the water samples which indicates the trend and distribution of the various concentrations of these parameters within the study area.

Table 4.10: Minimum, maximum and average values of physical and chemical parameters of groundwater samples

Parameters	Units	Minimum	Maximum	Mean
Temp	^{o}C	28	33	30
PH	pH units	3	7	6
EC	µS/cm	303	3999	1621
TDS	mg/L	150	2000	815
SAL	Ppm	1	12	5
TURB	NTU	0	11	2
Col	PCU	0	81	14
Na	mg/L	28	192	85
K	mg/L	3	74	26
Ca	mg/L	6	232	65
Mg	mg/L	1.6	38	15
Cl	mg/L	100	520	253
NO3	mg/L	1	57	11
SO4	mg/L	1	128	23
HCO_3	mg/L	5	268	62
PO_4	mg/L	0	26	7
Fe	mg/L	0.014	2.670	0.281
Zn	mg/L	0.002	0.070	0.012
Mn	mg/L	0.002	0.880	0.208
Co	mg/L	0.005	0.008	0.006
Ni	mg/L	0.002	0.116	0.036
Cr	mg/L	0.002	0.016	0.006
Pb	mg/L	0.002	0.214	0.033

4.6.1 Physical Parameters

The electrical conductivity of the water samples are due to the dissolution of mineral ions. From the water samples collected, 20 of the total water samples taken under investigation have measured conductivities above the WHO permissible limit of 1500 µS/cm. This represents exactly 50% of the water taken for the analysis which showed spatial variation within the area (Fig. 4.16).

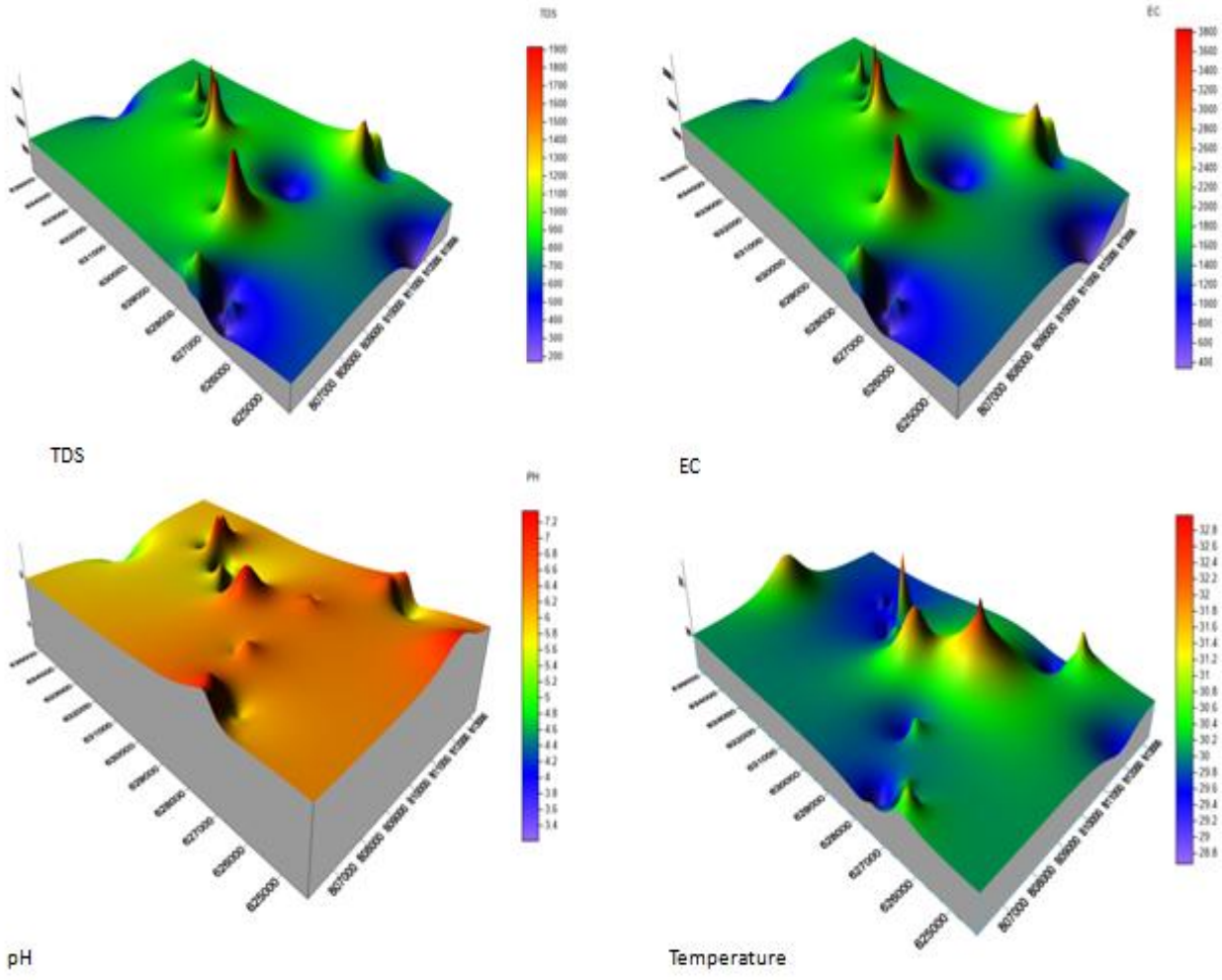

Figure 4.16: Spatial distribution of TDS, EC, Temperature and pH in the study area

This study has revealed that the electrical conductivity within the area ranged between 303 µS/cm to 3999 µS/cm, with the average recorded as 1557.5 µS/cm (Table 4.10). The higher EC values recorded were predominantly in the areas of reported cases of high chloride, iron and salinity content especially at the dump site and the Pantang hospital area. Some of these boreholes, have been left undeveloped and abandoned.

Within the study area, the temperature of the water samples collected ranged between 28.5°C to 33.5°C with an average of 30.04°C. The pH values observed ranged from as low as 3.0 to 7.4 indicating high acidity. None of the water sampled recorded a higher pH value beyond the WHO prescribed range of 6.5 to 8.5 but rather some fell below, which is within the acid range. pH values are mostly affected by industrial waste and dissolved gases which subsequently may have an effect on the taste of drinking water.

Water samples that records high level total dissolved solids minimizes the clarity of the water. The maximum value allowed by the WHO is 1000 mg/L (Wetzel, 2001). When the TDS was analysed, only 9 of the sampled wells and boreholes were beyond the standards whiles the remaining fell within the acceptable values. The nine wells that recorded high TDS values were observed at stations BAN 1 and BAN 4, and also at BAN 8, 10, 12, 13, 20, 21 and BAN 23. BAN 1, BAN 4, BAN 3 and BAN 10 were located at the dump site and the remaining at other areas including the stations BAN 20 which has been left undeveloped and abandoned. TDS values at these stations correlate well with the very low resistivity values generated from the stations mentioned. The higher TDS values could contribute to the

decrease in photosynthesis activities and may cause an increase in water temperature (NRCC, 2011).

4.6.2 Chemical Parameters

Concentration of $NO3^-$ permissible by the WHO is 10 mg/L. However, the $NO3^-$ concentration recorded ranged from 1 mg/L to 57 mg/L with an average of 10.75mg/L. The concentrations mostly increased around the dump site area (exceeding the WHO standards). Although the nitrate concentrations from the wells nearby the dump site are low, it has a higher tendency of being transported by advection, dispersion and diffusion mechanisms to pollute the other wells that are much closer especially those that are hydraulically connected (Achampong et al., 2013).

Aside the dump site, other areas also recorded higher concentrations of nitrate, which are probable due to anthropogenic activities in these areas. Notable amongst them are the farmland around GAEC (BAN16), an old mini dump site at the back of the Pantang hospital (BAN 37) and the hand dug well sampled at Haatso (BAN 35) closer to a stream. Convulsion and miscarriage in pregnant women are some of the adverse effects of high levels of nitrate in water when used as drinking water.

The concentration of chloride ranges from 100 to 520 mg/L and it predominately increases at the landfill site although higher concentrations were also recorded at different locations. In the study area. It is obviously one of the major inorganic anions in water and as such the salty taste felt in water is largely due to the higher concentrations of chloride (Yadav et al.,

2015). Although chloride is not noted to have any serious human health implications, the WHO has a limit of 250 mg/L acceptable in portable water. HCO_3^- ions found in the groundwater samples in study area ranged from 5 to 268.22 mg/L. Sulphate varies from 1 to 128 mg/L.

From the descriptive statistics (Table 4.10), the Na^+ and K^+ concentrations in groundwater range from 28 to 192 and 3 to 74 mg/L, respectively. Calcium concentration range from 6 to 232 mg/L, which is likely to be coming from minerals like feldspars, pyroxenes and amphiboles that are rich in calcium as these minerals are found within the Dahomeyan Structural Unit in the study area. The major source of Mg^{2+} in the groundwater is due to ion exchange of minerals in rocks and soils by water. The concentrations of Mg^{2+} ions found in the groundwater samples in study area ranged from 1.57 to 38 mg/L.

The heavy metals that were tested for the water samples collected includes Fe, Zn, Co, Ni, Cr, Pb and Mn. Ni, Co, and Cr were generally minimal or were not detected in the study area. From The electrical conductivity of the water at the dump site and those that are further away from the dump site were very high and beyond the WHO limit. The heavy metals are released mostly from broken down vehicles and other avenues such as industrial discharge which are dumped at the refuse site. The extent of the contamination from these metals are assessed using geochemical index. The presence of these trace metals are in a form of metallic ions. The presence of Fe content in groundwater for domestic purpose is not desirable as it makes water tastes bad and also stains clothing when used in washing.

The mean value of Pb concentration of 0.03258 mg/L exceeds the WHO standards limit of 0.01 mg/L which implies that there is relative abundance of Pb in the waters within the study area especially the hand dug wells at the dump site. Elevated lead concentrations detected at the dump site could be coming from disposed car batteries (Achampong et al., 2013). The presence of relatively high level of Pb in water poses a serious health challenge. Some of these health problems include kidney failure, neurological cell damages, hypertension and related heart diseases, reduction in fertility of human beings and also child birth defects.

Manganese present in the groundwater samples from the dump site may have contributed to the leachate plume. Four of the wells at the dump site BAN 2 to BAN 5 and two from the Pantang hospital area BAN 25 and BAN 26, making it a total of six wells which recorded higher concentrations of Mn. The rest of the boreholes recorded little or no concentrations when compared with the WHO permissible limit of 0.5mg/L. The presence of manganese in water also renders it distasteful and stains clothing as well.

Fe has the potential of causing a stomach upset when consumed into the human body through drinking water. Nine of the wells had high Fe content with 3 located at the dump site, 4 at GAEC area and 2 were observed in the wells at the Pantang hospital area and it might be coming from the alteration and weathering of rocks in the area. At the dump site different kinds of materials are thrown there and the high content of iron present in the wells identified could be from the disposal of these metals. The WHO limit of iron is 0.3 mg/L.

4.7 HYDROCHEMICAL FACIES

The physico-chemical data of the groundwater samples from the study area were plotted on a Piper tri-linear diagram (Piper, 1944) as shown in Figure 4.17. The piper diagram provides a suitable method to classify groundwater types, based on the ionic composition of different water samples collected for the study (Baba et al., 2008; Aly and Benaabidate, 2010; Aly et al., 2011; Semerjian, 2011). The analysis from the piper diagram has revealed that there are mainly two groundwater types in the study area.

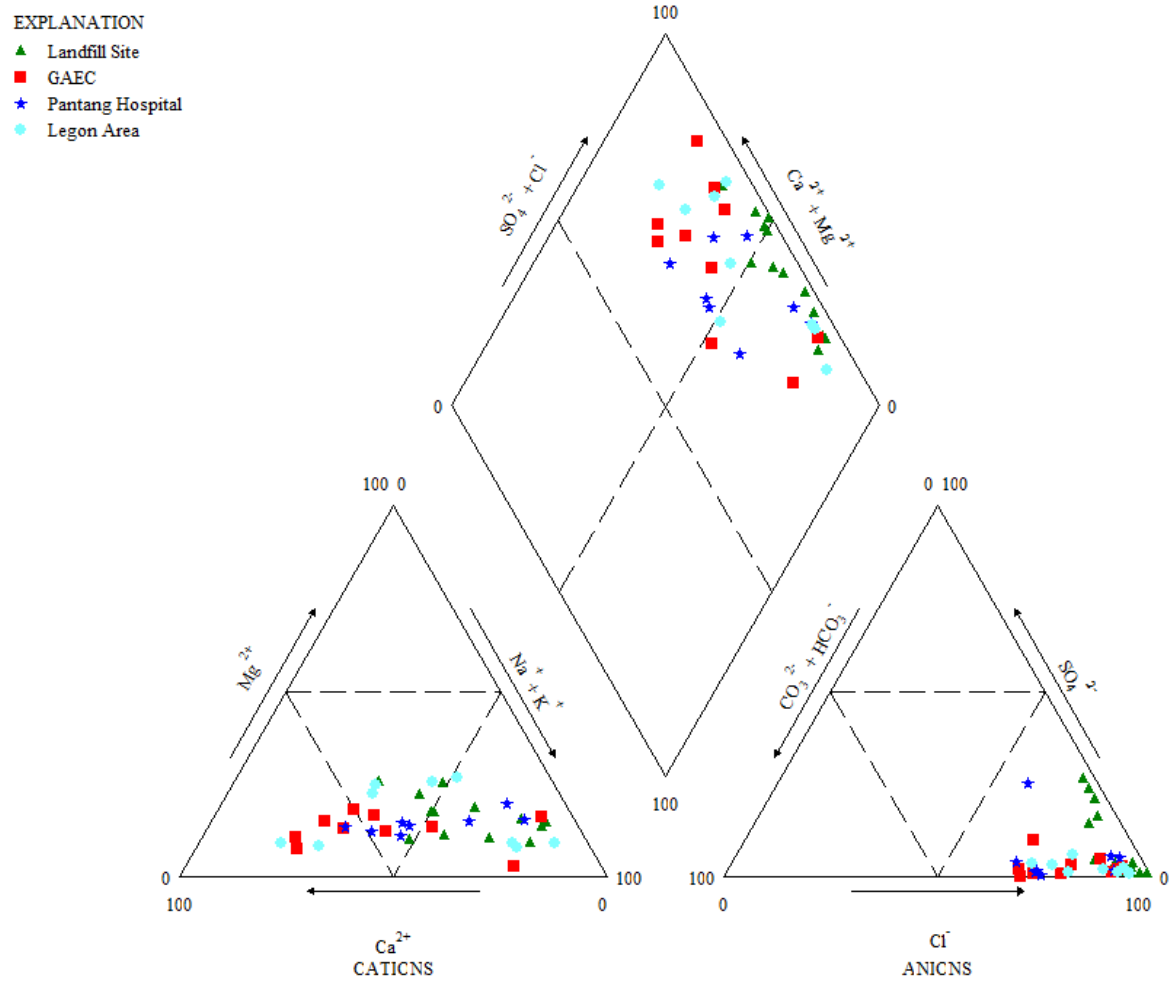

Figure 4.17: Piper diagram showing the hydrochemical facies of the groundwater type in the area after Piper, 1944.

From Figure 4.17, it can be observed that the plot shows NaCl and Na-HCO_3 as the main groundwater types in the area. The dominant cations are Na^+ and Ca^{2+} whiles Cl^- and HCO_3^- represents the dominant anions. It can also be observed on the piper diagram that, virtually all the data from the dump site classified by the triangle in colour green were plotted in the NaCl rich zone indicating that the salinity of the dump is very high and therefore the area is contaminated as compared to the water sampled from the other locations since the other water samples stretched across the two different zones of the water types identified in the area.

The chemistry of natural water is influenced by a variety of factors which includes chemistry of recharging precipitation waters, weathering of underlying rock, decay of organic matter, and a wide range of anthropogenic activities. The high salinity of the water in the area is a combination of weathering of phyllites which gives rise to clay minerals that dissolves in the groundwater as well as the anthropogenic activities from the dump site. The impact of the anthropogenic activities are higher at the dumpsite whiles the geogenic influence is seen much in the other areas.

4.8 ROCK WATER INTERACTION

The Gibbs plot of data from study area (Figs. 4.18 and 4.19) shows that the processes controlling the major ion composition of groundwater in the area is dominated by rock to crystalisation/evaporation dominance. Subsurface lithology, rock water interaction, and the process through which geochemical reactions take place are the factors that determines the concentration of dissolved ions in groundwater samples. The functional sources of dissolved

ions can be broadly assessed by plotting the samples, according to the variation in the ratio of Na/(Na+Ca) and Cl/(Cl+HCO3) as a function of TDS (Gibbs, 1970).

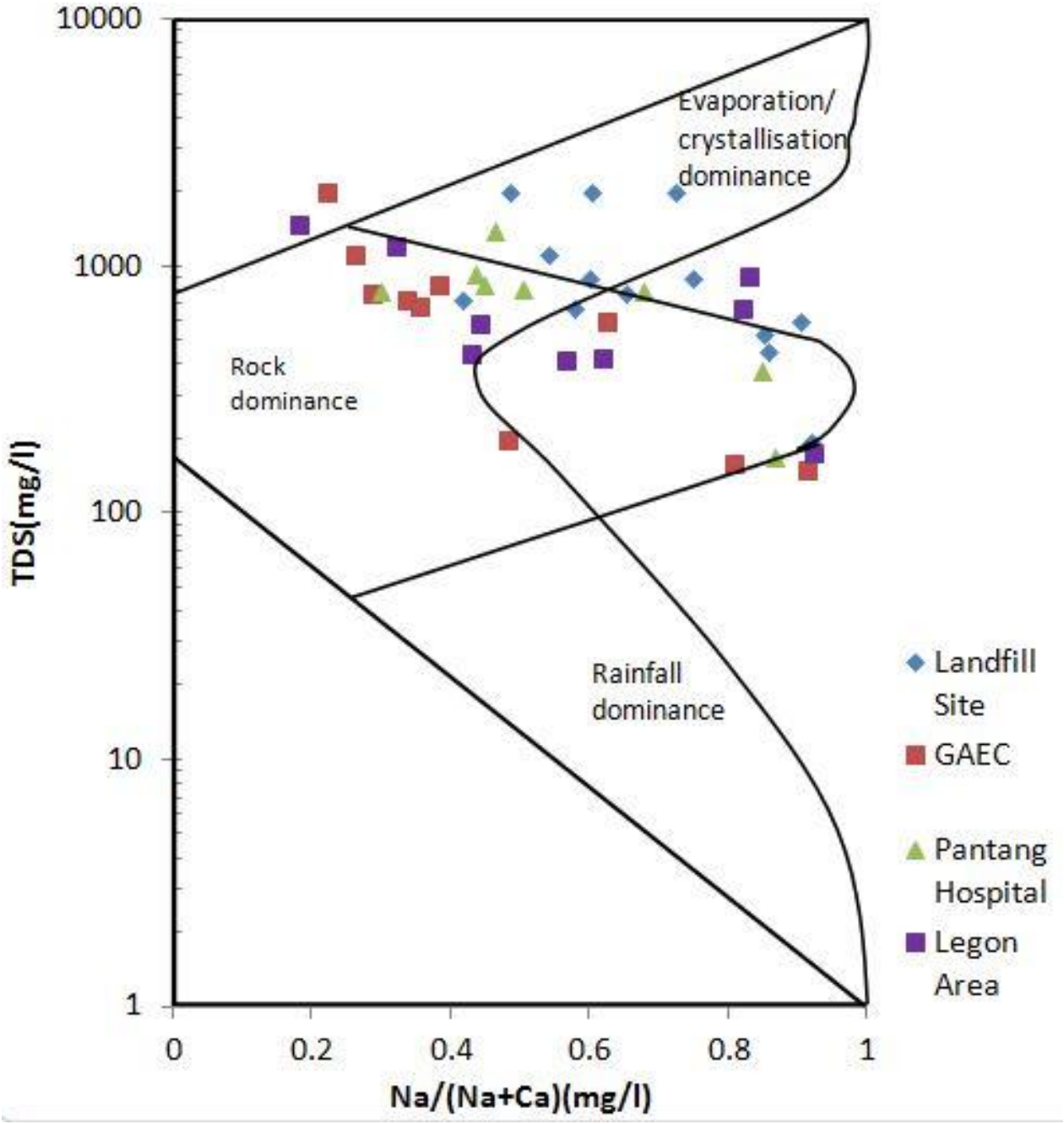

Figure 4.18: Mechanisms governing groundwater chemistry (after Gibbs, 1970)

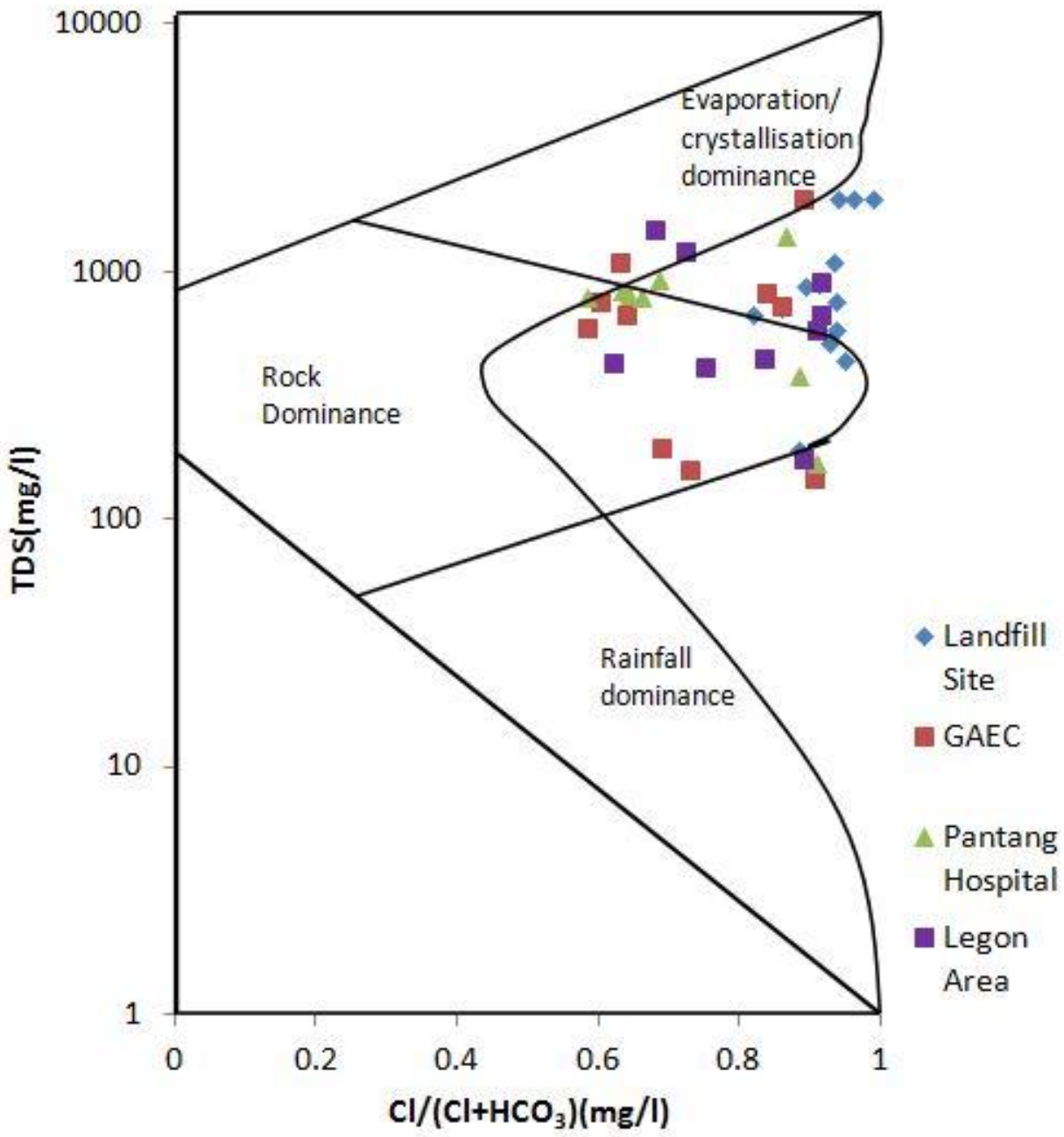

Figure 4.19: Mechanisms governing groundwater chemistry (after Gibbs, 1970)

4.9 WATER QUALITY FOR DRINKING BASED ON TDS AND TOTAL HARDNESS

The water samples collected have been analysed to check its suitability for drinking and agricultural purposes in the study area. The quality index of the drinking water was achieved by comparing the parameters such as the TDS and the total hardness with the World Health

Organisation standards (WHO, 2004). The standards set by the WHO indicates that 500 mg/L of TDS is the highest desirable and the maximum permissible is 1500 mg/L. The percentage of the most desirable limits and the maximum allowable limits are 27.5% and 62.5% respectively whiles 10% are beyond the maximum allowable limit. The percentage of the water hardness are 15% soft, 22.5% moderately hard, 22.5% hard and 40% very hard. The range is between 32 and 980 mg/L with a mean value of 65.05. The presence of the Mg^{2+} and Ca^{2+} content in the water is responsible for the total hardness (hard to very hard) contributing 62.5% of the groundwater samples in the area.

Table 4.11: Suitability of groundwater based on hardness

Total Hardness (mg/L)	**No. in the study area**	**% of samples**	**Water class**
<75	6	15%	Soft
75-150	9	22.5%	Moderately hard
150-300	9	22.5%	Hard
>300	16	40%	Very hard

4.10 GROUNDWATER SALINITY

Groundwater salinity is evaluated for its suitability in agricultural purposes based on parameters such as the sodium adsorption ratio (SAR), sodium percentage (Na%), residual sodium carbonate (RSC) and permeability index (PI) (Gowd, 2005). In the determination of the appropriateness of water for irrigation, the US Salinity Laboratory (USSL, 1954) classified groundwater on the basis of its electrical conductivity largely because it is a good measure of salinity hazard to crops as it reflects the TDS in the groundwater. Figure 4.20

shows that majority of the groundwater samples plotted in C3S1 region whiles few plotted in the C2S1 and very few plotting in C3S2 and C4S1; C4S2 and C2S2.

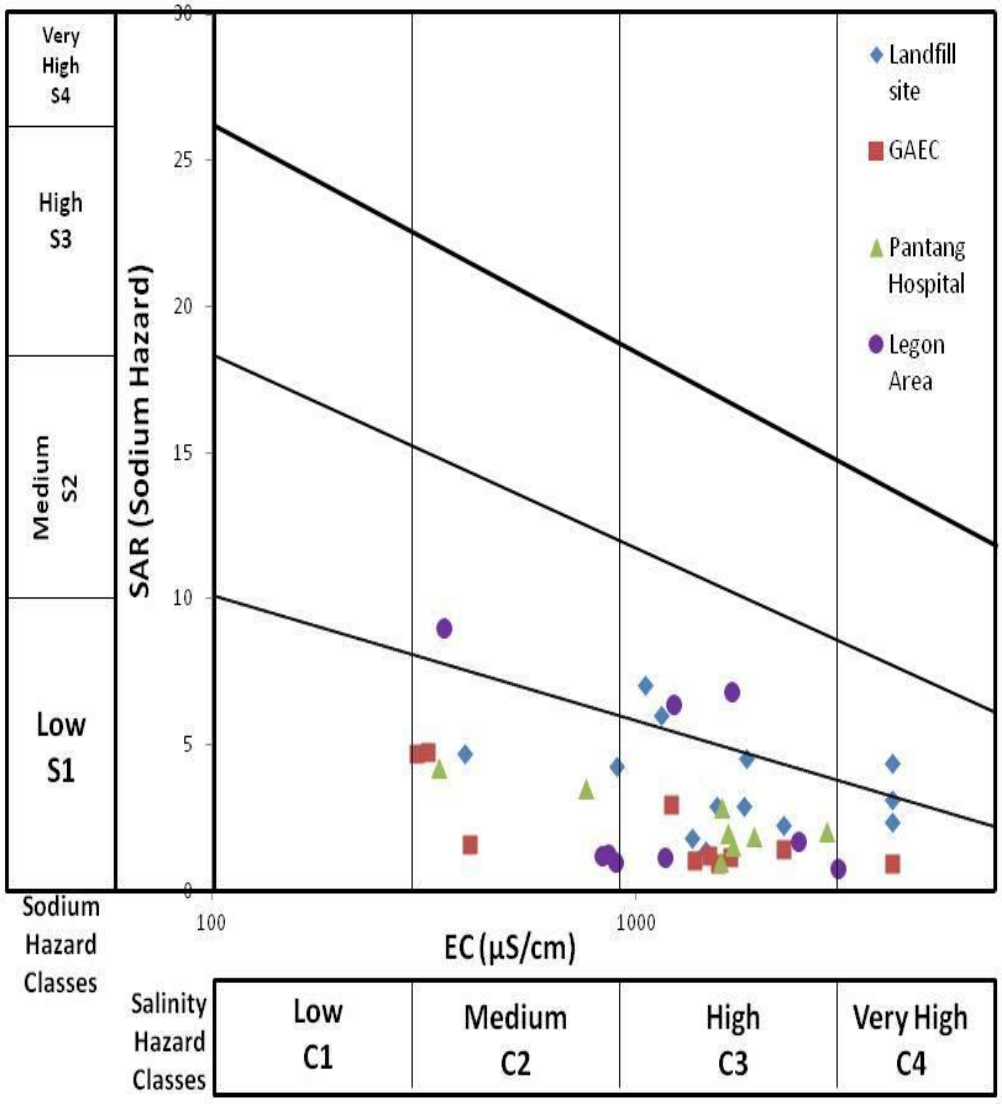

Figure 4.20: Classification of groundwater samples based on sodium hazard and salinity relations after Richard (1954).

It can however be observed that the samples from the Pantang dump site and the hospital area (Fig. 4.20) were largely within high salinity and low sodium hazard classes. In general, the samples are highly saline and thus will not be suitable for drinking except the ones

plotted in the medium salinity and the low sodium hazard regions. A lot of sodium concentration also prevents the soil from adsorption of the water and thus makes it unsuitable for irrigation in such instances. Sodium adsorption ratio (SAR) is also an important parameter for determining the suitability of groundwater for irrigation because it is a measure of alkali/ sodium hazard to crops (Subramani et al., 2005).

The formula used in calculating the SAR is given by Karanth (1987) as;

$$SAR = Na/[(Ca+Mg)/2]^{1/2} \quad (4.1)$$

where all parameters are expressed in meq/L.

From the analysis, SAR values range from 0.9 to 35.8 from the classification (Table 4.12). 90% of samples belong to the good and excellent category whiles 7% belongs to the doubtful and 3% unsuitable. It can therefore be inferred that the groundwater in the study area is generally good for irrigation with the exception of the samples from the dump site.

Table 4.12: Classification of groundwater for irrigation based on EC, SAR after (Richards, 1987)

Water Quality	**Electrical Conductivity(µS/cm)**	**Sodium adsorption ratio (SAR)**
Excellent	<250	<10
Good	250-750	10-18
Doubtful	750-2250	18-26
Unsuitable	>2250	>26

CHAPTER FIVE

CONCLUSION AND RECOMMENDATION

5.1 CONCLUSION

The combined effectiveness of electrical resistivity and hydrogeochemical cannot be neglected in the investigation of groundwater contamination, especially at a known zone of contamination such as the dump site. The research has shown that waste products disposed of at the dump site has infiltrated into the subsurface affecting the quality of groundwater in the area. From the geophysical survey, the pseudo and the resistivity cross-sections has revealed that the contaminant plume has gone beyond the water table at the dump site to about a depth of 7.2 m polluting the groundwater. The pseudo-section also shows that the contamination is on a downward trend and therefore has a tendency of affecting deeper depth with time.

The number of geologic layers, thicknesses and the resistivity values were determined when the VES were carried out. The total number of geoelectric layers revealed was four and it can be concluded that the terrain has four layers which correlated with the borehole logs provided in the area with very few generating three layers. The trace metals analysed in the study area indicated that the high concentrations of the metals at the dump site in a form of dissolved ions and contaminated fluids contributed much to the low resistivity and a very high electrical conductivity signatures.

The quality of the groundwater in the area were evaluated to determine its suitability for irrigation and drinking. The values obtained for SAR, indicates that the water around the

dump site is generally unsuitable for irrigation. It is therefore not recommended for drinking and irrigation purposes. The groundwater samples around the Legon, Pantang Hospital and GAEC areas are generally good for irrigation (Table 4.12).

With respect to the TDS, the percentage of the most desirable limits and the maximum allowable limits are 27.5% and 62.5% respectively whiles 10% are beyond the maximum allowable limit. The percentage of the water hardness are 15% soft, 22.5% moderately hard, 22.5% hard and 40% very hard. The presence of the Mg^{2+} and Ca^{2+} content in the water is responsible for the total hardness of hard to very hard contributing to 62.5% of the groundwater samples in the area thereby making it unsuitable for drinking.

The interpretation of hydrochemical analysis has revealed that the groundwater types in the study area is predominantly Na-Cl water type and Na-HCO_3 water type. Chloride and HCO_3^- are the dominant anions whiles sodium and calcium are the dominant cations in the study area. From Figures 4.18 and 4.19, the water samples are dominated by rock weathering to evaporation/crystalisation.

5.2 RECOMMENDATION

Application of direct current electrical resistivity in investigating groundwater contamination can be easy, economical and fast, it can also prove to be misleading when certain measures are not taken into consideration. Conditions such as the geology and the hydrogeology of the area, the nature of the contaminant, and the conductivity contrast between the natural groundwater and the contaminated water affects the success of the

survey. It is therefore advisable to take into account these measures when using resistivity to investigate groundwater contamination.

Although this study employed the combination of direct current resistivity and hydrochemistry, integrated approach of other geophysical techniques such as seismic, electromagnetic and induced polarisation without the hydrochemistry could be done in the area and other areas. This will compensate for the lapses that resistivity alone faces so that the success of using geophysics alone to investigate groundwater contamination can be evaluated.

REFERENCES

Abdalla, M. A. (2008). Integrated geophysical methods to delineate the contamination. Geophysical Research Abstracts, 10, EGU2008-A-02014.

Abdul Nassir, S. S., Loke, M. H., Lee, C.Y., and Nawawi, M. N. M. (2000). Salt-water Intrusion Mapping by Geoelectrical Imaging Surveys. Geophys. Prospect 48:647-661.

Accra Metropolitan Assembly. (2006). Ghana Districts Map. Retrieved from http://gaeast.ghanadistricts.gov.gh. (Assessed: 20 January, 2015)

Achampong, F., Anum, R. A., Obada, J., and Boadu, P. F. (2013). Contamination of Groundwater Around Garbage Dump. Case Study at The Pantang Landfill, 4(8), 2274-2290.

Adepelumi, A. A., Ako, B. D., Ajayi, T. R., Afolabi, O., Ometoso, E. J. (2008). Delineation of saltwater intrusion into the freshwater aquifer of Lekki. Penninsula, Lagos, Nigeria. Environ Geol 56: 927-933.

Adomako, D., Osae, S., Akiti, T. T., Faye, S. and Maloszewski, P. (2010). Geochemical and isotopic studies of groundwater conditions in the Densu River Basin of Ghana. Journal of Environmental Earth Science. DOI 10.1007/s12665-010- 0595-2.

Adetunji, V. O., and Odetokun, I. A. (2011). Groundwater contamination in Agbowo community , Ibadan Nigeria : Impact of septic tanks distances to wells, 7(3), 159–166.

Aghazadeh, N. and Mogaddam, A. A. (2010). Assessment of groundwater quality and its suitability for drinking and agricultural uses in the Oshnavieh Area, Northwest of Iran. J. Environ. Prot., 1: 30-40.

Agyei, E. K., van Landewijk, J. E. J. M., Armstrong, R. L., Harakal, J. E., Scott, K. L., (1987). Rb-Sr and K-Ar geometery of southeastern Ghana. Journal of African Earth Science. 6, 153-161.

Agyekum, A. W. (2002). Groundwater Resources of Ghana With Focus on International Shared Aquifer Boundaries. CSIR Water Research Institute Accra, Ghana.

Akankpo, O. and Igboekwe, M. U. (2011). Monitoring Groundwater Contamination Using Surface Electrical Resistivity and Geochemical Methods. Journal of Water Resource and Protection, 03(05), 318–324. http://doi.org/10.4236/jwarp.2011.35040.

Amfo Otu, R., Omari, S., and Boakye Dede, E. (2012). Assessment of Physico-chemical Quality of Groundwater Sources in Ga East Municipality of Ghana. Environment and Natural Resources Research, 2(3), 19–24. http://doi.org/10.5539/enrr.v2n3p19.

Anokwa, Y., Martin, N., Muff, R. (2005). Coastal stability map of greater accra metropolitan area 330000-335000. Water Research.

Apambire, W. B., Boyle, D. R., and Michel, F. A. (1997). Geochemistry, genesis, and health implications of fluoriferous groundwaters in the upper regions of Ghana. Environmental Geology, 33(1), 13–24. http://doi.org/10.1007/s002540050221.

APHA. (1995). Standard methods for the examination of water and waste water (19th ed.). Washington: American Public Health Association.

Appelo, C. A. J., and Postma, D. (2005). Geochemistry, groundwater, and pollution (2nd ed.). A. A. Balkema, Rotterdam, the Netherlands.

Aristodemou, E., Thomas-Betts, A. (2000). DC resistivity and induced polarisation investigations at a waste disposal site and its environments. Journal of Applied Geophysics, 44, 275–302.

Attoh, K., Dallmeyer, R. D., and Affaton, P. (1997). Precambrian Chronology of nappe assembly in the Pan-African Dahomeyide orogen, West Africa : evidence from 40Ar / 39Ar mineral ages, 82, 153–171.

Attwa, M., Günther, T., Grinat, M., and Binot, F. (2011). Evaluation of DC, FDEM and IP resistivity methods for imaging perched saltwater and a shallow channel within coastal tidal flat sediments. Journal of Applied Geophysics, 75(4), 656–670. http://doi.org/10.1016/j.jappgeo.2011.09.002.

Aly, A. A., Abbas, A. A., Benaabidate, L. (2011). Hydro-chemical and Quality of groundwater in Egypt, Case Study of Egypt Southern oases. NATO Science for Peace and Security Series C: Environmental Security. Springer.

Aly A. A., and Benaabidate L. (2010). Salinity of water resources in the Siwa Oasis: Monitoring and diagnosis in Water-Rock Interaction (Brikle, Torres Alvaro, eds). Taylor and Francis Group, London, UK.

Al-Tarazi, E., El-Naqa, A., El-Waheidi, M., and Abu Rajab, J. (2006). Electrical geophysical and hydrogeological investigations of groundwater aquifers in Ruseifa municipal landfill, Jordanm. Environmental Geology, 50, 1095–1103.

Al-Yaqout, A., and Hamoda, M. (2003). Education of landfill leachate in arid climate: a case study. Envir. International, 29, 593 - 600.

Aweto, E. K., and Mamah, L. I. (2014). Application of Resistivity Methods to Groundwater Protection Studies in Niger Delta. International Journal of Environmental Protection, (4) 3, 27-35 - 27.

Baba A., Erees F. S., and Hicsonmez U. (2008). An assessment of the quality of various bottled mineral water marketed in Turkey. Environmental Monitoring and Assessment, 139: 277-285.

Banoeng-Yakubo, B., Danso, S. and Tumbulto, J. (2005). Assessment of pollution status and vulnerability of water supply aquifers in Keta, Ghana. Final Report. pp 120.

Barker, R. D., (1990). Improving the quality of resistivity sounding data in landfill studies. In: Ward, S. H. (ed). Geotechnical and Environmental Geophysics. Vol. 2: Environmental and Groundwater. Tulsa: Society of Exploration Geophysicists 24 - 251.

Barker, R., Venkateswararao, T., and Thangarajan, M. (2001). Delineation of contaminant zone through electrical imaging techniques. Current Science, 81(3), 10.

Benson, R. C., (1991). Remote sensing and geophysical methods for evaluation of subsurface conditions, in Nielsen, D.M., Ed., Practical handbook of groundwater monitoring: Lewish Publishers, 143-194.

Blay, P. K. (1991). Applying subduction tectonics to the evolution of the Pan – African Dahomeyide deformed belt of Ghana, West Africa. Proceedings of the first local conference on Mineral Exploration and Development and their impact on the economy of Ghana, 7th December, 1990. Minerals Commission Publication, pp. 52-57.

British Geological Survey Report. (2011). Natural Environment Report. BGS Report No: GR_999999/1.

Carpenter, P. J., Ding, A., and Cheng, L. (2012). Identifying groundwater contamination using resistivity surveys at a landfill near Maoming, China. Nature Education Knowledge, (3) 7, 20.

Crook, J. P. (1970). Some preliminary notes on the classification of rocks of Eastern Ghana in Geological Survey Bulletin no. 38 – Symposium Fiftieth Anniversary – Ghana Geological Survey 1913 – 1963. pp 27 - 32.

Darko, P. K., Dua, A. A., and Dapaah-Siakwan, S. (2003). Groundwater Assessment: An element of integrated Water Resources Management: the case of Densu River Basin. Technical Report for the Water Resources Commission, Accra, Ghana.

Daily, W., Ramirez, A., Labreque., D. and Nitao, J. (1992). Electrical resistivity tomography of vadose water movements. Water Resource Research, 28, 1429-1442.

Denutsui, D., Akiti, T. T., Osae, S., Tutu, A. O., and Ayivor, J. E. (2012). Leachate Characterization and Assessment of Unsaturated Zone Pollution near Municipal Solid Waste Landfill Site at Oblogo, Accra-Ghana. Research Journal of Environmental and Earth Sciences. 4(1): 134-141.

Dickson, K. B. and Benneh, G. (1998). A New Geography of Ghana. Longman Group. London.

Domenico, P.A. and F.W. Schwartz, (1990). Physical and Chemical Hydrogeology. John Wiley and Sons, New York, pp: 824.

Duque, C., Calvache, M. L., Pedrera, A., Martín-Rosales, W., and López-Chicano, M. (2008). Combined time domain electromagnetic soundings and gravimetry to determine marine intrusion in a detrital coastal aquifer (Southern Spain). Journal of Hydrology, 349(3-4), 536–547. http://doi.org/10.1016/j.jhydrol.2007.11.031.

Duncan D., Harvey F., Walker M. and Australian Water Quality Centre (2007). Regulatory monitoring and testing Water and wastewater sampling. EPA Guidelines South Africa. pp 1-28.

Eaton, A. D., Clesceri, L., Greengerg, A. E (2005). (Ed), Standard Methods for the Examination of Water and Wastewater, American Public Health Association, 1015 Fifteenth street Washington.

Edet, a. E., and Okereke, C. S. (2002). Delineation of shallow groundwater aquifers in coastal plain sands of Calabar area (Southern Nigeria) using surface resistivity and hydrogeological data. Journal of African Earth Sciences, 35(3), 433–443. http://doi.org/10.1016/S0899-5362(02)00148-3

El-Hussaini, A. H., Ibrahim, H. A., and Sebaq, A. S. (2003). Application of electrical resistivity and self-potential for groundwater exploration and contamination study in the area northwest of Assiut City, Egypt. Journal of King Saud University, 16, 31–61.

Essumang, D.K., Adokoh, C. K., Afriyie, J. and Mensah., E. (2009). Source assessment and analysis of polycyclic aromatic hydrocarbon (PAH's) at the Oblogo waste disposal sites and some water bodies in and around the Accra Metropolis of Ghana. Journal of Water Resource and Protection., (1):456- 468.

Ford, D. C., and Williams P. (2007). Karst hydrogeology and geomorphology. New York: Wiley.

Franson M. A. H., Eaton A. D., Clesceri L, and Greegerg A. E. (1995). Standard Methods for the Examination of water and Wastewater (19th Edition), American Public Health Association, 1015 Fifteen Street Washington. Pg. 3-57 to 4-49.

Freeze, R. A. and J. A. Cherry, (1979). Groundwater. Prentice-Hall, Englewood Cliffs, NJ, USA.

Ga East Municipal Report. (2006). District Coordinating Report by the Planning Unit.

Ghana National Water Policy document. (2007). Ministry of Water Resources, Works and Housing.

Ghana Statistical Service. (2010). Ghana Population and Housing Census 2010, http://www.statsghana.gov.gh/docfiles/2010phc/Census2010. Summary report of final results.pdf (Assessed: 25 February, 2015).

Gibbs, R. J. (1970). Mechanisms controlling world water chemistry, Science, 17, 1088–1090.

Gowd, S. S. (2005). Assessment of groundwater quality for drinking and irrigation purpose: A case study of Peddavanka watershed, Anantapur District, Andhra Pradesh, India, Environmental Geology, 48, 702–712.

Grant, N. K. (1969). The Precambrian to early Paleozoic orogeny in Ghana, Togo, Dahomey and Nigeria. Geological Society of America Bulletin. 80: 45 – 55.

Griffis, R. J., Barning, K., Agezo, F. L., and Akosah, F. K. (2002). Gold Deposits of Ghana. Minerals Commission Report, Accra.

Griffis, R. J. and Agezo, F. L. (2000). Mineral Occurrences and Exploration Potential of Northern Ghana. Minerals Commission Report, Accra, 132p.

Gyau-Boakye, P., Kankam-Yeboah, K., Darko, P. K., Dapaah-Siakwan, S., and Duah, A. A. (2008). Groundwater as a vital resource for rural development: An example from Ghana. In: S. Adelana, A. MacDonald, T. A. Alemayehu and C. Tindimugaya, eds.

Applied groundwater studies in Africa, IAH selected papers Q3 on hydrogeology. vol. 13.

Habberjam, G. M. (1975). Apparent resistivity, anisotropy and strike measurements. Geophysical Prospecting 23, 211–247.

Habberjam, G.M., Watkins, G. E. (1967). The use of a square configuration in resistivity Prospecting: Geophysical Prospecting, 15, 221- 235.

Hwang, S., Shin, J., Park, I. and Lee, S. (2004). Assessment of Seawater Intrusion Using Geophysical Well Logging and Electrical Soundings in a Coastal Aquifer, Youngkwang- gun, Korea. Exp. Geophys., 35**,** 99-164.

Jianshua, S., Qi, F., Xiaohu, W., Yonghong, S., Haiyang, X. and Zongqiang, C. (2008). Major ion chemistry of groundwater in the extreme semi arid region northwest China. Environ Geol. doi10.1007/s00254-008-139-x.

Junner, N. R. and Hirst, T. (1946). The geology and hydrology of the Voltaian basin. Gold Coast Geological Survey Memoir., 8, 51.

Karanth, K. R. (1987). Groundwater assessment, development and management. Tata McGraw Hill, New Delhi, pp. 720.

Kearey, P., Brooks, M. and Hill, I. (2002). An Introduction to Geophysical Exploration. Blackwell Science, pp .262.

Keelson, K. B. (2014). Evaluation of landfill leachate management systems in Ghana. JENRM, 1 (1), 13-18.

Kesse, G. (1985). The mineral and rock resources of Ghana. United States: A. A. Balkema Publishers, Accord, MA.

Kleemeier, E. (2002). Rural Water Sector Reform in Ghana: A major change in Policy and Structure. Field note 2. PS Press Services Pvt. Ltd. Vanadana Mehra.

Koert, W. (1910). Begleit worte zur geologischer kante von Togo in Hans Mayer's Das Deutsche kolonia – ireich, Leipzig and Vienna, vol. 2.

Kortatsi, B. K. (2007). Hydrochemical framework of groundwater in the Ankobra Basin, Ghana. Aquatic Geochemistry, 13(1), 41–74. http://doi.org/10.1007/s10498-006-9006-4.

Kortatsi, B. K., Young, E. and Mensah-Bonsu, A. (2005). Potential Impact of Large Scale Abstraction on the Quality of Shallow Groundwater for Irrigation in the Keta Strip, Ghana. West African Journal of Applied Ecology, 8, 1-12.

Kortatsi, B. K., and Jorgensen, N. O. (2001). The origin of high salinity waters in the accra plains groundwaters. First International Conference on Saltwater Intrusion and Coastal Aquifers - Monitoring, Modeling and Management. Essaouira, Morroco, 10.

Kumar., C. D., Alappat, B. J. **(**2003**).** Monitoring Leachate Compoisiton at a municipal landfill site in New Delhi, India, Int. J. Environment and Pollution., 19(5), 454-465.

Kumaresan M. and Riyazuddin P. (2006). Major ion chemistry of environmental samples around sub urban of Chennai city. Current Science, 91(12), 1668-1677.

Lee, J.-Y., Song, S.H., (2007**).** Groundwater Chemistry and Ionic Ratios in a Western Coastal Aquifer of Buan, Korea; Implication for Seawater Intrusion. Geosci. Journ. Hyd., 3,259-270.

Li, Y., Li, J., Chen, S., and Diao, W. (2012). Establishing indices for groundwater contamination risk assessment in the vicinity of hazardous waste landfills in China. Environmental Pollution, 165, 77–90. http://doi.org/10.1016/j.envpol.2011.12.042.

Loh, G., and Hirdes, W. (1996). Explanatory Notes for the Geological Map of Southwest Ghana - 1:100,000 scale (Axim and Takoradi sheets). Ghana Geol. Surv. Bull. 49, 63p, Accra.

Majolagbe, A. O., Kasali, A. A, and Ghaniyu, L. O. (2011). Quality assessment of groundwater in the vicinity of dumpsites in Ifo and Lagos , Southwestern Nigeria, *2*(1), 289–298.

Makey, K. S., (1982). Natural Buffers for Sludge Leachate Stabilization. Groundwater, (20)4, 420- 429. doi:10.1111/j.1745-6584.1982.tb02762.

Mani, R. (1978). The geology of the Dahomeyan of Ghana; Geology of Ghana Project. Accra: Ghana Geological Survey Department.

MOFA, (2004). Projected livestock population for 1997-2007. Ministry of Food and Agriculture, Accra, Ghana.

Morrow, F. J., Ingham, M. R., and McConchie, J. A. (2010). Monitoring of tidal influences on the saline interface using resistivity traversing and cross-borehole resistivity tomography. Journal of Hydrology, 389(1-2), 69–77. http://doi.org/10.1016/j.

Mota, R., Monteiro Santos, F. A., Mateus, A., Marques, F. O., Gonçalves, M. A., Figueiras, J., and Amaral, H. (2004). Granite fracturing and incipient pollution beneath a recent landfill facility as detected by geoelectrical surveys. Journal of Applied Geophysics 57, 11 22.

Muff and Efa. (2006). Environmental and Engineering Geology for Urban Planning in the Accra-Tema Area. Ghana-Germany Technical Cooperation Project. Accra-Ghana.

National Research Council of Canada NRCC. (2011). Effect of Sodium and Potassium in the Canadian Environment. NO. 150154. Associate Committee on Scientific Criteria for Environmental Quality Otttawa.

Nartey, V. K., Hayford, E. K., and Ametsi, S. K. (2012). Assessment of the Impact of Solid Waste Dumpsites on Some Surface Water Systems in the Accra Metropolitan Area, Ghana. Journal of Water Resource and Protection, 04(08), 605–615. http://doi.org/10.4236/jwarp.2012.48070.

Nwankwo, N. C., and Emujakporue, G. O. (2012). Geophysical Method of Investigating Groundwater and Sub-Soil Contamination – A Case Study. American Journal of Environmental Engineering, 2(3), 49–53. http://doi.org/10.5923/j.ajee.20120203.02.

Nyarku, M. (2011). Major elements and lithostratigraphic study of the contact rocks of the Togo and the Dahomeyan formations in Ghana. Natural Science, 03(08), 646–650. http://doi.org/10.4236/ns.2011.38088

Obikoya, I. B., and Bennell, J. D. (2012). Geophysical Investigation of the Fresh-Saline Water Interface in the Coastal Area of Abergwyngregyn. Journal of Environmental Protection, 03(09), 1039–1046. http://doi.org/10.4236/jep.2012.39121.

Ogungbe, A. S., Onori, E. O., and Olaoye, M. A. (2012). Application of electrical resistivity techniques in the investigation of groundwater contamination : A case study of Ile – Epo Dumpsite , Lagos , *3*(1), 30–41.

Ortega-Guerrero., A. (2003). Origin and geochemical evolution of groundwater in a closed-basin clayey aquitard, Northern Mexico. Journal of Hydrology, 284, 26–44.

Osei, J., Osae, S. K., Fianko, J. R., Adomako, D., Anim, C. A. K., Ganyaglo, S. Y., Nyarku, M. and Nyarko, E. S. (2011). The impact of Oblogo landfill site in Accra-

Ghana on the surrounding environment. Research Journal of Environmental and Earth Sciences., 3(6), 633- 636.

Piper A. M. (1944). A graphic procedure in the geochemical interpretation of water analysis. Transactions American Geophysical Union, 25, 914-928.

Porsani, L., Filho, W. M., Ellis, V. R., Shimlis, J. D., Moura, H. P. (2004). The use of GRR and VES in delineating a contamination plume in a landfill site. A case study in SE Brazil. Journal of Applied Geophysics, l55, 199 – 209.

Quist, L. G., Bannerman, R. R. and Owusu, S. (1988). Groundwater in rural water supply in Ghana In: Ground Water in Rural Water Supply, Report of the West African Sub-Regional Workshop held in Accra, Ghana, 20-24 October 1986, UNESCO Technical Documents in Hydrology, Paris, pp 101-126.

Raman, N., and Narayanan, D. S. (2008). Impact of solid waste effect on ground water and soil quality nearer to pallavaram solid waste landfill site in chennai. Rjc Rasayan J. Chem. (1)4, 828-836.

Rao, S., Saroja, N., Nirmala, I. and Suryanarayana, K. (2005). Groundwater quality in a coastal area: A case study from Andhra Pradesh, India. Environ. Geol, 48, 543-550.

Richards, L. A. (1954). Diagnosis and improvement of saline and alkali soils. Agric. Hand Book 60, United States Department of Agriculture, Washington, D. C., pp 160.

Robertson, T. (1925). The sedimentary and volcanic rocks of western Togoland. Geological Magazine, (62) 1, 1 – 21.

Rushbrook, P and Pugh, M. (1999). Solid waste landfills in low and middle income countries: A technical guide to planning, design and operation. World Bank Technical Publication 426. World Bank.

Schneider, W.A., (1978). Generalized Regional Geology of Nigeria with Emphasis on Niger Delta and MPN offshore license Terms MPNMXR – 307, pp.57 -70.

Semerjian L. A. (2011). Quality assessment of various bottled waters marketed in Lebanon. Environmental Monitoring and Assessment, 172, 275-285.

Slater, L., Binley, A. M., Daily, W., and Johnson, R. (2000). Cross-hole electrical imaging of a controlled saline tracer injection. Journal of Applied Geophysics, 44(2-3), 85–102. http://doi.org/10.1016/S0926-9851(00)00002-1.

Slater, L., Binley, A., and Brown, D. (1996). Electrical imaging of fractures using groundwater salinity change. Ground Water, 35, 436-442.

Song, L., Zhu, J., Yan, Q., and Kang, H. (2012). Estimation of groundwater levels with vertical electrical sounding in the semiarid area of South Keerqin sandy aquifer, China. Journal of Applied Geophysics, 83, 11–18. http://doi.org/10.1016/j.jappgeo.2012.03.011

Sood, D. D, Reddy, A. V. R., and Ramamoorthy, N., (2004). Fundamentals of Radiochemistry (2nd Ed)., Perfect Prints, Jyoti Industrial Estate, India, pp 272 -279.

Srinivasamoorthy, K., Vasanthavigar, K. V. M., and Sarma, R. R. V. S. (2011). Integrated techniques to identify groundwater vulnerability to pollution in a highly industrialized terrain , Tamilnadu , India, 47–60. http://doi.org/10.1007/s10661-010-1857-x.

Srinivasamoorthy, K., Vijayaraghavan, K., Vasanthavigar, M., Sarma, V. S., Chidambaram, S., and Anandhan, P. (2010). Assessment of groundwater quality with special emphasis on fluoride contamination in crystalline bed rock aquifers of Mettur region, Tamilnadu, India. Arabian Journal of Geosciences. doi:10.1007/s12517-010-0162-x.

Srinivasamoorthy, K., Nanthakumar, C., Vasanthavigar, M., Vijayaraghavan, K., Rajivganthi, R., and Chidambaram, S. (2009). Groundwater quality assessment from a hard rock terrain, salem district of Tamilnadu, India. Arabian Journal of Geosciences. doi:10.1007/s12517-009-0076-7.

Stallman R. W. (1971) Aquifer-test design, observation and data analysis. Techniques of Water Resource Investigations of the US Geol Surv, Chap B1. Govt Printing Office Washington, DC.

Stuyfzand, P. (1986). A new hydrochemical classification of water types: principles and application to the coastal-dunes aquifer systems of the Netherlands. A selection of SWIM papers IAH, International Contributions to Hydrogeology, 11, 329-343.

Subramani, T., Elango, L., and Damodarasamy, S. R. (2005). Groundwater quality and its suitability for drinking and agricultural use in Chithar River Basin, Tamil Nadu, India. Environmental Geology, 47(8), 1099–1110. http://doi.org/10.1007/s00254-005-1243-0.

Tay, C., and Kortatsi, B. (2008). Groundwater Quality Studies : A Case Study of the Densu Basin , Ghana. West African Journal of Applied Ecology, 12.

Taylor, R., and Allen, A. (2001). Nature and Subject in Landfill. Impact Problem (Memorandum).

Taylor, R. W., and Fleming, A. H. (1988). Characterizing joint systems by azimuthal resistivity surveys. Ground Water, 26, 464 - 474.

Telford, W. M., Geldart, L. P., and Sheriff, R. E. (1990). Applied Geophysics, Cambridge: Cambridge University Press.

US Salinity Laboratory, (1954). Diagnosis and improvement of saline and alkali soils. Agricultural Handbook, USDA, No. 60, pp 160.

USGS Water Resource (2000). U.S. Department of the Interior U.S. Geological Survey.

Walton, J. (2010). Surface Investigations of Groundwater

Werner, A. D., Bakker, M., Post, V. E. A, Vandenbohede, A., Lu, C., Ataie-Ashtiani, B., and Barry, D. A. (2013). Seawater intrusion processes, investigation and management: Recent advances and future challenges. Advances in Water Resources, 51, 3–26. http://doi.org/10.1016/j.advwatres.2012.03.004.

Wetzel, R. G. (2001). Limnology, Lake and river systems. 3rd edition Academic Press, San Diego. pp 1006.

World Health Organisation (WHO), (2004). Guidelines for drinking water quality. Final task group meeting. WHO Press/World Health Organisation, Geneva.

Wilson, S. R., Ingham, M., and McConchie, J. A. (2006). The applicability of earth resistivity methods for saline interface definition. Journal of Hydrology, 316(1-4), 301–312. http://doi.org/10.1016/j.jhydrol.2005.05.004.

WRI. (2001). Groundwater Resources Assessment of Ghana. Technical Report, Water Research Institute (CSIR), Accra.

Wright, J. L., Hastings, D. A., Jones, W. B. and Williams, H. R., (1985). Geology and Mineral Resources of West Africa. 1st Edn., George Allen and Unwin (Publishers) Ltd., London, pp 187.

Yadav, S. D, P., Mishra, K., Chaudhary, N. K., and Mishra, P. (2015). Assessing Physico-Chemical Parameters of Potable Water in Dhankuta Municipality of Nepal. Science Journal of Analytical Chemistry, 3(2), 17–21.

Yeboah, S. A., and Ameyaw, Y. (2012). Analysis of Groundwater Quality for three selected Communities in the Ga East Municipal Assembly in the Greater Accra Region of Ghana. International Journal of Science and Nature, 3(4), 853-856.

Yidana, S. M., Ophori, D., Banoeng-Yakubo, B., and Samed, A. A. (2012). A factor model to explain the hydrochemistry and causes of fluoride enrichment in groundwater from the middle voltaian sedimentary aquifers in the Northern Region, Ghana. ARPN Journal of Engineering and Applied Sciences, 7(1), 50–68.

Yidana, S. M., Ganyaglo, S., Banoeng-Yakubo, B., and Akabzaa, T. (2011). A conceptual framework of groundwater flow in some crystalline aquifers in Southeastern Ghana. Journal of African Earth Sciences, 59(2-3), 185–194. http://doi.org/10.1016/j.jafrearsci.2010.10.005.

Yidana, S. M., (2010). Groundwater flow modeling and particle tracking for chemical transport in the southern Voltaian aquifers. Environ Earth Sci. 63:709–721.

Yidana, S. M., Ophori, D. and Obeng, B. (2007). Hydrochemical analysis of groundwater from the Keta Basin, Ghana. Journal of Environmental Hydrology, 15: 11 pp.

Zaidman, M. D. Middleton, R. T. West L. J., and Binley, A. M. (1999). Geophysical investigation of unsaturated zone transport in the Chalk in Yorkshire. Quarterly Journal of Geology and Hydro geology 1999, v. 32;p185-198. doi:10.1144/GSL.QJEGH..032.P3.08.

APPENDIX

APPENDIX A

Vertical electrical sounding (VES) models at all the 35

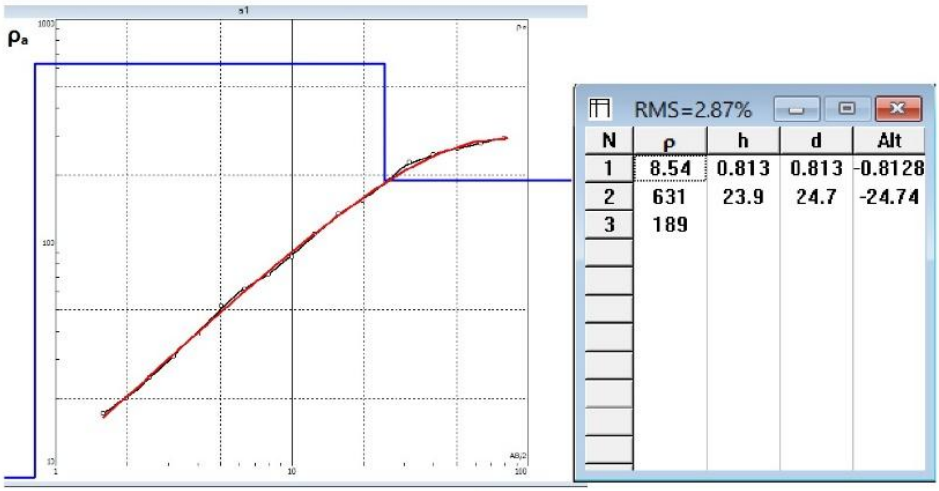

VESBAN1

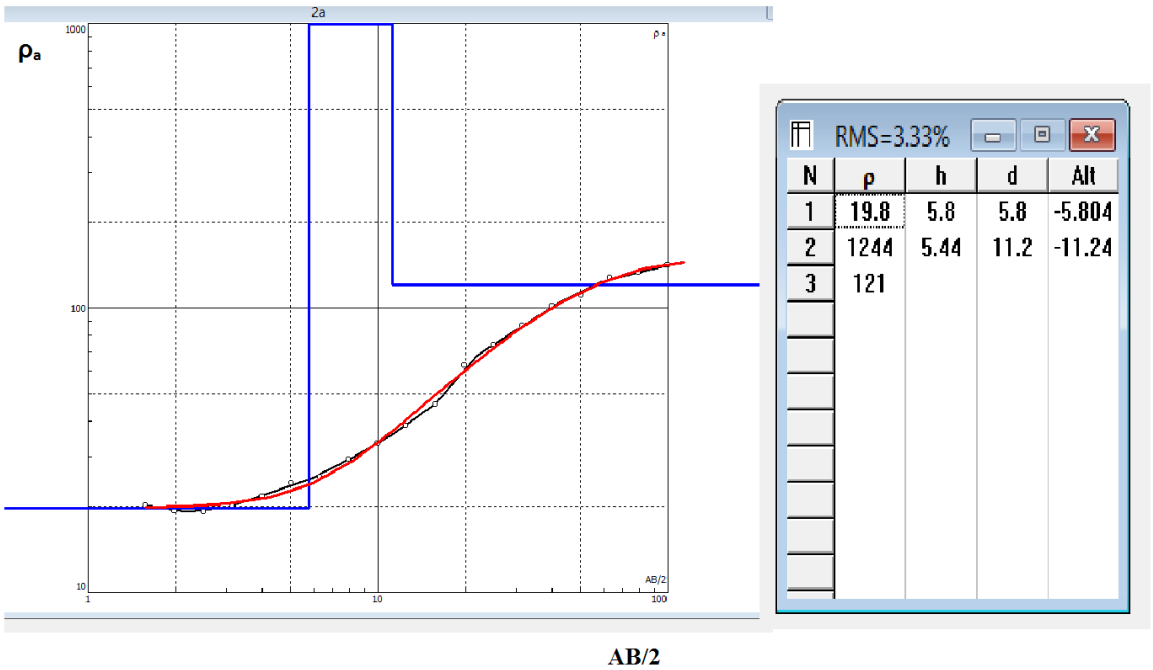

VESBAN2

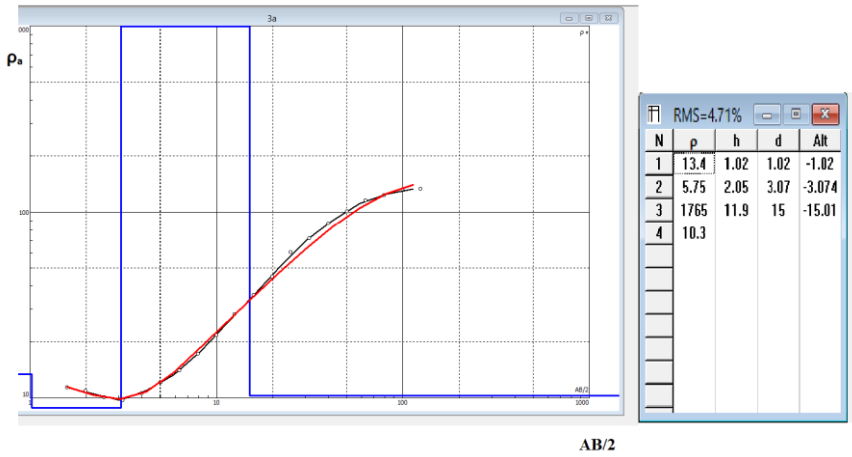

VESBAN3

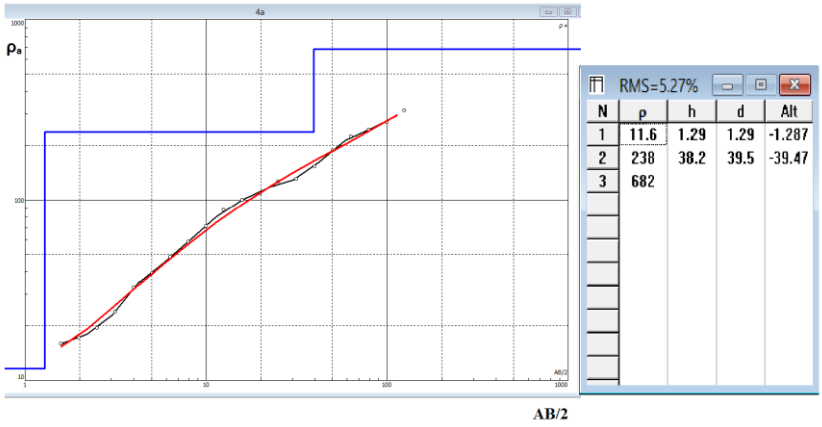

VES BAN4

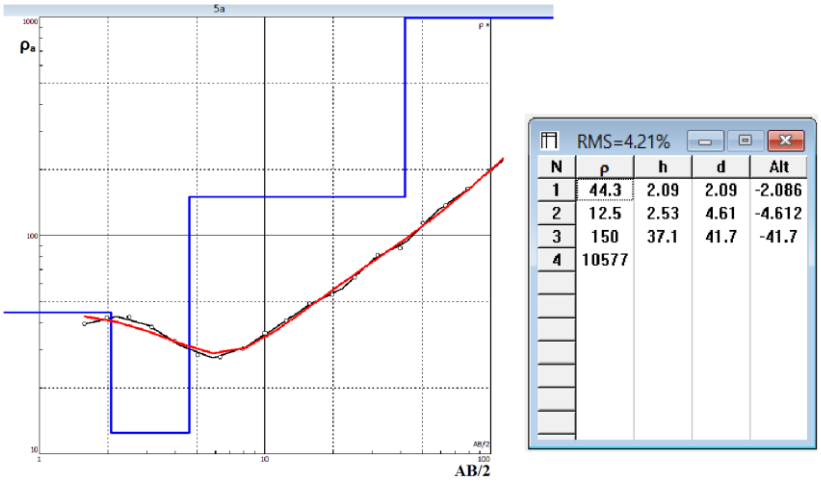

VES BAN5

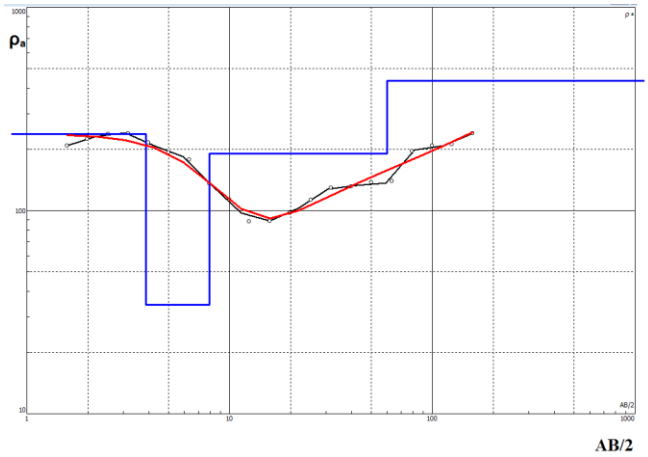

RMS=6.63%

N	ρ	h	d	Alt
1	238	3.86	3.86	-3.86
2	34.3	4.08	7.94	-7.94
3	190	51.8	59.7	-59.74
4	435			

VESBAN6

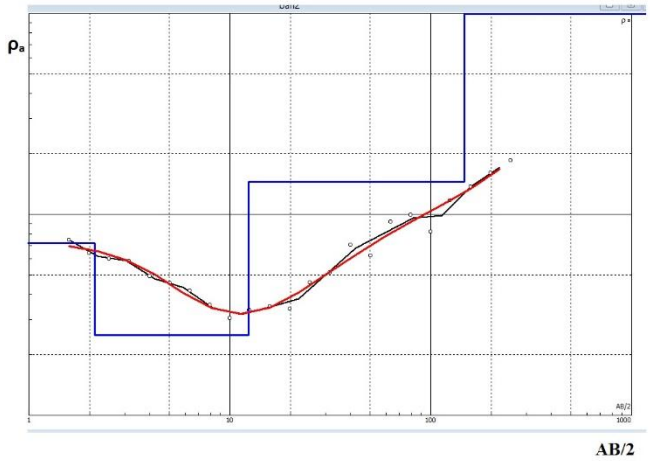

RMS=5.29%

N	ρ	h	d	Alt
1	72	2.12	2.12	-2.12
2	25	10.3	12.4	-12.42
3	145	135	147	-147.4
4	5663			

VESBAN7

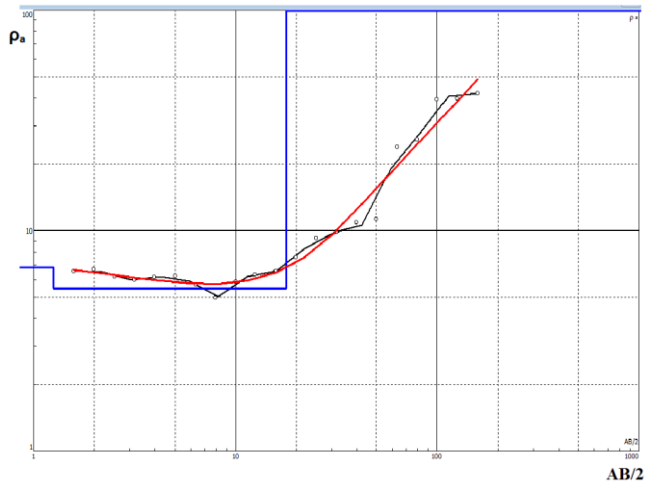

RMS=9.51%

N	ρ	h	d	Alt
1	6.85	1.25	1.25	-1.25
2	5.47	16.5	17.8	-17.75
3	2781			

VESBAN8

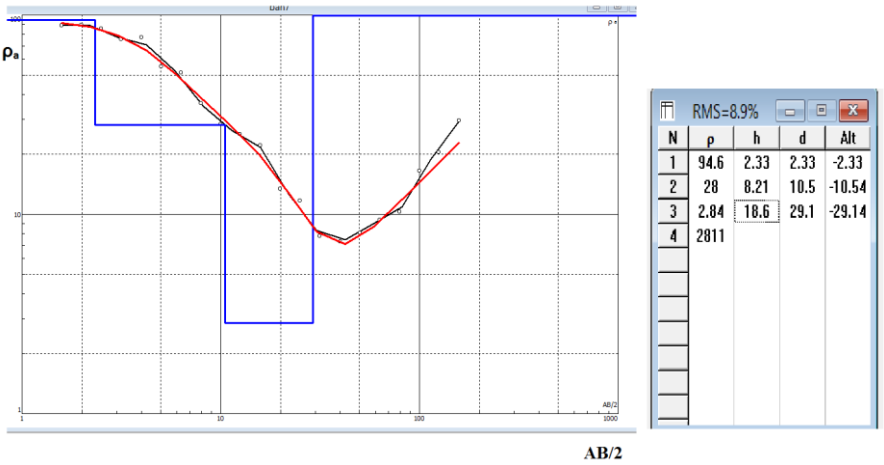

VESBAN9

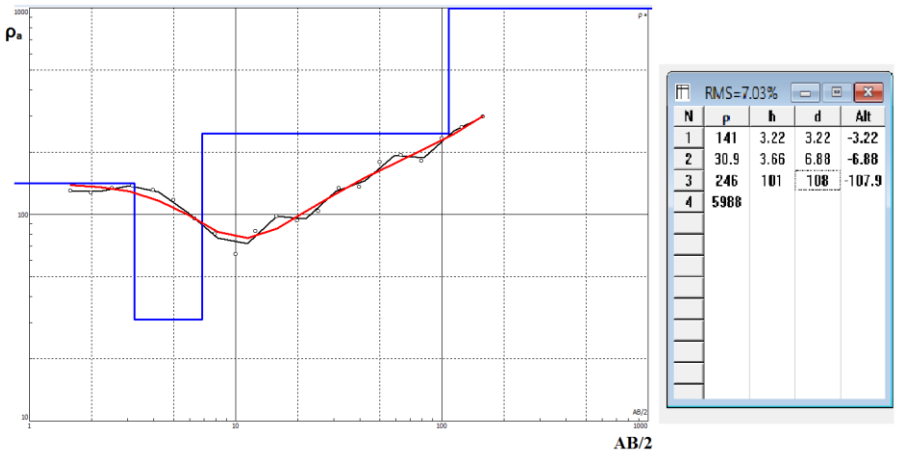

VESBAN10

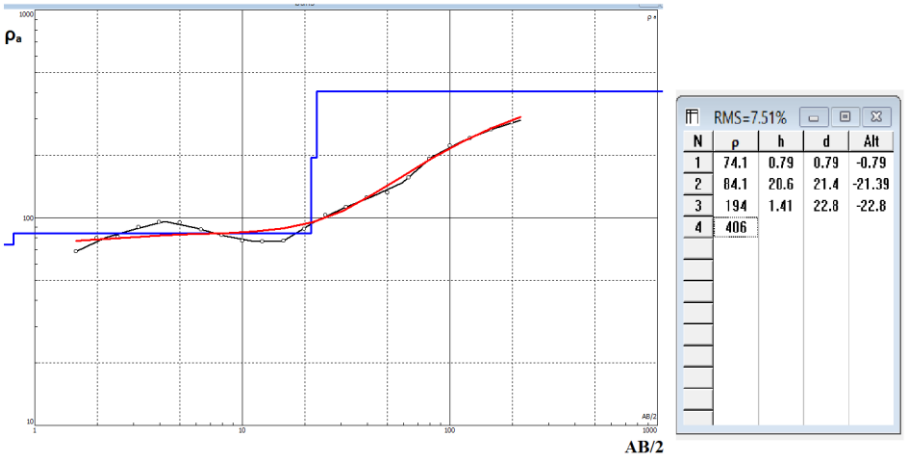

VESBAN11

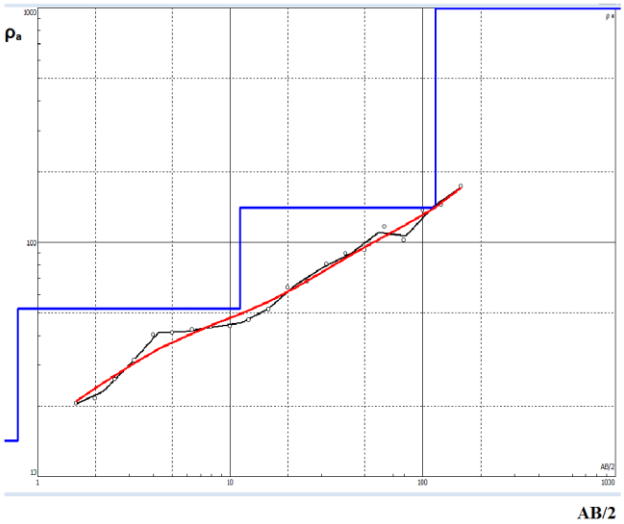

RMS=6.87%

N	ρ	h	d	Alt
1	14.2	0.79	0.79	-0.79
2	52.2	10.5	11.3	-11.29
3	140	105	116	-116.3
4	12568			

VESBAN12

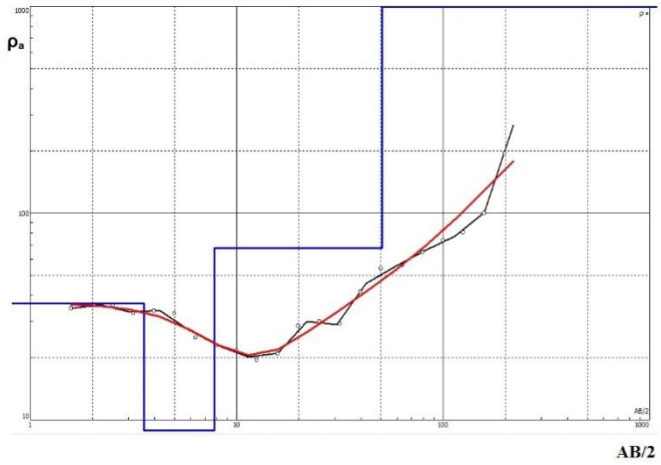

RMS=13.9%

N	ρ	h	d	Alt
1	36.5	3.56	3.56	-3.56
2	8.56	4.22	7.78	-7.78
3	68	43	50.8	-50.78
4	13949			

VESBAN13

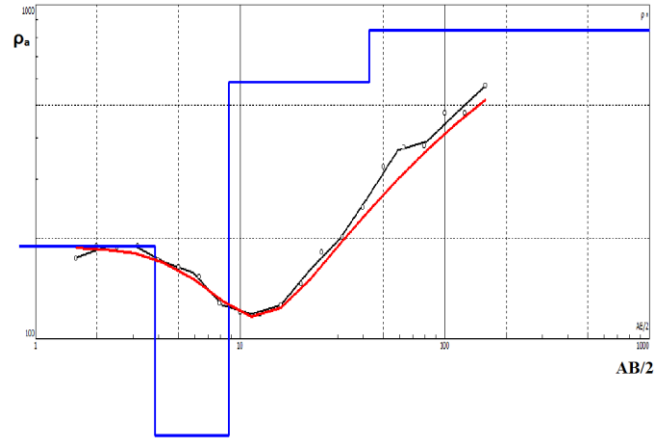

RMS=7.52%

N	ρ	h	d	Alt
1	189	3.83	3.83	-3.83
2	51.2	4.98	8.81	-8.81
3	586	34	42.8	-42.81
4	837			

VESBAN14

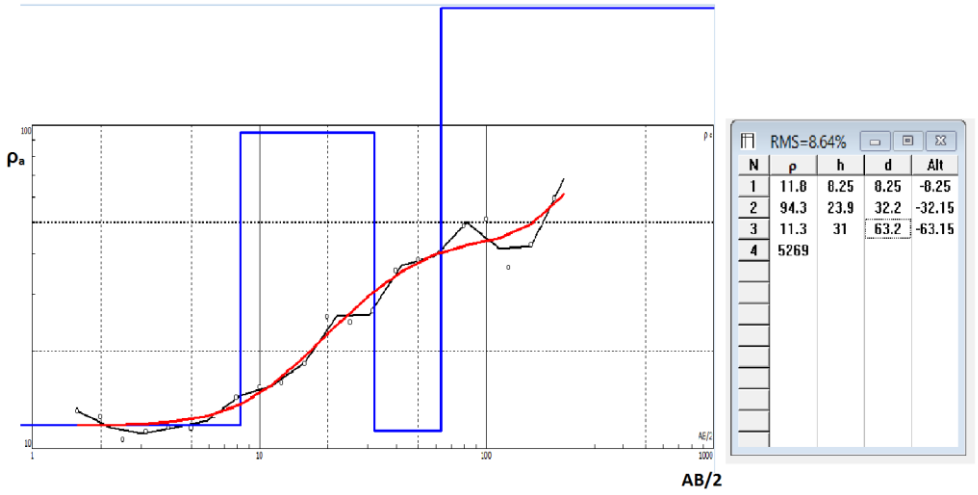

VESBAN15

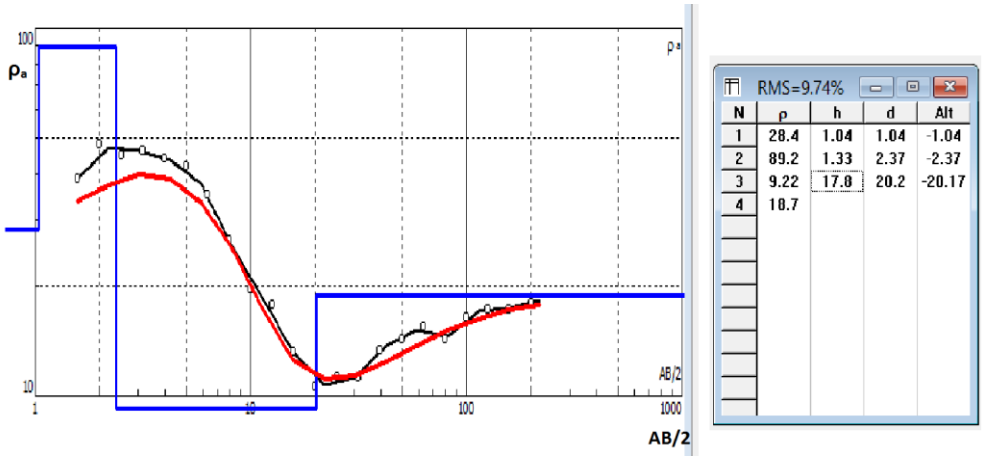

VESBAN16

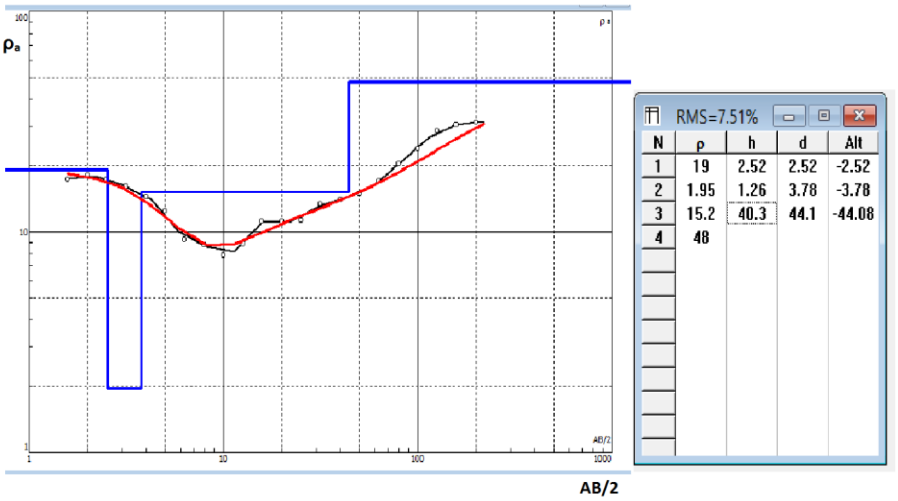

VESBAN17

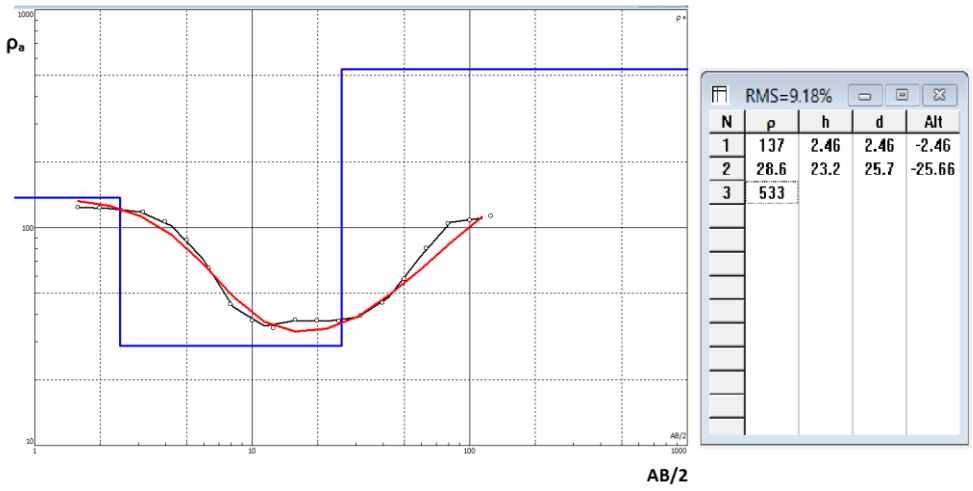

VESBAN18

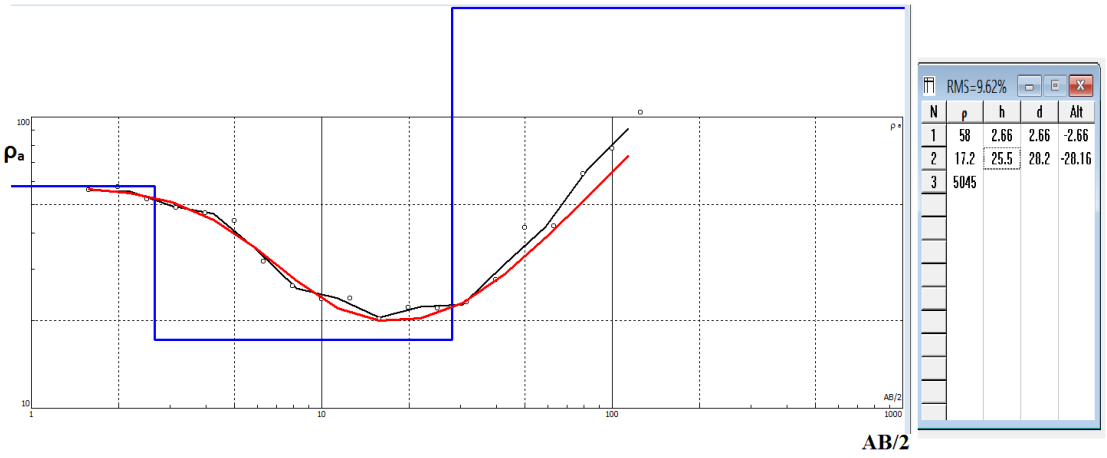

VESBAN19

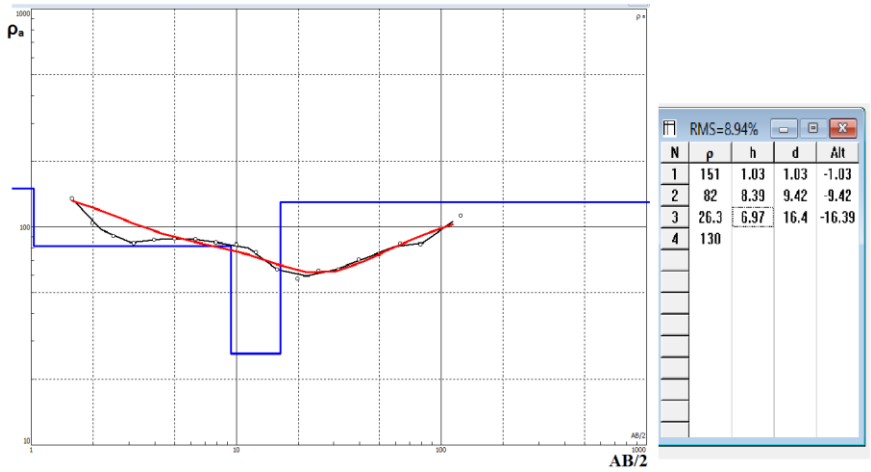

VESBAN20

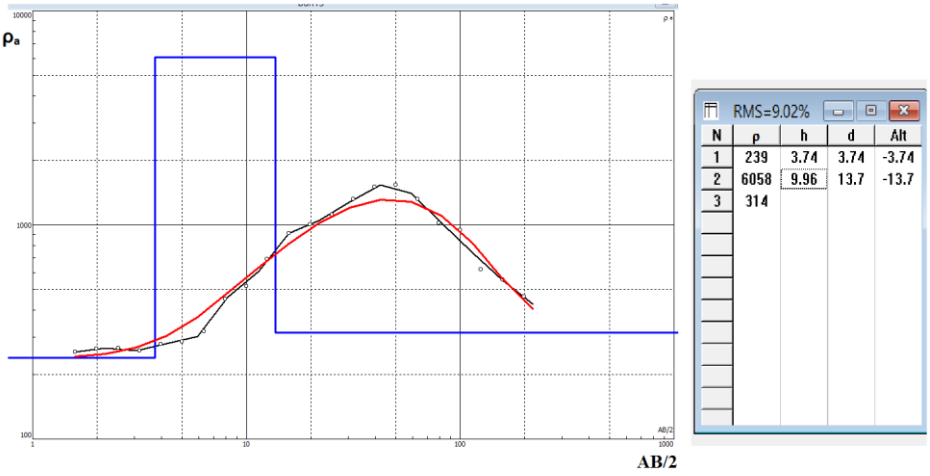

VESBAN21

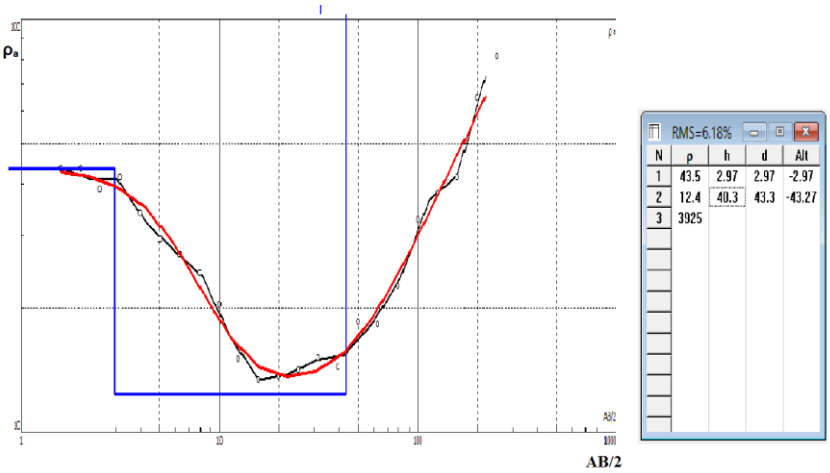

VESBAN22

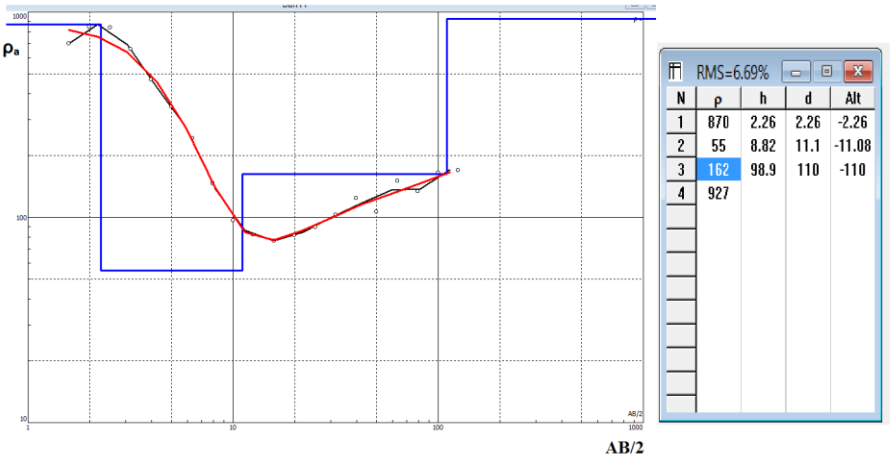

VESBAN23

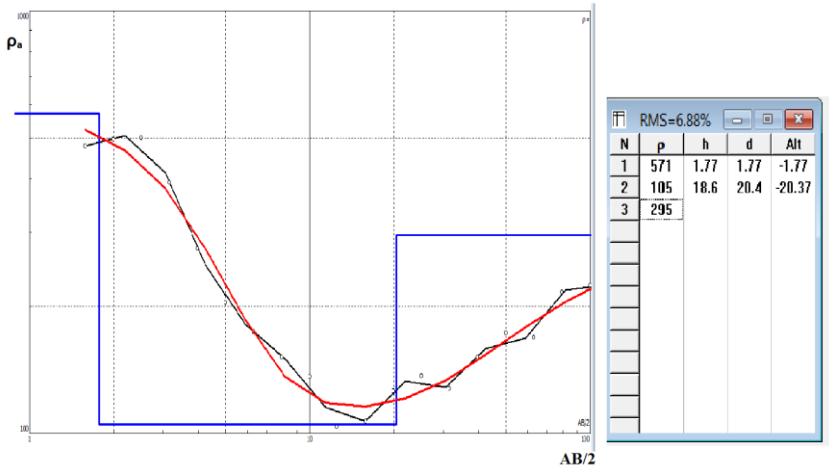

VESBAN24

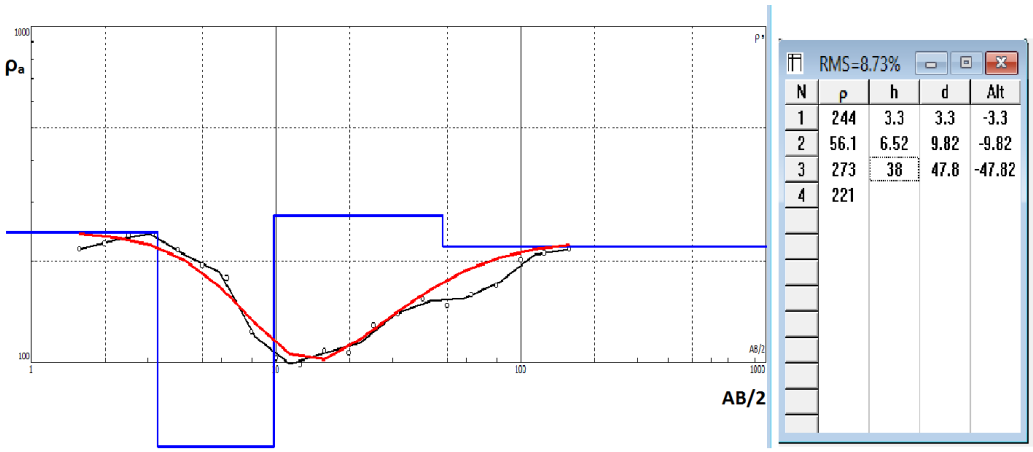

VESBAN25

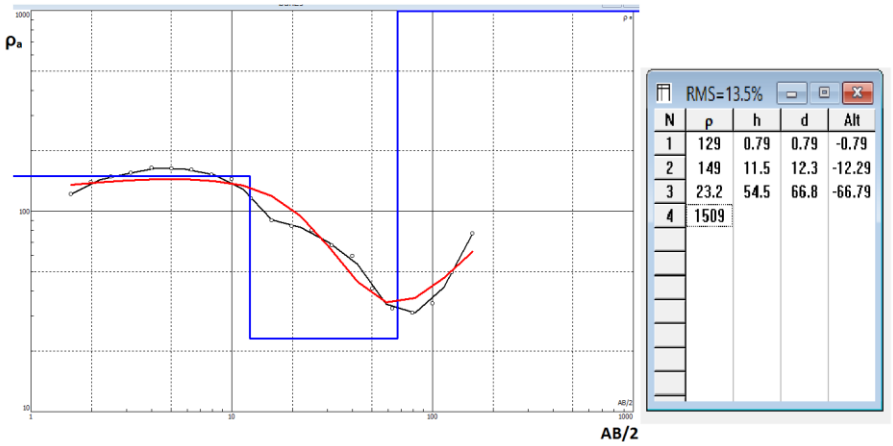

VESBAN26

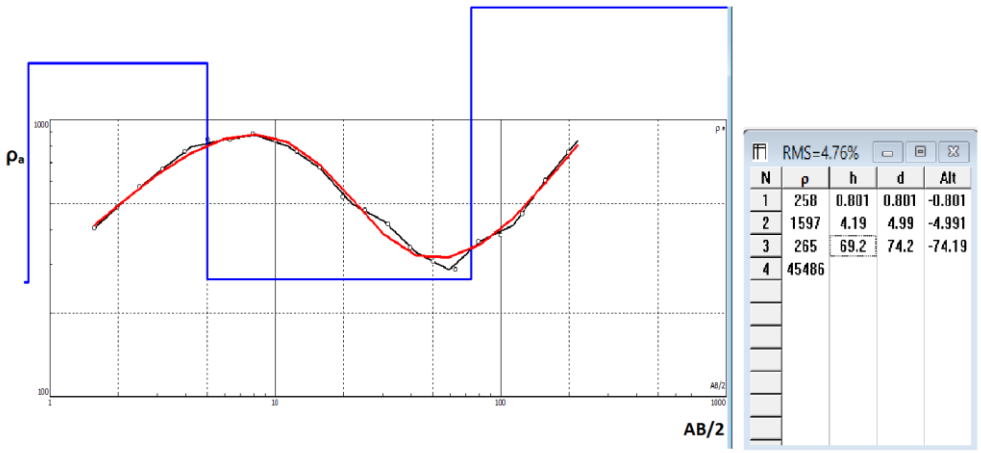

VESBAN27

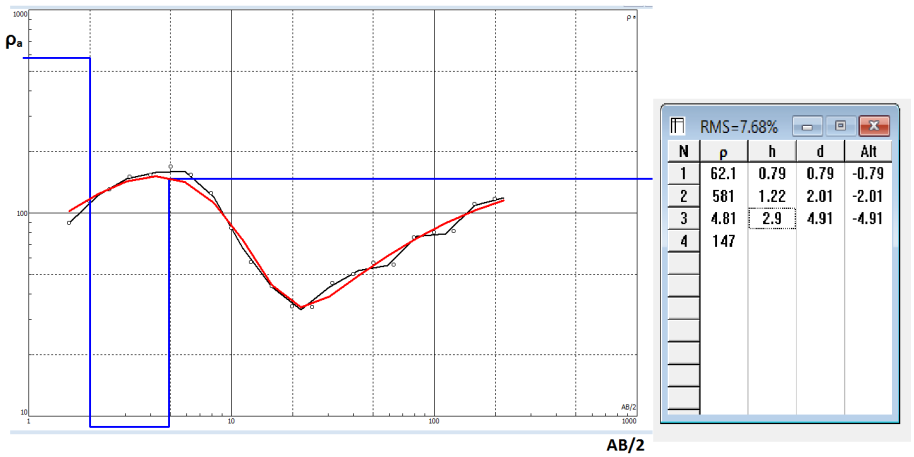

VESBAN28

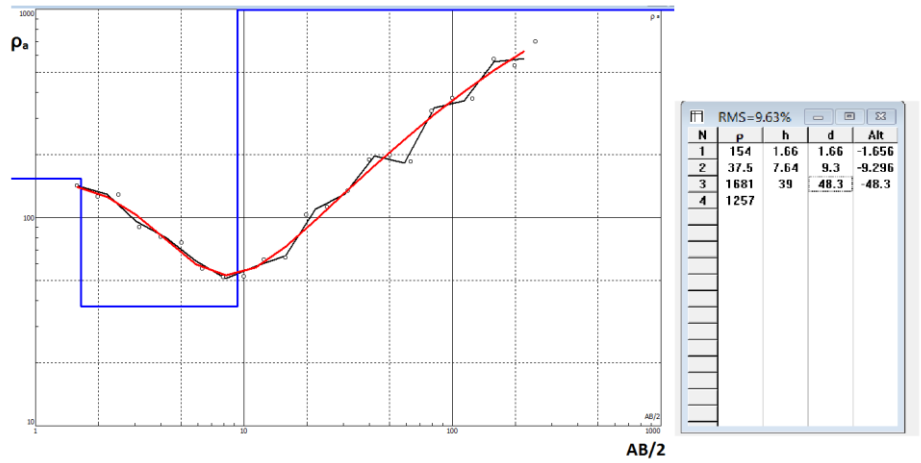

VESBAN29

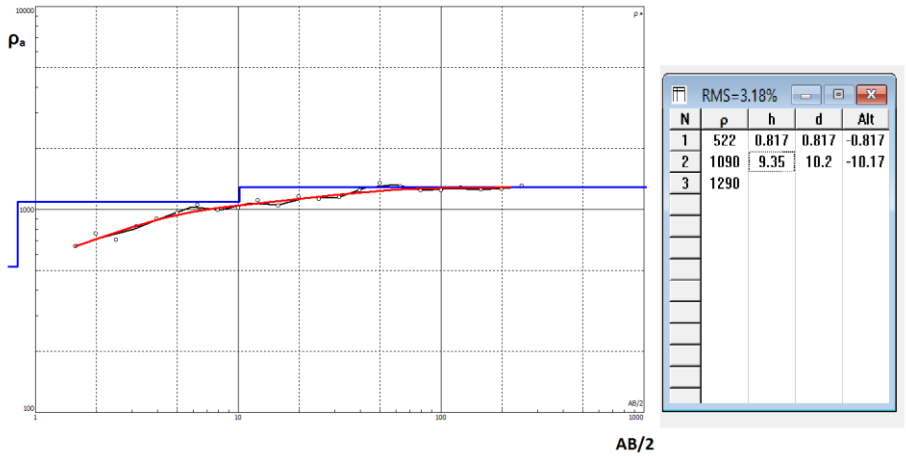

VESBAN30

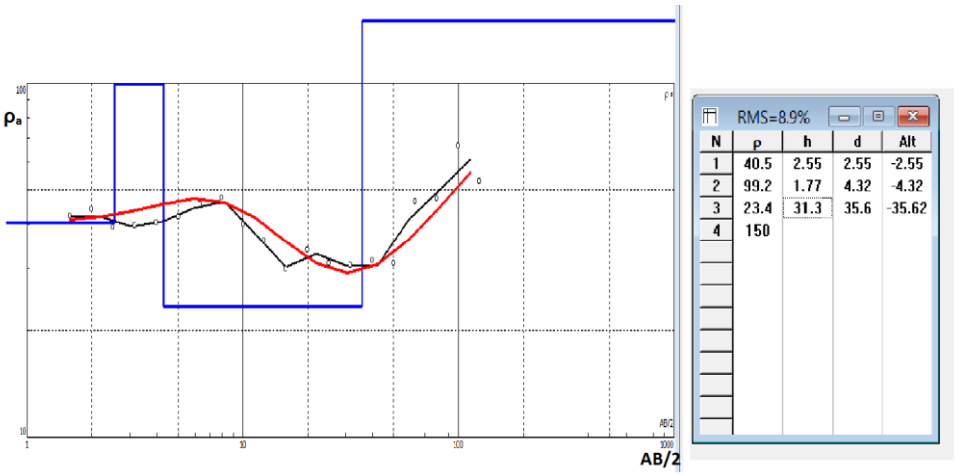

VESBAN31

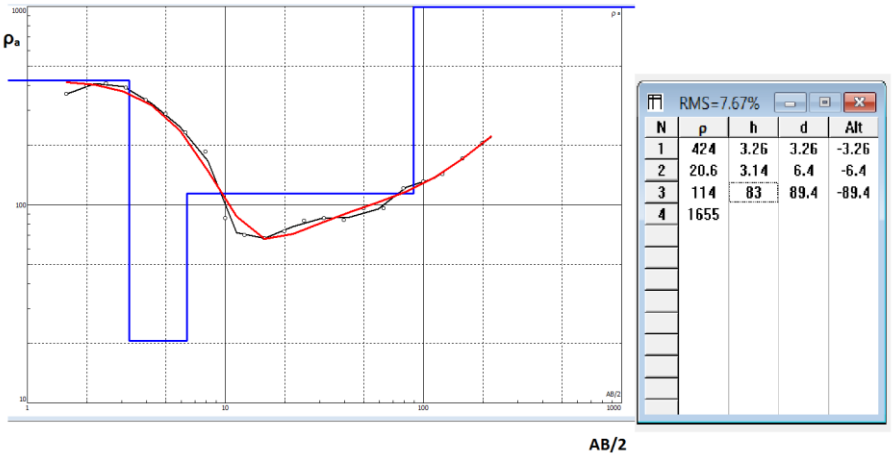

VESBAN32

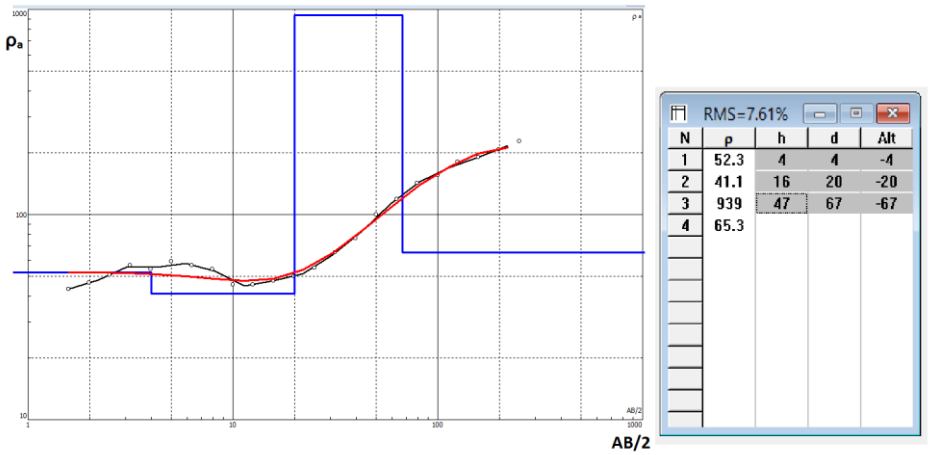

VESBAN33

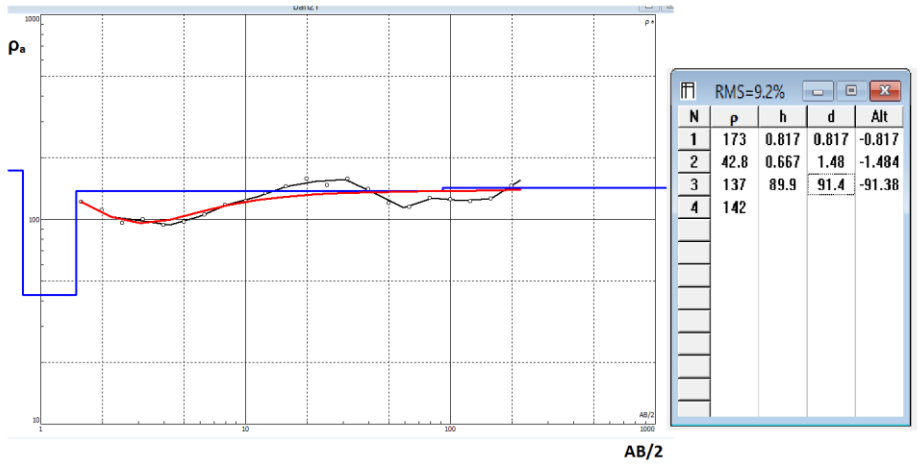

VESBAN34

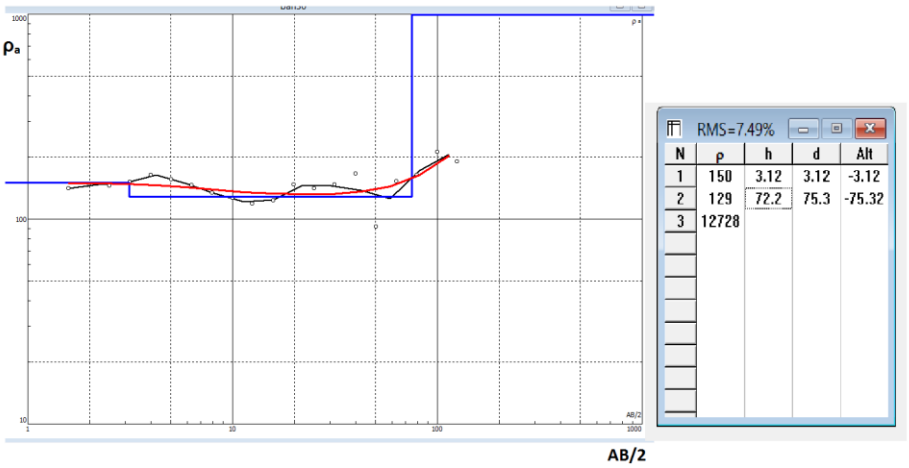

VESBAN35

APPENDIX B

Coordinates of VES and Sampling Stations

ID	EASTINGS	NORTHINGS	ELEVATION
BAN1	810352	631586	54
BAN2	810377	631157	61
BAN3	810466	631181	52
BAN4	810489	631222	68
BAN5	810541	631413	72
BAN6	811069	632043	76
BAN7	811220	632099	82
BAN8	810971	631712	81
BAN9	810487	631343	69
BAN10	810562	631146	67
BAN11	811194	631544	89
BAN12	813333	626860	92
BAN13	812868	627072	74
BAN14	810809	631568	79
BAN15	808155	628363	59
BAN16	808235	628415	58
BAN17	806704	626605	56
BAN18	806636	626922	67
BAN19	806877	626995	48
BAN20	808230	628052	61
BAN21	806497	627543	61
BAN22	811472	632482	88
BAN23	811521	632961	103
BAN24	811766	632613	88
BAN25	809973	629810	60
BAN26	811446	632564	88
BAN27	811610	632571	93
BAN28	811572	632429	89
BAN29	806154	627403	53
BAN30	806215	630887	103
BAN31	813006	631509	86
BAN32	809586	635325	84
BAN33	811700	624017	88
BAN34	811786	623983	92
BAN35	811654	624287	106
BAN36	806493	626546	50
BAN37	810804	628180	50
BAN38	810884	628223	50
BAN39	811859	632820	82
BAN40	810554	631440	64

APPENDIX C

Results of the Heavy Metals

ID	Fe	Zn	Mn	Co	Ni	Cr	Pb
BAN1	0.258	0.04	0.0254	<0.005	0.084	Nd	0.19
BAN2	0.42168	Nd	0.5421	<0.005	0.005	Nd	0.214
BAN3	0.8624	0.00241	0.6125	<0.005	0.0974	0.004	0.02
BAN4	0.37125	0.00752	0.5841	<0.005	0.0762	Nd	0.0183
BAN5	0.1389	0.01024	0.8762	<0.005	0.007	0.003	0.081
BAN6	0.133275	0.00225	<0.002	<0.005	0.0045	0.003	0.015
BAN7	0.102	0.00225	<0.002	<0.005	0.003	Nd	0.00825
BAN8	0.13875	0.00225	0.01275	<0.005	0.0075	0.00375	0.018
BAN9	0.05475	Nd	0.015	<0.005	Nd	Nd	0.0045
BAN10	0.075	0.01575	0.08925	<0.005	Nd	Nd	0.00525
BAN11	0.087	0.00975	0.01875	<0.005	Nd	Nd	0.006
BAN12	0.0735	Nd	0.006	<0.005	0.00525	Nd	0.02475
BAN13	0.04875	Nd	0.021	<0.005	Nd	Nd	0.0045
BAN14	0.05625	0.0015	0.015	<0.005	Nd	Nd	0.015
BAN16	0.70125	0.00525	0.108	0.00525	0.084	0.00525	0.02775
BAN17	0.06675	0.00225	0.31725	Nd	0.00225	Nd	0.00825
BAN18	2.67075	0.00225	0.024	0.0075	0.11625	0.01575	0.1575
BAN19	0.66675	0.0015	0.192	0.0045	0.07575	0.0045	0.02625
BAN20	1.94925	0.01425	0.4245	0.006	0.102	0.01275	0.1515
BAN21	0.06	Nd	0.0015	Nd	0.0045	Nd	0.0045
BAN22	0.45375	0.01425	0.3555	0.0045	0.00825	0.003	0.07575
BAN23	0.111	0.006	0.489	Nd	0.003	Nd	0.00825
BAN24	0.05775	0.00375	0.04275	Nd	Nd	Nd	0.00525
BAN25	0.0675	0.0015	0.5115	Nd	Nd	Nd	0.0075
BAN26	0.13725	Nd	0.50325	Nd	0.0045	Nd	0.009
BAN27	0.1185	0.0135	0.38925	Nd	0.003	Nd	0.0075
BAN28	0.52125	Nd	0.36825	0.00525	0.06	0.00225	0.006
BAN29	0.04875	Nd	0.003	Nd	Nd	Nd	0.00225
BAN31	0.07875	Nd	Nd	Nd	0.00525	Nd	0.01425
BAN32	0.06	0.06525	0.0018	Nd	Nd	Nd	0.0075
BAN33	0.05621	Nd	Nd	Nd	Nd	Nd	0.0089
BAN34	0.05472	Nd	Nd	Nd	Nd	Nd	0.0121
BAN35	0.05325	Nd	Nd	Nd	Nd	Nd	0.01725
BAN36	0.06075	Nd	0.01875	Nd	Nd	Nd	0.00225
BAN37	0.03525	0.006	0.002475	Nd	Nd	Nd	Nd
BAN38	0.051	0.00225	0.0045	Nd	Nd	Nd	0.0195
BAN39	0.03375	0.0015	Nd	Nd	Nd	Nd	0.00975
BAN40	0.03675	Nd	Nd	Nd	nd	Nd	Nd

APPENDIX D

Results of the Physical Parameters

ID	Temp	PH	EC	TDS	SAL	TSS	TURB	Col
BAN1	29.4	5.7	3998	1996	11.2	1	3	21
BAN2	30.4	4.48	1546	775	4.9	0	1	19
BAN3	28.9	6.13	1815	898	6.3	2	3	14
BAN4	31.1	5.31	2217	1109	8.4	1	2	23
BAN5	29.2	6.05	1451	729	4.3	0	2	9
BAN6	29.1	4.44	897	449	3.1	1	5	3
BAN7	29.5	5.28	1144	593	3.8	0	4	0
BAN8	28.5	4.8	3999	2000	12.1	1	1	18
BAN9	30.3	6.12	1790	895	5.5	0	0	8
BAN10	30.4	3.93	48	2000	12.5	2	2	37
BAN11	32.7	5.76	393	193	1.7	6	7	50
BAN12	29.7	6.91	2402	1205	7.5	0	1	12
BAN13	29	6.87	2970	1486	8.7	0	4	5
BAN14	29.6	5.95	1350	677	4.3	6	4	12
BAN16	29.2	6.26	1484	739	4.7	0	0	6
BAN17	29.9	6.11	1370	683	4.3	0	0	0
BAN18	29.4	6.09	405	197	1.4	3	8	69
BAN19	30.3	5.87	303	150	1.7	0	0	3
BAN20	30.5	6.76	3999	2000	11.4	6	7	81
BAN21	29	7.22	2215	1107	4.1	0	0	0
BAN22	29.3	7.05	1687	846	5	0	2	6
BAN23	29.3	3.02	2806	1406	8.3	0	0	0
BAN24	29.8	6.58	1890	943	5.7	0	0	0
BAN25	32.2	7.36	1556	777	4.8	0	11	6
BAN26	29.5	7.4	1640	820	4.8	0	0	0
BAN27	29.5	7.1	1581	801	5	2	7	48
BAN28	29.9	7.4	1592	795	4.7	0	0	0
BAN29	29.8	7.08	1207	602	3.8	1	2	1
BAN31	28.5	6.51	1046	527	3.3	0	1	11
BAN32	31.5	4.91	762	380	2.7	0	0	13
BAN33	29.5	5.28	1675	922	2.1	4	0	15
BAN34	30.1	5.33	1223	673	1.8	1	1	2.5
BAN35	29.5	7.14	353	176	1	0	0	0
BAN36	31.1	6.12	322	160	1.7	0	0	0
BAN37	30.2	5.56	1170	589	3.9	0	0	0
BAN38	31.6	5.38	895	448	3.1	0	0	0
BAN39	33.3	6.84	859	430	2.8	0	0	23
BAN40	31	6.2	828	416	2.8	0	0	5

APPENDIX E

Results of Chemical Parameters

STATION	Na^+	K^+	Ca^{2+}	Mg^{2+}	Cl^-	NO_3^-	SO_4^{2-}	HCO_3^-	TH	PO_4^-
BAN1	141	9.3	93	38	212	8.1	78	13.5	380	13.4
BAN2	115	28.1	61	35.4	256.1	13.5	110	17.3	467	7.64
BAN3	169	18.9	56.4	29	412	18.2	114	39.8	98	4.98
BAN4	85.6	73.5	72.3	23.5	257	14.1	128	18.3	175	15.7
BAN5	58.2	32.1	81.1	31	263	13	64	42.3	105	3.2
BAN6	88.5	15.3	14.4	10.9	239.9	5.3	12.4	12.1	68	12.0
BAN7	124	17.5	12.8	11.9	256.8	2.08	9.07	17.0	96	6.65
BAN8	140	70.5	53	14.3	425	8.05	4.90	17.0	664	3.00
BAN9	98.5	54	65.7	13.2	312	4.32	5.4	36.5	200	3.1
BAN10	97.3	71.8	102.4	15.0	520	3.56	6.3	4.87	920	4.65
BAN11	75.8	11.1	6.4	8.10	169.9	5.59	9.02	21.9	40	8.20
BAN12	89.5	12.9	189	14.9	350.2	5.91	6.09	134.1	96	9.07
BAN13	43.8	29.2	198.4	15.4	310.5	4.98	17.1	145	960	8.90
BAN14	50.5	29.8	36.8	12.2	189	18.2	13.6	41.4	128	12.0
BAN16	48.8	27.2	96	13.7	268.1	46.1	4.09	43.8	276	5.02
BAN17	35.2	19.8	64	14.0	125.3	3.97	25.0	70.7	336	5.09
BAN18	45	10.2	48	7.90	119.9	57	1.84	53.6	104	14.6
BAN19	85.6	16	8	10.5	213.4	3.09	9.05	21.9	32	0.04
BAN20	46	23.6	161.4	15.1	324.8	5.97	10.2	40.1	960	4.96
BAN21	82.6	17.3	232	15.1	455.9	4.12	8.35	268.2	764	5.59
BAN22	51.8	49.7	64	13.8	231.3	5.61	7.15	134.1	600	4.67
BAN23	78.6	57.5	91.2	14.4	251	6.09	6.09	39.01	524	4.01
BAN24	75.4	22.4	97.6	14.6	218	5.04	126	99.97	584	2.90
BAN25	35.9	17	89.6	13.8	230	20.2	9.13	151.1	356	9.12
BAN26	68.1	37.4	66.7	14.0	246	13.1	6.03	136.5	440	4.09
BAN27	39.6	38.8	92.8	13.8	219.5	5.18	17.8	156.0	360	3.00
BAN28	81	43.5	38.4	13.7	275	5.16	2.90	141.4	328	4.58
BAN29	96.5	10.6	57.6	13.9	281	3.09	0.75	199.9	228	6.07
BAN32	71.9	3.1	12.8	11.5	129.9	1.08	10.9	17.06	80	0.52
BAN33	184	3.9	37.7	10.6	323	3.2	3.48	29.3	180	0.58
BAN34	174	3.58	37.7	11.3	323	4.13	4.82	29.3	180	3.5
BAN35	192	5.6	16	11.2	315	5.14	5.02	39.01	60	6.93
BAN36	80.4	3.3	19.2	1.57	112	7.3	6.09	41.45	64	Nd
BAN37	34.1	8.7	43.2	13.5	198	4.09	6.73	19.50	204	6.17
BAN39	27.7	11	36.8	13.3	110	4.89	3.21	21.94	184	3.01
BAN40	28.5	31.8	17.6	12.8	99.9	18.3	7.02	60.95	116	8.93
BAN41	29.3	22.7	22.4	12.3	140	5.91	14.0	46.32	104	4.01
BAN42	83.9	16.3	12.8	10.5	200.3	54.2	15.3	19.50	68	15.2
BAN43	39.6	35.2	64	13.8	215.4	7.094	16.3	41.20	316	4.06

APPENDIX F

Resistivity Layers and Curve Types

Stations	Layers	Resistivities	Thickness	Depth	Curve Type
BAN 1	1	8.54	0.813	0.813	K
	2	631	23.9	24.7	
	3	189			
BAN2	1	19.8	5.8	5.8	K
	2	1244	5.44	11.2	
	3	121			
BAN3	1	13.4	1.02	1.02	HK
	2	5.75	2.05	3.07	
	3	1765	11.9	15	
	4	10.3			
BAN 4	1	11.6	1.29	1.29	A
	2	238	38.2	39.5	
	3	682			
BAN5	1	44.3	2.09	2.09	HA
	2	12.5	2.53	4.61	
	3	150	37.1	41.7	
	4	10577			
BAN6	1	238	3.86	3.86	HA
	2	34.3	4.08	7.94	
	3	190	51.8	59.7	
	4	435			
BAN7	1	72	2.12	2.12	HA
	2	25	10.3	12.4	
	3	145	135	147	
	4	5663			
BAN8	1	36.5	3.56	3.56	HA
	2	8.56	4.22	7.78	
	3	68	43	50.8	
	4	13949			
BAN9	1	14.2	0.79	0.79	AA
	2	52.2	10.5	11.3	
	3	140	105	116	
	4	12568			
BAN10	1	74.1	0.79	0.79	AA
	2	84.1	20.6	21.4	
	3	194	1.41	22.8	
	4	406			

BAN11	1	141	3.22	3.22	HA
	2	30.9	3.66	6.88	
	3	246	101	108	
	4	5988			
BAN12	1	94.6	2.33	2.33	QH
	2	28	8.21	10.5	
	3	2.84	18.6	29.1	
	4	2811			
BAN13	1	6.85	1.25	1.25	H
	2	5.47	16.5	17.8	
	3	2781			
BAN14	1	189	3.83	3.83	HA
	2	51.2	4.98	8.81	
	3	586	34	42.8	
	4	837			
BAN15	1	571	1.77	1.77	H
	2	105	18.6	20.4	
	3	295			
BAN16	1	870	2.26	2.26	HA
	2	55	8.82	11.1	
	3	162	98.9	110	
	4	927			
BAN17	1	43.5	2.97	2.97	H
	2	12.4	40.3	43.3	
	3	3925			
BAN18	1	239	3.74	3.74	K
	2	6058	9.96	13.7	
	3	314			
BAN19	1	151	1.03	1.03	QH
	2	82	8.39	9.42	
	3	26.3	6.97	16.4	
	4	130			
BAN20	1	58	2.66	2.666	H
	2	17.2	25.5	28.1	
	3	5045			
BAN21	1	137	2.46	2.46	H
	2	28.6	23.2	25.7	
	3	533			
BAN22	1	19	2.52	2.52	HA
	2	1.95	1.26	3.78	
	3	15.2	40.3	44.1	
	4	48			
BAN23	1	28.4	1.04	1.04	KH
	2	89.2	1.33	2.37	
	3	9.22	17.8	20.2	
	4	18.7			

BAN24	1	11.8	8.25	8.25	KH
	2	94.3	23.9	32.2	
	3	11.3	31	63.2	
	4	5269			
BAN25	1	244	3.3	3.3	HK
	2	56.1	6.52	9.83	
	3	273	38	47.8	
	4	221			
BAN26	1	173	0.817	0.817	HA
	2	42.8	0.667	1.48	
	3	137	89.9	91.4	
	4	142			
BAN27	1	52.3	4	4	HK
	2	41.1	16	20	
	3	939	47	67	
	4	65.3			
BAN28	1	424	3.26	3.26	HA
	2	20.6	3.14	6.4	
	3	114	83	89.4	
	4	1655			
BAN29	1	40.5	2.55	2.55	KH
	2	99.2	1.77	4.32	
	3	23.4	31.3	35.6	
	4	150			
BAN30	1	522	0.817	0.817	A
	2	1090	9.35	10.2	
	3	1290			
BAN31	1	154	1.66	1.66	HK
	2	37.5	7.64	9.3	
	3	1681	39	48.3	
	4	1257			
BAN32	1	62.1	0.79	0.79	KH
	2	581	1.22	2.01	
	3	4.81	2.9	4.91	
	4	147			
BAN33	1	258	0.801	0.801	KH
	2	1597	4.19	4.99	
	3	265	69.2	74.2	
	4	45486			
BAN34	1	129	0.79	0.79	KH
	2	149	11.5	12.3	
	3	23.2	54.5	66.8	
	4	1509			

BAN35	1	150	3.12	3.12	H
	2	129	72.2	75.3	
	3	12728			